

---

# MULTIVIZ: An Analysis Benchmark for Visualizing and Understanding Multimodal Models

---

Paul Pu Liang<sup>1</sup>, Yiwei Lyu<sup>1</sup>, Gunjan Chhablani<sup>2</sup>, Nihal Jain<sup>1</sup>, Zihao Deng<sup>1</sup>, Xingbo Wang<sup>3</sup>,

Louis-Philippe Morency<sup>1</sup>, Ruslan Salakhutdinov<sup>1</sup>

<sup>1</sup>Carnegie Mellon University, <sup>2</sup>Georgia Tech, <sup>3</sup>HKUST

<https://github.com/pliang279/MultiViz>

## Abstract

The promise of multimodal models for real-world applications has inspired research in visualizing and understanding their internal mechanics with the end goal of empowering stakeholders to visualize model behavior, perform model debugging, and promote trust in machine learning models. However, modern multimodal models are typically black-box neural networks, which makes it challenging to understand their internal mechanics. How can we visualize the internal modeling of multimodal interactions in these models? Our paper aims to fill this gap by proposing MULTIVIZ, a method for analyzing the behavior of multimodal models by scaffolding the problem of interpretability into 4 stages: (1) *unimodal importance*: how each modality contributes towards downstream modeling and prediction, (2) *cross-modal interactions*: how different modalities relate with each other, (3) *multimodal representations*: how unimodal and cross-modal interactions are represented in decision-level features, and (4) *multimodal prediction*: how decision-level features are composed to make a prediction. MULTIVIZ is designed to operate on diverse modalities, models, tasks, and research areas. Through experiments on 8 trained models across 6 real-world tasks, we show that the complementary stages in MULTIVIZ together enable users to (1) *simulate* model predictions, (2) assign *interpretable concepts* to features, (3) perform *error analysis* on model misclassifications, and (4) use insights from error analysis to *debug* models. MULTIVIZ is publicly available, will be regularly updated with new interpretation tools and metrics, and welcomes inputs from the community.

## 1 Introduction

The recent promise of multimodal models that integrate information from heterogeneous sources of data has led to their proliferation in numerous real-world settings such as multimedia [60, 75], affective computing [62, 81], robotics [50, 54], and healthcare [27, 107]. Subsequently, their impact towards real-world applications has inspired recent research in visualizing and understanding their internal mechanics [15, 32, 77, 99, 115] as a step towards accurately benchmarking their limitations for more reliable deployment [17, 35, 40]. However, modern parameterizations of multimodal models are typically black-box neural networks, such as pretrained transformers [36, 57, 67, 98]. How can we visualize and understand the internal modeling of multimodal information and interactions in these models?

As a step in interpreting multimodal models, this paper introduces an analysis and visualization benchmark called MULTIVIZ (see Figure 1). To tackle the challenges of visualizing model behavior, we scaffold the problem of interpretability into 4 stages: (1) *unimodal importance*: identifying the contributions of each modality towards downstream modeling and prediction, (2) *cross-modal interactions*: uncovering the various ways in which different modalities can relate with each other and the types of new information possibly discovered as a result of these relationships, (3) *multimodal representations*: how unimodal and cross-modal interactions are represented in decision-level features, and (4) *multimodal prediction*: how decision-level features are composed to make a prediction for a given task. In addition to including current approaches for unimodal importance [32, 73, 86] and

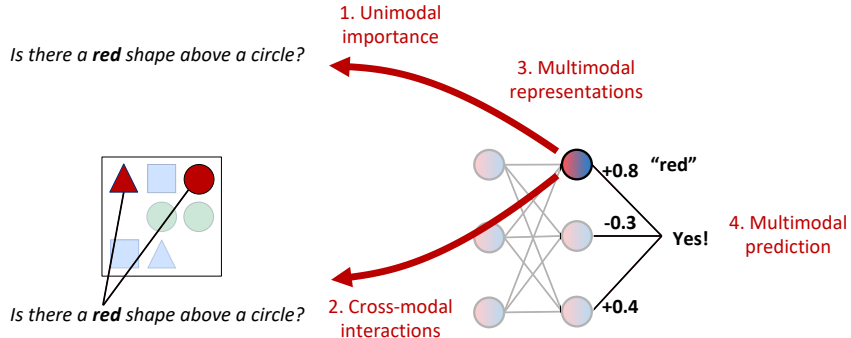


Figure 1: We scaffold the problem of multimodal interpretability into several stages and propose MULTIVIZ, a comprehensive analysis benchmark encompassing a set of fine-grained analysis tools for each stage: (1) **unimodal importance** identifies the contributions of each modality, (2) **cross-modal interactions** uncover how different modalities relate with each other and the types of new information possibly discovered as a result of these relationships, (3) **multimodal representations** study how unimodal and cross-modal interactions are represented in decision-level features, and (4) **multimodal prediction** studies how these features are composed to make a prediction.

cross-modal interactions [37, 69], we additionally propose new methods for interpreting cross-modal interactions, multimodal representations, and prediction to complete these stages in MULTIVIZ. By viewing multimodal interpretability through the lens of these 4 stages, MULTIVIZ contributes a *modular* and *human-in-the-loop* visualization toolkit for the community to visualize popular multimodal datasets and models, compare with other interpretation perspectives, and for stakeholders to understand multimodal models in their research domains.

MULTIVIZ is designed to support many modality inputs while also operating on diverse modalities, models, tasks, and research areas. Through experiments on 6 real-world multimodal tasks (spanning fusion [7, 43, 115], retrieval [80], and question-answering [33, 44]), 6 modalities, and 8 models, we show that MULTIVIZ helps users gain a deeper understanding of model behavior as measured via a proxy task of model simulation. We further demonstrate that MULTIVIZ helps human users assign interpretable language concepts to previously uninterpretable features and perform error analysis on model misclassifications. Finally, using takeaways from error analysis, we present a case study of human-in-the-loop model debugging. Overall, MULTIVIZ provides a practical toolkit for interpreting the internal mechanics of multimodal models for human understanding and debugging. MULTIVIZ datasets, models, and code can be found at <https://github.com/pliang279/MultiViz>.

## 2 MULTIVIZ: Towards Visualizing and Understanding Multimodal Models

This section presents MULTIVIZ, our proposed analysis benchmark for analyzing the behavior of multimodal models. As a general setup, we assume multimodal datasets take the form  $\mathcal{D} = \{(\mathbf{x}_1, \mathbf{x}_2, y)_{i=1}^n\} = \{(x_1^{(1)}, x_1^{(2)}, \dots, x_2^{(1)}, x_2^{(2)}, \dots, y)_{i=1}^n\}$ , with boldface  $\mathbf{x}$  denoting the entire modality, each  $x_1, x_2$  indicating modality atoms (i.e., fine-grained sub-parts of modalities that we would like to analyze, such as individual words in a sentence, object regions in an image, or time-steps in time-series data), and  $y$  denoting the label. These datasets enable us to train a multimodal model  $\hat{y} = f(\mathbf{x}_1, \mathbf{x}_2; \theta)$  which we are interested in visualizing.

Modern parameterizations of multimodal models  $f$  are typically black-box neural networks, such as multimodal transformers [36, 98] and pretrained models [57, 67]. How can we visualize and understand the internal modeling of multimodal information and interactions in these models? Having an accurate understanding of their decision-making process would enable us to benchmark their opportunities and limitations for more reliable real-world deployment. However, interpreting  $f$  is difficult. In many multimodal problems, it is useful to first scaffold the problem of interpreting  $f$  into several intermediate stages from low-level unimodal inputs to high-level predictions. Each of these stages provides complementary information on the decision-making process (see Figure 1):

- (1) **Unimodal importance** investigates the contributions of each modality towards downstream modeling and prediction.
- (2) **Cross-modal interactions** uncover the various ways in which different modalities can relate to each other and the types of new information discovered as a result of these relationships.

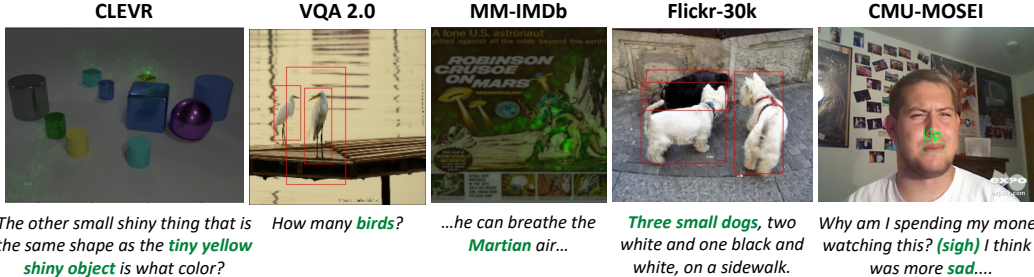


Figure 2: Examples of cross-modal interactions discovered by our proposed second-order gradient approach: first taking a gradient of model  $f$  with respect to an input word (e.g.,  $x_1 = \text{birds}$ ), before taking a second-order gradient with respect to all image pixels  $\mathbf{x}_2$  indeed results in all birds in the image being highlighted.

(3) **Multimodal representations** probe how unimodal and cross-modal interactions are represented as intermediate features in multimodal models.

(4) **Multimodal prediction** analyzes how discovered unimodal and cross-modal interactions are composed to form higher-level features suitable for a particular prediction task.

We now describe each step in detail and propose methods to analyze each step.

## 2.1 Unimodal importance (U)

Unimodal importance aims to understand the contributions of each modality towards modeling and prediction. It builds upon ideas of gradient-based visualizations (e.g., Guided backpropagation [32] or Grad-CAM [15, 88]) and feature attributions (e.g., LIME [34, 86, 109], Shapley values [73, 87, 95]). We implement unimodal feature attribution methods as a module  $\text{UNI}(f_\theta, y, \mathbf{x})$  taking in a trained model  $f_\theta$ , an output/feature  $y$  which analysis is performed with respect to, and the modality of interest  $\mathbf{x}$ .  $\text{UNI}$  returns importance weights across atoms  $x$  of modality  $\mathbf{x}$ .

## 2.2 Cross-modal interactions (C)

Cross-modal interactions describe various ways in which atoms from different modalities can relate with each other and the types of new information possibly discovered as a result of these relationships. Recent work [37, 69] has formalized a definition of cross-modal interactions by building upon literature in statistical non-additive interactions:

**Definition 1** (Statistical Non-Additive Interaction [28, 93, 100, 101]). A function  $f$  learns a feature interaction  $\mathcal{I}$  between 2 unimodal atoms  $x_1$  and  $x_2$  if and only if  $f$  cannot be decomposed into a sum of unimodal subfunctions  $g_1, g_2$  such that  $f(x_1, x_2) = g_1(x_1) + g_2(x_2)$ .

This definition of non-additive interactions is general enough to include different ways that interactions can happen, including multiplicative interactions from complementary views of the data (i.e., an interaction term  $x_1 \mathbb{W} x_2$  [42]), or cooperative interactions from equivalent views (i.e., an interaction term  $\text{majority}(f(x_1), f(x_2))$  [22]). Using this definition, **MULTIVIZ** first includes two recently proposed methods for understanding cross-modal interactions: **EMAP** [37] decomposes  $f(x_1, x_2) = g_1(x_1) + g_2(x_2) + g_{12}(x_1, x_2)$  into strictly unimodal representations  $g_1, g_2$ , and cross-modal representation  $g_{12} = f - \mathbb{E}_{x_1}(f) - \mathbb{E}_{x_2}(f) + \mathbb{E}_{x_1, x_2}(f)$  to quantify the degree of global cross-modal interactions across an entire dataset. **DIME** [69] further extends EMAP using feature visualization on each disentangled representation locally (per datapoint). However, these approaches require approximating expectations over modality subsets, which may not scale beyond 2 modalities. To fill this gap, we propose an efficient approach for visualizing these cross-modal interactions by observing that the following gradient definition directly follows from Definition 1:

**Definition 2** (Gradient definition of statistical non-additive interaction [28, 101]). A function  $f$  exhibits non-additive interactions among 2 unimodal atoms  $x_1$  and  $x_2$  if  $\mathbb{E}_x \left[ \frac{\partial f(x)}{\partial x_1 \partial x_2} \right]^2 > 0$ .

Definition 2 inspires us to extend first-order gradient and perturbation-based approaches [34, 86, 109] to second-order gradient methods. Specifically, given a model  $f$ , we first take a gradient of  $f$  with respect to an input word (e.g.,  $x_1 = \text{dog}$ ), before taking a second-order gradient with respect to all input image pixels  $\mathbf{x}_2$ , which should result in only the dog in the image being highlighted (see Figure 2 for examples on real datasets). We implement a general module  $\text{CM}(f_\theta, y, x_1, \mathbf{x}_2)$  for



Figure 3: We visualize multimodal representations through local and global analysis. Given an input datapoint, **local analysis** visualizes the unimodal and cross-modal interactions that activate a feature. **Global analysis** informs the user of similar datapoints that also maximally activate that feature, and is especially useful in assigning human-interpretable concepts to features by looking at similarly activated input regions across datapoints (e.g., the concept of color in this case).

cross-modal visualizations, taking in a trained model  $f_\theta$ , an output/feature  $y$ , the first modality’s atom of interest  $x_1$ , and the entire second modality of interest  $x_2$ . CM returns importance weights across atoms  $x_2$  of modality  $x_2$ , and can build on top of any first-order unimodal attribution method (i.e., gradient visualization [32], LIME [86], or Shapley values [73], see Appendix C.2).

### 2.3 Multimodal representations

Given these highlighted unimodal and cross-modal interactions at the input level, the next stage aims to understand how these interactions are represented at the feature representation level. Specifically, given a trained multimodal model  $f$ , define the matrix  $M_z \in \mathbb{R}^{N \times d}$  as the penultimate layer of  $f$  representing (uninterpretable) deep feature representations implicitly containing information from both unimodal and cross-modal interactions. For the  $i$ th datapoint,  $z = M_z(i)$  collects a set of individual feature representations  $z_1, z_2, \dots, z_d \in \mathbb{R}$ . We aim to interpret these feature representations through both local and global analysis (see Figure 3 for an example):

**Local representation analysis ( $R_\ell$ )** informs the user on parts of the original datapoint that activate feature  $z_j$ . To do so, we run unimodal and cross-modal visualization methods with respect to feature  $z_j$  (i.e.,  $\text{UNI}(f_\theta, z_j, \mathbf{x})$ ,  $\text{CM}(f_\theta, z_j, x_1, x_2)$ ) in order to explain the input unimodal and cross-modal interactions represented in feature  $z_j$ . Local analysis is useful in explaining model predictions on the original datapoint by studying the input regions activating feature  $z_j$ .

**Global representation analysis ( $R_g$ )** provides the user with the top  $k$  datapoints  $\mathcal{D}_k(z_j) = \{(\mathbf{x}_1, \mathbf{x}_2, y)_{i=(1)}^k\}$  that also maximally activate feature  $z_j$ . By further unimodal and cross-modal visualizations on datapoints in  $\mathcal{D}_k(z_j)$ , global analysis is especially useful in helping humans assign interpretable language concepts to each feature by looking at similarly activated input regions across datapoints (e.g., the concept of color in Figure 3). Global analysis can also help to find related datapoints the model also struggles with for error analysis.

### 2.4 Multimodal prediction (P)

Finally, the prediction step takes the set of feature representations  $z_1, z_2, \dots, z_d$  and composes them to form higher-level abstract concepts suitable for a task. We approximate the prediction process with a linear combination of penultimate layer features by integrating a sparse linear prediction model with neural network features [105]. Given the penultimate layer  $M_z \in \mathbb{R}^{N \times d}$ , we fit a linear model  $\mathbb{E}(Y|X = x) = M_z^\top \beta$  (bias  $\beta_0$  omitted for simplicity) and solve for sparsity using:

$$\hat{\beta} = \arg \min_{\beta} \frac{1}{2N} \|M_z^\top \beta - y\|_2^2 + \lambda_1 \|\beta\|_1 + \lambda_2 \|\beta\|_2^2. \quad (1)$$

The resulting understanding starts from the set of learned weights with the highest non-zero coefficients  $\beta_{\text{top}} = \{\beta_{(1)}, \beta_{(2)}, \dots\}$  and corresponding ranked features  $z_{\text{top}} = \{z_{(1)}, z_{(2)}, \dots\}$ .  $\beta_{\text{top}}$  tells the user how features  $z_{\text{top}}$  are composed to make a prediction, and  $z_{\text{top}}$  can then be visualized with respect to unimodal and cross-modal interactions using the representation stage (Section 2.3).

---

**Algorithm 1** Visualizing and understanding multimodal models using MULTIVIZ.

---

**Given:** Dataset  $\mathcal{D} = \{(\mathbf{x}_1, \mathbf{x}_2, y)_{i=1}^n\} = \{(x_1^{(1)}, \dots, x_2^{(1)}, \dots, y)_{i=1}^n\}$  and trained model  $f_\theta$ .  
**Given:** Unimodal and cross-modal visualization subroutines  $\text{UNI}(f_\theta, y, \mathbf{x})$ ,  $\text{CM}(f_\theta, y, \mathbf{x}_1, \mathbf{x}_2)$ .  
 Obtain deep features  $M_z = f_\theta(\mathbf{x}_1, \mathbf{x}_2)$  for datapoint of interest.  
 Fit sparse linear model:  $f_{\theta, \text{sparse}} = M_z^\top \hat{\beta}$  by solving equation (2).  
 Obtain predictions  $\hat{y} = f_{\theta, \text{sparse}}(\mathbf{x}_1, \mathbf{x}_2)$  and ranked features  $z_{\text{top}}$  with largest coefficients.  
 Visualize overall unimodal importance wrt  $\hat{y}$ :  $U_1 = \text{UNI}(f_\theta, \hat{y}, \mathbf{x}_1)$ ,  $U_2 = \text{UNI}(f_\theta, \hat{y}, \mathbf{x}_2)$ .  
 Visualize overall cross-modal interactions wrt  $\hat{y}$ :  $C = \text{CM}(f_\theta, \hat{y}, \mathbf{x}_1, \mathbf{x}_2)$ ,  $\text{CM}(f_\theta, \hat{y}, \mathbf{x}_2, \mathbf{x}_1)$ .  
**for** each top feature  $z$  in  $z_{\text{top}}$  **do**  
 # local analysis for original datapoint  
 Visualize unimodal and cross-modal interactions of original datapoint wrt  $z$ .  
 # global analysis across similar datapoints  
 Obtain top  $k$  datapoints that also maximally activate  $z$ .  
**for** each new top  $k$  datapoint  $(\mathbf{x}_1, \mathbf{x}_2, y)$  **do**  
 Visualize unimodal and cross-modal interactions of new datapoint wrt  $z$ .

---

Table 1: MULTIVIZ enables fine-grained analysis across 6 datasets spanning 3 research areas, 6 input modalities ( $\ell$ : language,  $i$ : image,  $v$ : video,  $a$ : audio,  $t$ : time-series,  $ta$ : tabular), and 8 models.

Area	Dataset	Model	Modalities	# Samples	Prediction task
Fusion	CMU-MOSEI [115]	MULT [98]	$\{\ell, v, a\} \rightarrow y$	22,777	sentiment, emotions
	MM-IMDB [7]	LRTF [66]	$\{\ell, i\} \rightarrow y$	25,959	movie genre classification
	MIMIC [43]	LF [10]	$\{t, ta\} \rightarrow y$	36,212	mortality, ICD-9 codes
Retrieval	FLICKR-30K [80]	ViLT [49]	$\ell \leftrightarrow i$	158,000	image-caption retrieval
	FLICKR-30K [80]	CLIP [84]	$\ell \leftrightarrow i$	158,000	image-caption retrieval
QA	CLEVR [44]	CNN-LSTM-SA [44]	$\{i, \ell\} \rightarrow y$	853,554	QA
	CLEVR [44]	MDETR [45]	$\{i, \ell\} \rightarrow y$	853,554	QA
	VQA 2.0 [33]	LXMERT [97]	$\{i, \ell\} \rightarrow y$	1,100,000	QA

## 2.5 Putting everything together

We summarize these proposed approaches for understanding each step of the multimodal process and show the overall pipeline in Algorithm 1 and Figure 1. To enable human studies, MULTIVIZ provides an interactive API where users can choose multimodal datasets and models and be presented with a set of visualizations at each stage (see Appendix D).

## 3 Experiments

Our experiments are designed to verify the usefulness and complementarity of the 4 MULTIVIZ stages. We start with a model simulation experiment to test the utility of each stage towards overall model understanding (Section 3.1). We then dive deeper into the individual stages by testing how well MULTIVIZ enables representation interpretation (Section 3.2) and error analysis (Section 3.3), before presenting a case study of model debugging from error analysis insights (Section 3.4). We showcase the following selected experiments and defer results on other datasets to Appendix F.

**Setup:** We use a large suite of datasets from MultiBench [63] which spans real-world fusion, retrieval, and QA tasks. For each dataset, we test a corresponding state-of-the-art model spanning MULT [98], LRTF [66], LF [10], ViLT [49], CLIP [84], CNN-LSTM-SA [44], MDETR [45], and LXMERT [97]. These cover models both pretrained and trained from scratch. We summarize all 6 datasets and 8 models tested in Table 1 and provide implementation details in Appendix E.

### 3.1 Model simulation

We first design a model simulation experiment to determine if MULTIVIZ helps users of multimodal models gain a deeper understanding of model behavior. If MULTIVIZ indeed generates human-understandable explanations, humans should be able to accurately simulate model predictions given these explanations only, as measured by correctness with respect to actual model predictions and annotator agreement (Krippendorff's alpha [51]). To investigate the utility of each stage in MULTIVIZ, we design a human study to see what 15 humans (3 for each local ablation setting) predict:

- (1) **U:** Users are only shown the unimodal importance (U) of each modality towards label  $y$ .

Table 2: **Model simulation**: human annotators who have access to all stages visualized in MULTIVIZ are able to accurately and consistently simulate model predictions (regardless of whether the model made the correct prediction), representing a step towards model understanding.

Research area Dataset Model	QA		Fusion		Fusion	
	VQA 2.0 [33]		MM-IMDB [7]		CMU-MOSEI [115]	
	LXMERT [97]		LRTF [66]		MULT [98]	
Metric	Correctness	Agreement	Correctness	Agreement	Correctness	Agreement
U	55.0 $\pm$ 0.0	0.39	50.0 $\pm$ 13.2	0.34	71.7 $\pm$ 17.6	0.39
U + C	65.0 $\pm$ 5.0	0.50	53.7 $\pm$ 7.6	0.51	76.7 $\pm$ 10.4	0.45
U + C + R <sub>ℓ</sub>	61.7 $\pm$ 7.6	0.57	56.7 $\pm$ 7.6	0.59	78.3 $\pm$ 2.9	0.42
U + C + R <sub>ℓ</sub> + R <sub>g</sub>	71.7 $\pm$ 15.3	0.61	61.7 $\pm$ 7.6	0.43	100.0 $\pm$ 0.0	1.00
MULTIVIZ	<b>81.7 <math>\pm</math> 2.9</b>	<b>0.86</b>	<b>65.0 <math>\pm</math> 5.0</b>	<b>0.60</b>	<b>100.0 <math>\pm</math> 0.0</b>	<b>1.00</b>

Table 3: **Left**: Humans are able to consistently assign concepts to previously uninterpretable multimodal features using both local and global representation analysis. **Right**: Humans are also able to categorize model errors into one of 3 stages they occur in when given full MULTIVIZ visualizations.

Research area Dataset Model	QA		Research area Dataset Model	QA		QA		
	VQA 2.0 [33]			CLEVR [44]		VQA 2.0 [33]		
	LXMERT [97]			CNN-LSTM-SA [44]		LXMERT [97]		
Metric	Confidence	Agree.	Metric	Confidence	Agree.	Confidence	Agree.	
R <sub>ℓ</sub>	1.94 $\pm$ 0.42	0.21	No viz	2.72 $\pm$ 0.73	0.47	2.15 $\pm$ 0.70	0.24	
R <sub>ℓ</sub> + R <sub>g</sub> (no viz)	3.42 $\pm$ 0.55	0.54	MULTIVIZ	<b>4.26 <math>\pm</math> 0.35</b>	<b>0.87</b>	<b>3.85 <math>\pm</math> 0.50</b>	<b>0.79</b>	
R <sub>ℓ</sub> + R <sub>g</sub>	<b>4.58 <math>\pm</math> 0.41</b>	<b>0.60</b>						

- (2) **U + C**: Users are also shown cross-modal interactions (C) highlighted towards label  $y$ .
- (3) **U + C + R<sub>ℓ</sub>**: Users are also shown local analysis (R<sub>ℓ</sub>) of unimodal and cross-modal interactions of top features  $z_{\text{top}} = \{z_{(1)}, z_{(2)}, \dots\}$  maximally activating label  $y$ .
- (4) **U + C + R<sub>ℓ</sub> + R<sub>g</sub>**: Users are additionally shown global analysis (R<sub>g</sub>) through similar datapoints that also maximally activate top features  $z_{\text{top}}$  for label  $y$ .
- (5) **MULTIVIZ (U + C + R<sub>ℓ</sub> + R<sub>g</sub> + P)**: The entire MULTIVIZ method by further including visualizations of the final prediction (P) stage: sorting top ranked feature neurons  $z_{\text{top}} = \{z_{(1)}, z_{(2)}, \dots\}$  with respect to their coefficients  $\beta_{\text{top}} = \{\beta_{(1)}, \beta_{(2)}, \dots\}$  and showing these coefficients to the user.

We show these results in Table 2 and find that having access to all stages visualized in MULTIVIZ leads to significantly highest accuracy of model simulation on VQA 2.0 with consistent agreement with other annotators. On fusion tasks with MM-IMDB and CMU-MOSEI, we also find that including each visualization stage consistently leads to higher correctness and agreement in human simulation, despite the fact that fusion models may not require cross-modal interactions to solve the task [37]. More importantly, humans are able to simulate model predictions regardless of whether the model made the correct prediction or not. Moreover, the annotators who were given full MULTIVIZ interpretations reported that they found local and global representation analysis particularly useful: global analysis with other datapoints that also maximally activate feature representations were important for identifying similar concepts and assigning them to multimodal features. We also include additional simulation experiments on other datasets in Appendix F.1.

### 3.2 Representation interpretation

We now take a deeper look to check that MULTIVIZ generates accurate explanations of multimodal representations. Using local and global representation visualizations, can humans consistently assign interpretable concepts in natural language to previously uninterpretable features? We study this question by tasking 9 human annotators (3 for each setting) to assign concepts to each feature  $z$  when given access to visualizations of (1) R<sub>ℓ</sub> (local analysis of unimodal and cross-modal interactions in  $z$ ), (2) R<sub>ℓ</sub> + R<sub>g</sub> (no viz) (including global analysis through similar datapoints that also maximally activate feature  $z$ ), and (3) R<sub>ℓ</sub> + R<sub>g</sub> (adding highlighted unimodal and cross-modal interactions of global datapoints). Since there are no ground-truth labels for feature concepts, we rely on annotator confidence (1-5 scale) and annotator agreement [51] as a proxy for accuracy. From Table 3 (left), we find that having access to both local and global visualizations are crucial towards interpreting multimodal features. We show examples of human-assigned concepts in Figure 4 (more in

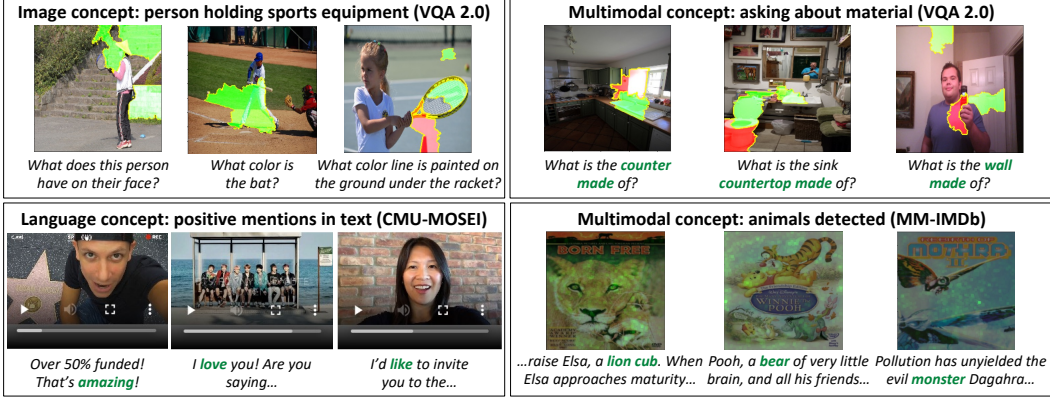


Figure 4: Examples of human-annotated **concepts** using MULTIVIZ on feature representations. We find that the features separately capture image-only, language-only, and multimodal concepts.

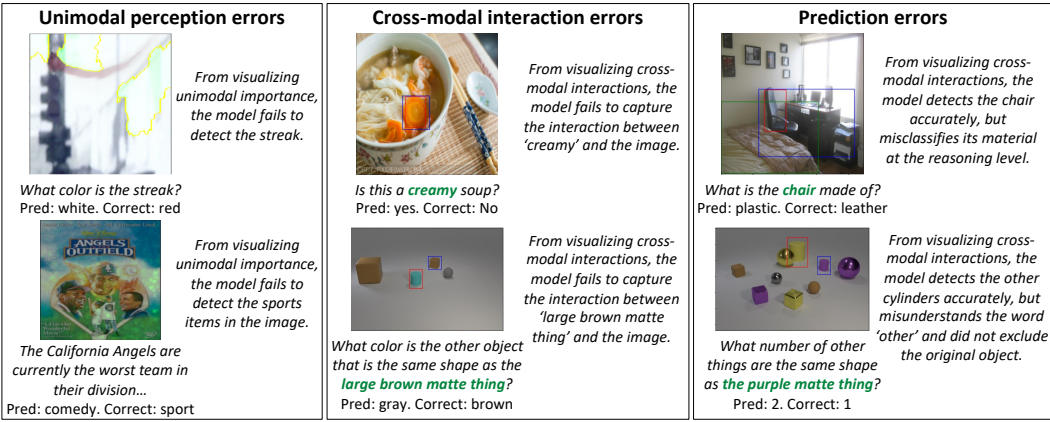


Figure 5: Examples of human-annotated **error analysis** using MULTIVIZ on multimodal models. Using all stages provided in MULTIVIZ enables fine-grained classification of model errors (e.g., errors in unimodal processing, cross-modal interactions, and predictions) for targeted debugging.

Appendix F.3). It is interesting to note that the features separately capture image-only, language-only, and multimodal concepts.

### 3.3 Error analysis

We further examine a case study of error analysis on trained models. We task 3 human users to use MULTIVIZ and highlight the errors that a multimodal model exhibits by categorizing these errors into one of 3 specific stages that they occur in: failures in (1) unimodal perception, (2) capturing cross-modal interaction, and (3) prediction with perceived unimodal and cross-modal information. Again, we rely on annotator confidence (1-5 scale) and agreement [51] due to lack of ground-truth error categorization, and compare with **No viz**, a baseline that does not provide any model visualizations to the user. From Table 3 (right), we find that MULTIVIZ enables humans to consistently categorize model errors into one of 3 stages. We show examples that human annotators classified into unimodal perception, cross-modal interaction, and prediction errors in Figure 5 (more in Appendix F.4).

### 3.4 A case study in model debugging

Following error analysis, we take a deeper investigation into one of the errors on a pretrained LXMERT [97] model fine-tuned on VQA 2.0 [33]. Specifically, we first found the top 5 penultimate-layer neurons that are most activated on erroneous datapoints. Inspecting these neurons carefully through MULTIVIZ local and global representation analysis, human annotators found that 2 of the 5 neurons were consistently related to questions asking about color, which highlighted the model’s failure to identify color correctly (especially **blue**). The model has an accuracy of only 5.5% amongst all **blue**-related points (i.e., either have **blue** as correct answer or predicted answer), and these failures account for 8.8% of all model errors. We show examples of such datapoints and their MULTIVIZ

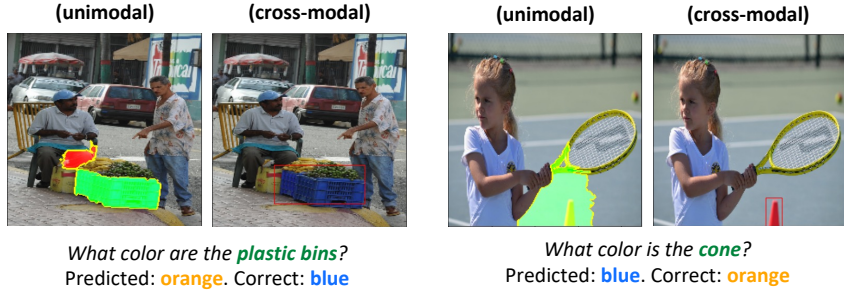


Figure 6: A case study on **model debugging**: we task 3 human users to use MULTIVIZ visualizations and highlight the errors that a pretrained LXMERT [97] model fine-tuned on VQA 2.0 [33] exhibits, and find 2 penultimate-layer neurons highlighting the model’s failure to identify color (especially **blue**). Targeted localization of the error to this specific stage (prediction) and representation concept (**blue**) via MULTIVIZ enabled us to identify a bug in the popular Hugging Face LXMERT repository.

visualizations in Figure 6. Observe that the model is often able to capture unimodal and cross-modal interactions perfectly, but fails to identify color at the prediction stage.

Curious as to the source of this highly-specific error, we looked deeper into the source code for the entire pipeline of LXMERT, including that of its image encoder, Faster R-CNN [85]<sup>1</sup>. We in fact uncovered a bug in data preprocessing for Faster R-CNN in the popular Hugging Face repository that swapped the image data storage format from RGB to BGR formats responsible for these errors. This presents a concrete use case of MULTIVIZ: through visualizing each stage, we were able to (1) isolate the source of the bug (at prediction and not unimodal perception or cross-modal interactions), and (2) use representation analysis to localize the bug to the specific color concept.

In Appendix F.5, we further detail our initial attempt at tackling this error by using MULTIVIZ analysis to select additional targeted datapoints in an active learning scenario, which proved to be much more effective (higher improvement with fewer data) as compared to baselines that add data randomly or via uncertainty sampling [55, 56, 89], which may be of independent interest.

## 4 Related Work

Interpretable machine learning as a research field aims to further our understanding of AI models, empower stakeholders to build trust in AI models, perform model debugging, and use these insights for joint decision-making between humans and AI [11, 17, 30]. We categorize related work into:

**Unimodal importance:** Recent work in interpretable multimodal learning can be categorized into two sections: (1) constructing interpretable multimodal models via careful model design [77, 99, 115] or (2) performing post-hoc explanations of black-box multimodal models [15, 32]. In the former, several approaches have individually focused on building interpretable components for unimodal importance through soft [77] and hard attention mechanisms [16]. When aiming to explain black-box multimodal models, related work rely primarily on gradient-based visualizations (Guided backpropagation [32] or Grad-CAM [15, 88]) to highlight regions of the image which the model attends to.

**Cross-modal interactions:** Approaches have parametrized cross-modal interactions using data structures such as graphs [61, 115] or routing networks [99], which enables easier interpretation as compared to fully dense alternatives such as multiplicative [42] or tensor-based [62, 66, 112] parameterizations. To better understand cross-modal interactions in more general multimodal models, recent work investigates the activation patterns of pretrained language and vision transformer models [13, 58], performs diagnostic experiments through specially curated inputs [26, 76], or trains auxiliary explanation modules [47, 77]. Particularly related to our work is EMAP [37] for disentangling the effects of unimodal (additive) contributions from cross-modal interactions in multimodal tasks, as well as M2Lens [104], an interactive visual analytics system to visualize multimodal models for sentiment analysis through both unimodal and cross-modal contributions.

**Multimodal representation and prediction:** Existing approaches have used language syntax as a guide for compositionality into higher-level abstract features useful for prediction. For example, neuro-symbolic approaches [4, 102] or neural module networks [6] compose modules based on

<sup>1</sup>we used the popular Hugging Face implementation at <https://huggingface.co/unc-nlp/lxmert-vqa-uncased>

the syntax of language (i.e., the question in VQA). Similarly, logical reasoning has motivated the integration of logical statements with neural networks [31, 96]. While these approaches provide reliable interpretations by virtue of model design, they are typically restricted to a certain set of modalities or tasks. We propose a more general approach that (1) is able to visualize arbitrary multimodal models, and (2) does not assume anything about the modality or task.

**Dataset and model biases:** One core motivation for interpretable ML is to better understand the model’s decision-making process. These tools have uncovered several biases in models and datasets (e.g., unimodal biases in the language modality of VQA tasks [2, 5, 12, 40, 33]). Similar visualizations also led to improvements in image captioning by relying less on gender biases and spurious correlations [35]. Inspired by these insights, we believe that MULTIVIZ will enable the identification of dataset and model biases across a wider range of modalities and tasks.

## 5 Limitations and Broader Impact

Multimodal data and models are ubiquitous in a range of real-world applications. MULTIVIZ is our attempt at a standardized and modular framework for visualizing these multimodal models. While we believe these tools will eventually help stakeholders gain a deeper understanding of multimodal models as a step towards reliable real-world deployment, we believe that special care must be taken in the following regard to ensure that these interpretation tools are reliably deployed:

**Reliability of visualizations:** There has been recent work examining the reliability of model interpretability methods for real-world practitioners [82, 94]. Lipton [65] examines the motivations underlying interest in interpretability, finding them to be diverse and occasionally discordant. Krishna et al. [53] find that state-of-the-art explanation methods may disagree in terms of the explanations they output. Chandrasekaran et al. [15] further conclude that existing explanations on VQA model do not actually make its responses and failures more predictable to a human. We refer the reader to Chen et al. [17] for a critique on the disconnect between technical objectives targeted by interpretable ML research and the high-level goals stated as consumers’ use cases, as well as Bhatt et al. [11] for an analysis of how interpretable and explainable ML tools can be used in real-world deployment. Human-in-the-loop interpretation and evaluation could be a promising direction towards connecting technical solutions with real-world stakeholders, while also offering users an interactive medium to incorporate feedback in multimodal models.

**Evaluating interpretability:** Progress towards interpretability is challenging to evaluate [14, 20, 41, 90, 94]. Model interpretability (1) is highly subjective across different population subgroups [8, 53], (2) requires high-dimensional model outputs as opposed to low-dimensional prediction objectives [77], and (3) has desiderata that change across research fields, populations, and time [74]. We plan to continuously expand MULTIVIZ through community inputs for new interpretation methods in each stage and metrics to evaluate interpretability methods (see Appendix G for details).

## 6 Conclusion

This paper proposes MULTIVIZ, a comprehensive benchmark for analyzing and visualizing multimodal models. MULTIVIZ scaffolds the interpretation problem into 4 modular stages of unimodal importance, cross-modal interactions, multimodal representations, and multimodal prediction, before providing existing and newly proposed analysis tools in each stage. MULTIVIZ is designed to be *modular* (encompassing existing analysis tools and encouraging research towards understudied stages), *general* (supporting diverse modalities, models, and tasks), and *human-in-the-loop* (providing a visualization tool for human model interpretation, error analysis, and debugging), qualities which we strive to upkeep by ensuring its public access and regular updates from community feedback.

## Acknowledgements

This material is based upon work partially supported by the National Science Foundation (Awards #1722822 and #1750439) and National Institutes of Health (Awards #R01MH125740, #R01MH096951, and #U01MH116925). PPL is partially supported by a Facebook PhD Fellowship and a Carnegie Mellon University’s Center for Machine Learning and Health Fellowship. RS is partially supported by NSF IIS1763562 and ONR Grant N000141812861. Any opinions, findings, conclusions, or recommendations expressed in this material are those of the author(s) and do not necessarily reflect the views of the National Science Foundation, National Institutes of Health, Facebook, Carnegie Mellon University’s Center for Machine Learning and Health, or Office of Naval Research, and no official endorsement should be inferred. Finally, we would also like to acknowledge NVIDIA’s GPU support.

## References

- [1] Estelle Aflalo, Meng Du, Shao-Yen Tseng, Yongfei Liu, Chenfei Wu, Nan Duan, and Vasudev Lal. VI-interpret: An interactive visualization tool for interpreting vision-language transformers. In *Proceedings of the IEEE/CVF Conference on Computer Vision and Pattern Recognition*, pages 21406–21415, 2022. [64](#)
- [2] Aishwarya Agrawal, Dhruv Batra, and Devi Parikh. Analyzing the behavior of visual question answering models. In *Proceedings of the 2016 Conference on Empirical Methods in Natural Language Processing*, pages 1955–1960, 2016. [9](#)
- [3] Aishwarya Agrawal, Jiasen Lu, Stanislaw Antol, Margaret Mitchell, C. Lawrence Zitnick, Devi Parikh, and Dhruv Batra. VQA: Visual question answering. *International Journal of Computer Vision*, 2017. [34](#)
- [4] Saeed Amizadeh, Hamid Palangi, Alex Polozov, Yichen Huang, and Kazuhito Koishida. Neuro-symbolic visual reasoning: Disentangling. In *International Conference on Machine Learning*, pages 279–290. PMLR, 2020. [8, 64](#)
- [5] Ankesh Anand, Eugene Belilovsky, Kyle Kastner, Hugo Larochelle, and Aaron Courville. Blindfold baselines for embodied qa. *arXiv preprint arXiv:1811.05013*, 2018. [9](#)
- [6] Jacob Andreas, Marcus Rohrbach, Trevor Darrell, and Dan Klein. Neural module networks. In *Proceedings of the IEEE conference on computer vision and pattern recognition*, pages 39–48, 2016. [8, 65](#)
- [7] John Arevalo, Thamar Solorio, Manuel Montes-y Gómez, and Fabio A González. Gated multimodal units for information fusion. In *5th International conference on learning representations 2017 workshop*, 2017. [2, 5, 6, 32](#)
- [8] Siddhant Arora, Danish Pruthi, Norman Sadeh, William W Cohen, Zachary C Lipton, and Graham Neubig. Explain, edit, and understand: Rethinking user study design for evaluating model explanations. *arXiv preprint arXiv:2112.09669*, 2021. [9, 19, 20, 65](#)
- [9] Tadas Baltrušaitis, Peter Robinson, and Louis-Philippe Morency. Openface: an open source facial behavior analysis toolkit. In *2016 IEEE Winter Conference on Applications of Computer Vision (WACV)*, pages 1–10. IEEE, 2016.
- [10] Tadas Baltrušaitis, Chaitanya Ahuja, and Louis-Philippe Morency. Multimodal machine learning: A survey and taxonomy. *IEEE transactions on pattern analysis and machine intelligence*, 41(2):423–443, 2018. [5, 35](#)
- [11] Umang Bhatt, Alice Xiang, Shubham Sharma, Adrian Weller, Ankur Taly, Yunhan Jia, Joydeep Ghosh, Ruchir Puri, José MF Moura, and Peter Eckersley. Explainable machine learning in deployment. In *Proceedings of the 2020 Conference on Fairness, Accountability, and Transparency*, pages 648–657, 2020. [8, 9, 19, 20, 65](#)
- [12] Remi Cadene, Corentin Dancette, Matthieu Cord, Devi Parikh, et al. Rubi: Reducing unimodal biases for visual question answering. *Advances in Neural Information Processing Systems*, 32:841–852, 2019. [9](#)
- [13] Jize Cao, Zhe Gan, Yu Cheng, Licheng Yu, Yen-Chun Chen, and Jingjing Liu. Behind the scene: Revealing the secrets of pre-trained vision-and-language models. In *European Conference on Computer Vision*, pages 565–580. Springer, 2020. [8](#)
- [14] Chun Sik Chan, Huanqi Kong, and Liang Guanqing. A comparative study of faithfulness metrics for model interpretability methods. In *Proceedings of the 60th Annual Meeting of the Association for Computational Linguistics (Volume 1: Long Papers)*, pages 5029–5038, 2022. [9, 19, 20, 65](#)
- [15] Arjun Chandrasekaran, Viraj Prabhu, Deshraj Yadav, Prithvijit Chattopadhyay, and Devi Parikh. Do explanations make vqa models more predictable to a human? In *EMNLP*, 2018. [1, 3, 8, 9, 19, 20, 21](#)
- [16] Minghai Chen, Sen Wang, Paul Pu Liang, Tadas Baltrušaitis, Amir Zadeh, and Louis-Philippe Morency. Multimodal sentiment analysis with word-level fusion and reinforcement learning. In *Proceedings of the 19th ACM International Conference on Multimodal Interaction*, pages 163–171, 2017. [8, 64](#)
- [17] Valerie Chen, Jeffrey Li, Joon Sik Kim, Gregory Plumb, and Ameet Talwalkar. Interpretable machine learning: Moving from mythos to diagnostics. *Queue*, 19(6):28–56, 2022. [1, 8, 9, 19, 20, 65](#)
- [18] Donald G Childers and CK Lee. Vocal quality factors: Analysis, synthesis, and perception. *the Journal of the Acoustical Society of America*, 90(5):2394–2410, 1991.

[19] Abhishek Das, Samyak Datta, Georgia Gkioxari, Stefan Lee, Devi Parikh, and Dhruv Batra. Embodied question answering. In *Proceedings of the IEEE Conference on Computer Vision and Pattern Recognition*, pages 1–10, 2018. 34

[20] Sanjoy Dasgupta, Nave Frost, and Michal Moshkovitz. Framework for evaluating faithfulness of local explanations. *arXiv preprint arXiv:2202.00734*, 2022. 9, 19, 20, 65

[21] Gilles Degottex, John Kane, Thomas Drugman, Tuomo Raitio, and Stefan Scherer. Covarep—a collaborative voice analysis repository for speech technologies. In *Acoustics, Speech and Signal Processing (ICASSP), 2014 IEEE International Conference on*, pages 960–964. IEEE, 2014.

[22] Daisy Yi Ding and Robert Tibshirani. Cooperative learning for multi-view analysis. *arXiv preprint arXiv:2112.12337*, 2021. 3

[23] Thomas Drugman and Abeer Alwan. Joint robust voicing detection and pitch estimation based on residual harmonics. In *Interspeech*, pages 1973–1976, 2011.

[24] Stéphane Dupont and Juergen Luettin. Audio-visual speech modeling for continuous speech recognition. *IEEE transactions on multimedia*, 2(3):141–151, 2000. 32

[25] Paul Ekman. Universal facial expressions of emotion.

[26] Stella Frank, Emanuele Bugliarello, and Desmond Elliott. Vision-and-language or vision-for-language? on cross-modal influence in multimodal transformers. In *Proceedings of the 2021 Conference on Empirical Methods in Natural Language Processing*, pages 9847–9857, 2021. 8

[27] Christos A Frantzidis, Charalampos Bratsas, Manousos A Klados, Evdokimos Konstantinidis, Chrysa D Lithari, Ana B Vivas, Christos L Papadelis, Eleni Kaldoudi, Costas Pappas, and Panagiotis D Bamidis. On the classification of emotional biosignals evoked while viewing affective pictures: an integrated data-mining-based approach for healthcare applications. *IEEE Transactions on Information Technology in Biomedicine*, 14(2):309–318, 2010. 1

[28] Jerome H Friedman and Bogdan E Popescu. Predictive learning via rule ensembles. *The annals of applied statistics*, 2(3):916–954, 2008. 3, 21

[29] Timnit Gebru, Jamie Morgenstern, Briana Vecchione, Jennifer Wortman Vaughan, Hanna Wallach, Hal Daumé III, and Kate Crawford. Datasheets for datasets. *arXiv preprint arXiv:1803.09010*, 2018. 34

[30] Leilani H Gilpin, David Bau, Ben Z Yuan, Ayesha Bajwa, Michael Specter, and Lalana Kagal. Explaining explanations: An overview of interpretability of machine learning. In *2018 IEEE 5th International Conference on data science and advanced analytics (DSAA)*, pages 80–89. IEEE, 2018. 8

[31] Tejas Gokhale, Pratyay Banerjee, Chitta Baral, and Yezhou Yang. Vqa-lol: Visual question answering under the lens of logic. In *European conference on computer vision*, pages 379–396. Springer, 2020. 9

[32] Yash Goyal, Akrit Mohapatra, Devi Parikh, and Dhruv Batra. Towards transparent ai systems: Interpreting visual question answering models. *arXiv preprint arXiv:1608.08974*, 2016. 1, 3, 4, 8, 21

[33] Yash Goyal, Tejas Khot, Douglas Summers-Stay, Dhruv Batra, and Devi Parikh. Making the v in vqa matter: Elevating the role of image understanding in visual question answering. In *Proceedings of the IEEE Conference on Computer Vision and Pattern Recognition*, pages 6904–6913, 2017. 2, 5, 6, 7, 8, 9, 34, 61, 62

[34] Xiaochuang Han, Byron C Wallace, and Yulia Tsvetkov. Explaining black box predictions and unveiling data artifacts through influence functions. In *Proceedings of the 58th Annual Meeting of the Association for Computational Linguistics*, pages 5553–5563, 2020. 3, 21

[35] Lisa Anne Hendricks, Kaylee Burns, Kate Saenko, Trevor Darrell, and Anna Rohrbach. Women also snowboard: Overcoming bias in captioning models. In *Proceedings of the European Conference on Computer Vision (ECCV)*, pages 771–787, 2018. 1, 9

[36] Lisa Anne Hendricks, John Mellor, Rosalia Schneider, Jean-Baptiste Alayrac, and Aida Nematzadeh. Decoupling the role of data, attention, and losses in multimodal transformers. *Transactions of the Association for Computational Linguistics*, 9:570–585, 2021. 1, 2

[37] Jack Hessel and Lillian Lee. Does my multimodal model learn cross-modal interactions? it’s harder to tell than you might think! In *Proceedings of the 2020 Conference on Empirical Methods in Natural Language Processing (EMNLP)*, pages 861–877, 2020. 2, 3, 6, 8, 20, 21

[38] Ronghang Hu and Amanpreet Singh. Transformer is all you need: Multimodal multitask learning with a unified transformer. *arXiv preprint arXiv:2102.10772*, 2021. 64

[39] iMotions. Facial expression analysis, 2017. URL [goo.gl/1rh1JN](http://goo.gl/1rh1JN).

[40] Allan Jabri, Armand Joulin, and Laurens van der Maaten. Revisiting visual question answering baselines. In *European conference on computer vision*, pages 727–739. Springer, 2016. 1, 9

[41] Alon Jacovi and Yoav Goldberg. Towards faithfully interpretable nlp systems: How should we define and evaluate faithfulness? In *Proceedings of the 58th Annual Meeting of the Association for Computational Linguistics*, pages 4198–4205, 2020. 9, 19, 20, 65

[42] Siddhant M Jayakumar, Wojciech M Czarnecki, Jacob Menick, Jonathan Schwarz, Jack Rae, Simon Osindero, Yee Whye Teh, Tim Harley, and Razvan Pascanu. Multiplicative interactions and where to find them. In *International Conference on Learning Representations*, 2020. 3, 8

[43] Alistair EW Johnson, Tom J Pollard, Lu Shen, H Lehman Li-Wei, Mengling Feng, Mohammad Ghassemi, Benjamin Moody, Peter Szolovits, Leo Anthony Celi, and Roger G Mark. Mimic-iii, a freely accessible critical care database. *Scientific data*, 3(1):1–9, 2016. 2, 5, 33, 37, 39, 42

[44] Justin Johnson, Bharath Hariharan, Laurens Van Der Maaten, Li Fei-Fei, C Lawrence Zitnick, and Ross Girshick. Clevr: A diagnostic dataset for compositional language and elementary visual reasoning. In *Proceedings of the IEEE conference on computer vision and pattern recognition*, pages 2901–2910, 2017. 2, 5, 6, 34, 36, 53

[45] Aishwarya Kamath, Mannat Singh, Yann LeCun, Ishan Misra, Gabriel Synnaeve, and Nicolas Carion. Mdetr-modulated detection for end-to-end multi-modal understanding. *arXiv preprint arXiv:2104.12763*, 2021. 5, 36, 53

[46] John Kane and Christer Gobl. Wavelet maxima dispersion for breathy to tense voice discrimination. *IEEE Transactions on Audio, Speech, and Language Processing*, 21(6):1170–1179, 2013.

[47] Atsushi Kanehira, Kentaro Takemoto, Sho Inayoshi, and Tatsuya Harada. Multimodal explanations by predicting counterfactuality in videos. In *Proceedings of the IEEE/CVF Conference on Computer Vision and Pattern Recognition*, pages 8594–8602, 2019. 8

[48] Douwe Kiela, Suvrat Bhooshan, Hamed Firooz, Ethan Perez, and Davide Testuggine. Supervised multimodal bitransformers for classifying images and text. *arXiv preprint arXiv:1909.02950*, 2019. 32

[49] Wonjae Kim, Bokyung Son, and Ildoo Kim. Vilt: Vision-and-language transformer without convolution or region supervision. In *International Conference on Machine Learning*, pages 5583–5594. PMLR, 2021. 5, 35, 53

[50] Elsa A Kirchner, Stephen H Fairclough, and Frank Kirchner. Embedded multimodal interfaces in robotics: applications, future trends, and societal implications. In *The Handbook of Multimodal-Multisensor Interfaces: Language Processing, Software, Commercialization, and Emerging Directions-Volume 3*, pages 523–576. 2019. 1

[51] Klaus Krippendorff. Computing krippendorff's alpha-reliability. 2011. 5, 6, 7

[52] Ranjay Krishna, Yuke Zhu, Oliver Groth, Justin Johnson, Kenji Hata, Joshua Kravitz, Stephanie Chen, Yannis Kalantidis, Li-Jia Li, David A Shamma, et al. Visual genome: Connecting language and vision using crowdsourced dense image annotations. *International journal of computer vision*, 123(1):32–73, 2017. 64

[53] Satyapriya Krishna, Tessa Han, Alex Gu, Javin Pombra, Shahin Jabbari, Steven Wu, and Himabindu Lakkaraju. The disagreement problem in explainable machine learning: A practitioner's perspective. *arXiv preprint arXiv:2202.01602*, 2022. 9, 19, 20, 65

[54] Michelle A Lee, Yuke Zhu, Krishnan Srinivasan, Parth Shah, Silvio Savarese, Li Fei-Fei, Animesh Garg, and Jeannette Bohg. Making sense of vision and touch: Self-supervised learning of multimodal representations for contact-rich tasks. In *2019 International Conference on Robotics and Automation (ICRA)*, pages 8943–8950. IEEE, 2019. 1

[55] David D Lewis and Jason Catlett. Heterogeneous uncertainty sampling for supervised learning. In *Machine learning proceedings 1994*, pages 148–156. Elsevier, 1994. 8, 61, 62

[56] David D Lewis and William A Gale. A sequential algorithm for training text classifiers. In *SIGIR'94*, pages 3–12. Springer, 1994. 8, 61, 62

[57] Liunian Harold Li, Mark Yatskar, Da Yin, Cho-Jui Hsieh, and Kai-Wei Chang. Visualbert: A simple and performant baseline for vision and language. *arXiv preprint arXiv:1908.03557*, 2019. [1](#), [2](#)

[58] Liunian Harold Li, Mark Yatskar, Da Yin, Cho-Jui Hsieh, and Kai-Wei Chang. What does bert with vision look at? In *Proceedings of the 58th Annual Meeting of the Association for Computational Linguistics*, pages 5265–5275, 2020. [8](#)

[59] Paul Liang. Awesome multimodal ml. <https://github.com/pliang279/awesome-multimodal-ml>, 2020. [40](#)

[60] Paul Pu Liang, Ziyin Liu, AmirAli Bagher Zadeh, and Louis-Philippe Morency. Multimodal language analysis with recurrent multistage fusion. In *EMNLP*, 2018. [1](#), [32](#)

[61] Paul Pu Liang, Ruslan Salakhutdinov, and Louis-Philippe Morency. Computational modeling of human multimodal language: The mosei dataset and interpretable dynamic fusion. 2018. [8](#), [32](#), [64](#)

[62] Paul Pu Liang, Zhun Liu, Yao-Hung Hubert Tsai, Qibin Zhao, Ruslan Salakhutdinov, and Louis-Philippe Morency. Learning representations from imperfect time series data via tensor rank regularization. In *ACL*, 2019. [1](#), [8](#)

[63] Paul Pu Liang, Yiwei Lyu, Xiang Fan, Zetian Wu, Yun Cheng, Jason Wu, Leslie Chen, Peter Wu, Michelle A Lee, Yuke Zhu, Ruslan Salakhutdinov, and Louis-Philippe Morency. Multibench: Multiscale benchmarks for multimodal representation learning. *NeurIPS Datasets and Benchmarks Track*, 2021. [5](#), [32](#), [46](#), [49](#), [64](#)

[64] Paul Pu Liang, Peter Wu, Liu Ziyin, Louis-Philippe Morency, and Ruslan Salakhutdinov. Cross-modal generalization: Learning in low resource modalities via meta-alignment. In *Proceedings of the 29th ACM International Conference on Multimedia*, pages 2680–2689, 2021. [33](#)

[65] Zachary C Lipton. The mythos of model interpretability: In machine learning, the concept of interpretability is both important and slippery. *Queue*, 16(3):31–57, 2018. [9](#), [19](#), [20](#)

[66] Zhun Liu, Ying Shen, Varun Bharadhwaj Lakshminarasi, Paul Pu Liang, AmirAli Bagher Zadeh, and Louis-Philippe Morency. Efficient low-rank multimodal fusion with modality-specific factors. In *Proceedings of the 56th Annual Meeting of the Association for Computational Linguistics (Volume 1: Long Papers)*, pages 2247–2256, 2018. [5](#), [6](#), [8](#), [35](#)

[67] Jiasen Lu, Dhruv Batra, Devi Parikh, and Stefan Lee. Vilbert: pretraining task-agnostic visiolinguistic representations for vision-and-language tasks. In *Proceedings of the 33rd International Conference on Neural Information Processing Systems*, pages 13–23, 2019. [1](#), [2](#), [64](#), [65](#)

[68] Jelena Luketina, Nantas Nardelli, Gregory Farquhar, Jakob N Foerster, Jacob Andreas, Edward Grefenstette, Shimon Whiteson, and Tim Rocktäschel. A survey of reinforcement learning informed by natural language. In *IJCAI*, 2019. [64](#)

[69] Yiwei Lyu, Paul Pu Liang, Zihao Deng, Ruslan Salakhutdinov, and Louis-Philippe Morency. Dime: Fine-grained interpretations of multimodal models via disentangled local explanations. *arXiv preprint arXiv:2203.02013*, 2022. [2](#), [3](#), [21](#)

[70] Andreas Madsen, Nicholas Meade, Vaibhav Adlakha, and Siva Reddy. Evaluating the faithfulness of importance measures in nlp by recursively masking allegedly important tokens and retraining. *arXiv preprint arXiv:2110.08412*, 2021. [20](#), [65](#)

[71] Jiayuan Mao, Chuang Gan, Pushmeet Kohli, Joshua B. Tenenbaum, and Jiajun Wu. The Neuro-Symbolic Concept Learner: Interpreting Scenes, Words, and Sentences From Natural Supervision. In *International Conference on Learning Representations*, 2019. URL <https://openreview.net/forum?id=rJgMlhRctm>. [64](#)

[72] Kenneth Marino, Ruslan Salakhutdinov, and Abhinav Gupta. The more you know: Using knowledge graphs for image classification. In *2017 IEEE Conference on Computer Vision and Pattern Recognition (CVPR)*, pages 20–28. IEEE, 2017. [64](#)

[73] Luke Merrick and Ankur Taly. The explanation game: Explaining machine learning models using shapley values. In *International Cross-Domain Conference for Machine Learning and Knowledge Extraction*, pages 17–38. Springer, 2020. [1](#), [3](#), [4](#), [21](#)

[74] W James Murdoch, Chandan Singh, Karl Kumbier, Reza Abbasi-Asl, and Bin Yu. Definitions, methods, and applications in interpretable machine learning. *Proceedings of the National Academy of Sciences*, 116(44):22071–22080, 2019. [9](#), [19](#), [20](#), [65](#)

[75] Milind Naphade, John R Smith, Jelena Tasic, Shih-Fu Chang, Winston Hsu, Lyndon Kennedy, Alexander Hauptmann, and Jon Curtis. Large-scale concept ontology for multimedia. *IEEE multimedia*, 13(3):86–91, 2006. 1

[76] Letitia Parcalabescu, Albert Gatt, Anette Frank, and Iacer Calixto. Seeing past words: Testing the cross-modal capabilities of pretrained v&l models on counting tasks. In *Proceedings of the 1st Workshop on Multimodal Semantic Representations (MMSR)*, pages 32–44, 2021. 8

[77] Dong Huk Park, Lisa Anne Hendricks, Zeynep Akata, Anna Rohrbach, Bernt Schiele, Trevor Darrell, and Marcus Rohrbach. Multimodal explanations: Justifying decisions and pointing to the evidence. In *Proceedings of the IEEE Conference on Computer Vision and Pattern Recognition*, pages 8779–8788, 2018. 1, 8, 9, 19, 20, 64, 65

[78] Jeffrey Pennington, Richard Socher, and Christopher D Manning. Glove: Global vectors for word representation. In *EMNLP*, volume 14, pages 1532–1543, 2014.

[79] Juan-Manuel Pérez-Rúa, Valentin Vielzeuf, Stéphane Pateux, Moez Baccouche, and Frédéric Jurie. Mfas: Multimodal fusion architecture search. In *Proceedings of the IEEE Conference on computer vision and pattern recognition*, pages 6966–6975, 2019. 32

[80] Bryan A Plummer, Liwei Wang, Chris M Cervantes, Juan C Caicedo, Julia Hockenmaier, and Svetlana Lazebnik. Flickr30k entities: Collecting region-to-phrase correspondences for richer image-to-sentence models. In *Proceedings of the IEEE international conference on computer vision*, pages 2641–2649, 2015. 2, 5, 33, 53

[81] Soujanya Poria, Erik Cambria, Rajiv Bajpai, and Amir Hussain. A review of affective computing: From unimodal analysis to multimodal fusion. *Information Fusion*, 2017. 1

[82] Danish Pruthi, Mansi Gupta, Bhuvan Dhingra, Graham Neubig, and Zachary C Lipton. Learning to deceive with attention-based explanations. In *Proceedings of the 58th Annual Meeting of the Association for Computational Linguistics*, pages 4782–4793, 2020. 9, 19, 20

[83] Sanjay Purushotham, Chuizheng Meng, Zhengping Che, and Yan Liu. Benchmarking deep learning models on large healthcare datasets. *Journal of Biomedical Informatics*, 83:112–134, 2018. ISSN 1532-0464. doi: <https://doi.org/10.1016/j.jbi.2018.04.007>. URL <https://www.sciencedirect.com/science/article/pii/S1532046418300716>. 33

[84] Alec Radford, Jong Wook Kim, Chris Hallacy, Aditya Ramesh, Gabriel Goh, Sandhini Agarwal, Girish Sastry, Amanda Askell, Pamela Mishkin, Jack Clark, et al. Learning transferable visual models from natural language supervision. In *International Conference on Machine Learning*, pages 8748–8763. PMLR, 2021. 5, 35

[85] Shaoqing Ren, Kaiming He, Ross Girshick, and Jian Sun. Faster r-cnn: Towards real-time object detection with region proposal networks. *Advances in neural information processing systems*, 28, 2015. 8

[86] Marco Tulio Ribeiro, Sameer Singh, and Carlos Guestrin. " why should i trust you?" explaining the predictions of any classifier. In *Proceedings of the 22nd ACM SIGKDD international conference on knowledge discovery and data mining*, pages 1135–1144, 2016. 1, 3, 4, 21

[87] Raquel Rodríguez-Pérez and Jürgen Bajorath. Interpretation of machine learning models using shapley values: application to compound potency and multi-target activity predictions. *Journal of computer-aided molecular design*, 34(10):1013–1026, 2020. 3, 21

[88] Ramprasaath R Selvaraju, Michael Cogswell, Abhishek Das, Ramakrishna Vedantam, Devi Parikh, and Dhruv Batra. Grad-cam: Visual explanations from deep networks via gradient-based localization. In *Proceedings of the IEEE international conference on computer vision*, pages 618–626, 2017. 3, 8, 21

[89] Burr Settles. Active learning literature survey. 2009. 8, 61, 62

[90] Harshay Shah, Prateek Jain, and Praneeth Netrapalli. Do input gradients highlight discriminative features? *Advances in Neural Information Processing Systems*, 34, 2021. 9, 19, 20, 65

[91] Karen Simonyan and Andrew Zisserman. Very deep convolutional networks for large-scale image recognition. In *International Conference on Learning Representations*, 2015.

[92] Richard Socher, Milind Ganjoo, Christopher D Manning, and Andrew Ng. Zero-shot learning through cross-modal transfer. In *Advances in Neural Information Processing Systems*, pages 935–943, 2013. 64

[93] Daria Sorokina, Rich Caruana, Mirek Riedewald, and Daniel Fink. Detecting statistical interactions with additive groves of trees. In *Proceedings of the 25th international conference on Machine learning*, pages 1000–1007, 2008. 3

[94] Suraj Srinivas and Francois Fleuret. Rethinking the role of gradient-based attribution methods for model interpretability. In *International Conference on Learning Representations*, 2020. 9, 19, 20, 65

[95] Mukund Sundararajan and Amir Najmi. The many shapley values for model explanation. In *International conference on machine learning*, pages 9269–9278. PMLR, 2020. 3, 21

[96] Riko Suzuki, Hitomi Yanaka, Masashi Yoshikawa, Koji Mineshima, and Daisuke Bekki. Multimodal logical inference system for visual-textual entailment. In *Proceedings of the 57th Annual Meeting of the Association for Computational Linguistics: Student Research Workshop*, pages 386–392, 2019. 9

[97] Hao Tan and Mohit Bansal. LXMERT: learning cross-modality encoder representations from transformers. *CoRR*, abs/1908.07490, 2019. URL <http://arxiv.org/abs/1908.07490>. 5, 6, 7, 8, 36, 61, 62

[98] Yao-Hung Hubert Tsai, Shaojie Bai, Paul Pu Liang, J Zico Kolter, Louis-Philippe Morency, and Ruslan Salakhutdinov. Multimodal transformer for unaligned multimodal language sequences. In *Proceedings of the 57th Annual Meeting of the Association for Computational Linguistics*, pages 6558–6569, 2019. 1, 2, 5, 6, 35

[99] Yao-Hung Hubert Tsai, Martin Ma, Muqiao Yang, Ruslan Salakhutdinov, and Louis-Philippe Morency. Multimodal routing: Improving local and global interpretability of multimodal language analysis. In *Proceedings of the 2020 Conference on Empirical Methods in Natural Language Processing (EMNLP)*, pages 1823–1833, 2020. 1, 8, 64

[100] Michael Tsang, Dehua Cheng, and Yan Liu. Detecting statistical interactions from neural network weights. In *International Conference on Learning Representations*, 2018. 3

[101] Michael Tsang, Dehua Cheng, Hanpeng Liu, Xue Feng, Eric Zhou, and Yan Liu. Feature interaction interpretability: A case for explaining ad-recommendation systems via neural interaction detection. In *International Conference on Learning Representations*, 2019. 3, 21

[102] Ramakrishna Vedantam, Karan Desai, Stefan Lee, Marcus Rohrbach, Dhruv Batra, and Devi Parikh. Probabilistic neural symbolic models for interpretable visual question answering. In *International Conference on Machine Learning*, pages 6428–6437, 2019. 8

[103] Alvin Wan, Lisa Dunlap, Daniel Ho, Jihan Yin, Scott Lee, Suzanne Petryk, Sarah Adel Bargal, and Joseph E Gonzalez. Nbdt: Neural-backed decision tree. In *International Conference on Learning Representations*, 2020. 20, 64

[104] Xingbo Wang, Jianben He, Zhihua Jin, Muqiao Yang, Yong Wang, and Huamin Qu. M2lens: Visualizing and explaining multimodal models for sentiment analysis. *IEEE Transactions on Visualization and Computer Graphics*, 28(1):802–812, 2021. 8, 64

[105] Eric Wong, Shibani Santurkar, and Aleksander Madry. Leveraging sparse linear layers for debuggable deep networks. In *International Conference on Machine Learning*, pages 11205–11216. PMLR, 2021. 4, 22

[106] Jialin Wu and Raymond Mooney. Faithful multimodal explanation for visual question answering. In *Proceedings of the 2019 ACL Workshop BlackboxNLP: Analyzing and Interpreting Neural Networks for NLP*, pages 103–112, 2019. 20, 65

[107] Keyang Xu, Mike Lam, Jingzhi Pang, Xin Gao, Charlotte Band, Piyush Mathur, Frank Papay, Ashish K Khanna, Jacek B Cywinski, Kamal Maheshwari, et al. Multimodal machine learning for automated icd coding. In *Machine Learning for Healthcare Conference*, pages 197–215. PMLR, 2019. 1

[108] Kexin Yi, Jiajun Wu, Chuang Gan, Antonio Torralba, Pushmeet Kohli, and Josh Tenenbaum. Neural-symbolic vqa: Disentangling reasoning from vision and language understanding. *Advances in neural information processing systems*, 31:1031–1042, 2018. 65

[109] Jason Yosinski, Jeff Clune, Thomas Fuchs, and Hod Lipson. Understanding neural networks through deep visualization. In *In ICML Workshop on Deep Learning*. Citeseer, 2015. 3, 21

[110] Jiahong Yuan and Mark Liberman. Speaker identification on the scotus corpus. *Journal of the Acoustical Society of America*, 123(5):3878, 2008.

- [111] Amir Zadeh, Rowan Zellers, Eli Pincus, and Louis-Philippe Morency. Mosi: multimodal corpus of sentiment intensity and subjectivity analysis in online opinion videos. *arXiv preprint arXiv:1606.06259*, 2016. [38](#)
- [112] Amir Zadeh, Minghai Chen, Soujanya Poria, Erik Cambria, and Louis-Philippe Morency. Tensor fusion network for multimodal sentiment analysis. In *Proceedings of the 2017 Conference on Empirical Methods in Natural Language Processing*, pages 1103–1114, 2017. [8](#)
- [113] Amir Zadeh, Michael Chan, Paul Pu Liang, Edmund Tong, and Louis-Philippe Morency. Social-iq: A question answering benchmark for artificial social intelligence. In *Proceedings of the IEEE/CVF Conference on Computer Vision and Pattern Recognition*, pages 8807–8817, 2019. [34](#)
- [114] Amir Zadeh, Paul Pu Liang, and Louis-Philippe Morency. Foundations of multimodal co-learning. *Information Fusion*, 64:188–193, 2020. [64](#)
- [115] AmirAli Bagher Zadeh, Paul Pu Liang, Soujanya Poria, Erik Cambria, and Louis-Philippe Morency. Multimodal language analysis in the wild: Cmu-mosei dataset and interpretable dynamic fusion graph. In *ACL*, 2018. [1](#), [2](#), [5](#), [6](#), [8](#), [32](#), [38](#), [64](#)
- [116] Liangli Zhen, Peng Hu, Xu Wang, and Dezhong Peng. Deep supervised cross-modal retrieval. In *Proceedings of the IEEE/CVF Conference on Computer Vision and Pattern Recognition*, pages 10394–10403, 2019. [33](#)
- [117] Victor Zhong, Tim Rocktäschel, and Edward Grefenstette. Rtfm: Generalising to new environment dynamics via reading. In *International Conference on Learning Representations*, 2020. [64](#)
- [118] Victor Zhong, Austin W Hanjie, Karthik Narasimhan, Luke Zettlemoyer, Austin W Hanjie, Victor Zhong, Karthik Narasimhan, Machel Reid, Victor Zhong, Victor Zhong, et al. Silg: The multi-environment symbolic interactive language grounding benchmark. *NeurIPS*, 2021. [64](#)

## Checklist

1. For all authors...
  - (a) Do the main claims made in the abstract and introduction accurately reflect the paper's contributions and scope? [\[Yes\]](#)
  - (b) Did you describe the limitations of your work? [\[Yes\]](#) see Appendix B.
  - (c) Did you discuss any potential negative societal impacts of your work? [\[Yes\]](#) see Appendix A.
  - (d) Have you read the ethics review guidelines and ensured that your paper conforms to them? [\[Yes\]](#)
2. If you are including theoretical results...
  - (a) Did you state the full set of assumptions of all theoretical results? [\[N/A\]](#)
  - (b) Did you include complete proofs of all theoretical results? [\[N/A\]](#)
3. If you ran experiments (e.g. for benchmarks)...
  - (a) Did you include the code, data, and instructions needed to reproduce the main experimental results (either in the supplemental material or as a URL)? [\[Yes\]](#) code is provided in the supplementary material and on <https://github.com/pliang279/MultiViz>.
  - (b) Did you specify all the training details (e.g., data splits, hyperparameters, how they were chosen)? [\[Yes\]](#) see Appendix F.
  - (c) Did you report error bars (e.g., with respect to the random seed after running experiments multiple times)? [\[Yes\]](#) we include standard deviations for all results where appropriate.
  - (d) Did you include the total amount of compute and the type of resources used (e.g., type of GPUs, internal cluster, or cloud provider)? [\[Yes\]](#) see Appendix F.
4. If you are using existing assets (e.g., code, data, models) or curating/releasing new assets...
  - (a) If your work uses existing assets, did you cite the creators? [\[Yes\]](#) we cited existing code, datasets, and models MULTIVIZ builds on where appropriate.
  - (b) Did you mention the license of the assets? [\[Yes\]](#) we release MULTIVIZ under the MIT license, see <https://github.com/pliang279/MultiViz/blob/main/LICENSE.md>.
  - (c) Did you include any new assets either in the supplemental material or as a URL? [\[Yes\]](#) we release MULTIVIZ datasets, models, interpretation code, and experimental code at <https://github.com/pliang279/MultiViz>.
  - (d) Did you discuss whether and how consent was obtained from people whose data you're using/curating? [\[Yes\]](#) see Appendix E.
  - (e) Did you discuss whether the data you are using/curating contains personally identifiable information or offensive content? [\[Yes\]](#) see Appendix E.
5. If you used crowdsourcing or conducted research with human subjects...
  - (a) Did you include the full text of instructions given to participants and screenshots, if applicable? [\[Yes\]](#) see Appendix F.
  - (b) Did you describe any potential participant risks, with links to Institutional Review Board (IRB) approvals, if applicable? [\[Yes\]](#) see Appendix F.
  - (c) Did you include the estimated hourly wage paid to participants and the total amount spent on participant compensation? [\[Yes\]](#) see Appendix F.

## Appendix

### Contents

<b>A Broader Impact</b>	<b>19</b>
<b>B Limitations</b>	<b>20</b>
<b>C Analysis Details</b>	<b>21</b>
C.1 Unimodal importance . . . . .	21
C.2 Cross-modal interactions . . . . .	21
C.3 Multimodal representations . . . . .	21
C.4 Multimodal prediction . . . . .	22
<b>D MULTIVIZ Visualization Tool</b>	<b>23</b>
D.1 MULTIVIZ code framework . . . . .	23
D.2 The MULTIVIZ website . . . . .	24
<b>E Datasets and Models</b>	<b>32</b>
E.1 Datasets provided in MULTIVIZ . . . . .	32
E.1.1 Multimodal fusion . . . . .	32
E.1.2 Multimodal retrieval . . . . .	33
E.1.3 Multimodal question answering . . . . .	34
E.2 Documentation . . . . .	34
E.3 Benchmark distribution . . . . .	43
E.4 Hosting and maintenance . . . . .	43
E.5 Author statement . . . . .	43
E.6 License . . . . .	43
E.7 Metadata . . . . .	43
E.8 Persistence of MULTIVIZ . . . . .	43
<b>F Additional Experiments and Details</b>	<b>45</b>
F.1 Model simulation . . . . .	45
F.1.1 Setup . . . . .	45
F.1.2 VQA 2.0 . . . . .	46
F.1.3 MM-IMDb . . . . .	46
F.1.4 CMU-MOSEI . . . . .	49
F.2 Cross-modal interactions . . . . .	53
F.2.1 CLEVR . . . . .	53
F.2.2 FLICKR-30K . . . . .	53
F.3 Representation interpretation . . . . .	55
F.3.1 VQA 2.0 . . . . .	55
F.3.2 CLEVR . . . . .	56
F.3.3 MM-IMDB . . . . .	56
F.4 Error analysis . . . . .	59
F.4.1 Setup . . . . .	59
F.4.2 VQA 2.0 . . . . .	59
F.4.3 CLEVR . . . . .	60
F.5 Model debugging . . . . .	61
F.5.1 VQA 2.0 . . . . .	61
F.6 Summary of takeaway messages . . . . .	63
<b>G Future Directions</b>	<b>64</b>
G.1 New datasets and models . . . . .	64
G.2 New classes of interpretation tools . . . . .	64
G.2.1 Unimodal importance . . . . .	64
G.2.2 Cross-modal interactions . . . . .	64
G.2.3 Multimodal prediction . . . . .	64
G.3 Evaluating interpretability . . . . .	65
G.4 Engagement with real-world stakeholders . . . . .	65

## A Broader Impact

Multimodal data and models are ubiquitous in a range of real-world applications. MULTIVIZ is our attempt at a standardized and modular framework for visualizing these multimodal models. While we believe these tools will eventually help stakeholders gain a deeper understanding of multimodal models as a step towards reliable real-world deployment, we believe that special care must be taken in the following regard to ensure that these interpretation tools are reliably deployed:

**Reliability of visualizations:** There has been recent work examining the reliability of model interpretability methods for real-world practitioners [82, 94]. Lipton [65] examines the motivations underlying interest in interpretability, finding them to be diverse and occasionally discordant. Krishna et al. [53] find that state-of-the-art explanation methods may disagree in terms of the explanations they output. Chandrasekaran et al. [15] further conclude that existing explanations on VQA model do not actually make its responses and failures more predictable to a human. We refer the reader to Chen et al. [17] for a critique on the disconnect between technical objectives targeted by interpretable ML research and the high-level goals stated as consumers’ use cases, as well as Bhatt et al. [11] for an analysis of how interpretable and explainable ML tools can be used in real-world deployment. Human-in-the-loop interpretation and evaluation could be a promising direction towards connecting technical solutions with real-world stakeholders, while also offering users an interactive medium to incorporate feedback in multimodal models.

**Evaluating interpretability:** Progress towards interpretability is challenging to evaluate [14, 20, 41, 90, 94]. Model interpretability (1) is highly subjective across different population subgroups [8, 53], (2) requires high-dimensional model outputs as opposed to low-dimensional prediction objectives [77], and (3) has desiderata that change across research fields, populations, and time [74]. We plan to continuously expand MULTIVIZ through community inputs for new interpretation methods in each stage and metrics to evaluate interpretability methods (see Appendix G for details).

## B Limitations

We outline the following limitations of our work and several ideas towards alleviating these shortcomings.

1. **Reliability of visualizations:** There has been recent work examining the reliability of model interpretability methods for real-world practitioners [15, 53, 65, 82, 94]. We refer the reader to Chen et al. [17] for a critique on the disconnect between technical objectives targeted by interpretable ML research and the high-level goals stated as consumers’ use cases, as well as Bhatt et al. [11] for an analysis of how interpretable and explainable ML tools can be used in real-world deployment. Human-in-the-loop interpretation and evaluation could be a promising direction towards connecting technical solutions with real-world stakeholders, while also offering users an interactive medium to incorporate feedback in multimodal models.
2. **Pitfalls of gradient-based interpretation:** We are aware of the limitations underlying gradient-based interpretation of black-box models [65, 94] with issues surrounding their faithfulness and usefulness. Future work should examine the opportunities and risks of gradient-based approaches, particularly in the context of cross-modal interactions.
3. **The role of cross-modal interactions:** There has been work showing that certain multimodal tasks do not need models to pick up cross-modal interactions to achieve good performance [37]. Indeed, for tasks like cross-modal retrieval, simply learning one interaction between a word and its corresponding image region is enough for typical datasets. This makes interpretation of cross-modal interactions difficult, since even well-performing models may not need to pick up all cross-modal interactions.
4. **Human-centered interpretation:** While we tried to be comprehensive in providing visualizations to the user, more information beyond a certain point is probably not useful and may overwhelm the user. We plan to work closely with human-computer interaction researchers to rethink usability and design of our proposed interpretation tools through careful user studies. MULTIVIZ will also welcome feedback from the public to improve its usability.
5. **Beyond linear reasoning:** Currently, we simplify the potentially-complex reasoning process by interpreting it as a linear prediction layer. We plan future work beyond linear prediction by investigating interpretable tree [103] and hierarchical reasoning layers in multimodal models (see Appendix G for details).
6. **Beyond MULTIVIZ stages:** While we believe that many multimodal problems can benefit from breaking them down into our proposed interpretation stages, we also acknowledge that certain problems may not benefit from this perspective. For example, problems in multimodal translation (mapping from one modality to another, such as image captioning) will not involve prediction layers and instead require new stages to interpret the generation process, and problems in multimodal co-learning (cross-modal transfer) will also require new stages to interpret knowledge transfer. In Appendix G, we include more details on new datasets we plan to add to MULTIVIZ to enable the study of new multimodal interpretability problems, and other interpretation tools we plan to add.
7. **Evaluating interpretability:** Progress towards interpretability is challenging to evaluate [14, 20, 41, 90, 94]. Model interpretability (1) is highly subjective across different population subgroups [8, 53], (2) requires high-dimensional model outputs as opposed to low-dimensional prediction objectives [77], and (3) has desiderata that change across research fields, populations, and time [74]. We plan to continuously expand MULTIVIZ through community inputs for new interpretation methods in each stage and metrics to evaluate interpretability methods. Some metrics we have in mind include those for measuring faithfulness, as proposed in recent work [14, 20, 41, 70, 90, 94, 106].

## C Analysis Details

### C.1 Unimodal importance

Unimodal importance aims to understand the contributions of each modality towards modeling and prediction. It builds upon ideas of gradient-based visualizations (e.g., Guided backpropagation [32] or Grad-CAM [15, 88]) and feature attributions (e.g., LIME [34, 86, 109], Shapley values [73, 87, 95]).

Taking **LIME** [86] for an example, given model  $f$ , we would like to return weights over each of the  $x_1$  and  $x_2$ 's such that important modalities are accurately weighted. LIME perturbs the set of  $x_1$  and  $x_2$ 's, observes how model predictions change, and fits a local linear model with respect to that datapoint. The areas with the highest positive weights are presented as the important ones. Other feature attribution and visualization approaches, such as **Gradient-based** [15, 88] or **Shapley values** [73, 87, 95], work similarly [109].

We implement unimodal feature attribution methods as a module  $\text{UNI}(f_\theta, y, \mathbf{x})$  taking in a trained model  $f_\theta$ , an output/feature  $y$  which analysis is performed with respect to, and the modality of interest  $\mathbf{x}$ .  $\text{UNI}$  returns importance weights across atoms  $x$  of modality  $\mathbf{x}$ .

### C.2 Cross-modal interactions

Cross-modal interactions describe various ways in which atoms from different modalities can relate with each other and the types of new information possibly discovered as a result of these relationships. **MULTIVIZ** first includes two recently proposed methods for understanding cross-modal interactions:

**EMAP** [37] decomposes  $f(x_1, x_2) = g_1(x_1) + g_2(x_2) + g_{12}(x_1, x_2)$  into strictly unimodal representations  $g_1, g_2$ , and cross-modal representation  $g_{12} = f - \mathbb{E}_{x_1}(f) - \mathbb{E}_{x_2}(f) + \mathbb{E}_{x_1, x_2}(f)$  to quantify the degree of global (across an entire dataset) cross-modal interactions captured by a model.

**DIME** [69] further extends EMAP by designing an efficient method for feature visualization on each disentangled representation locally (per datapoint).

**Higher-order Gradient** is our proposed method for efficiently quantifying the presence of cross-modal interactions. Based on the gradient definition of statistical non-additive interaction [28, 101], a function  $f$  exhibits non-additive interactions among 2 unimodal atoms  $x_1$  and  $x_2$  if  $\mathbb{E}_x \left[ \frac{\partial f(x)}{\partial x_1 \partial x_2} \right]^2 > 0$ . This definition inspires us to extend first-order gradient and perturbation-based approaches [34, 86, 109] to second-order gradient methods. We plan to make several approximations: only estimating single instances  $(x_1, x_2)$  at a time which avoids the expectation, and computing the magnitude  $w(x_1, x_2) = \left( \frac{\partial f(x)}{\partial x_1 \partial x_2} \right)^2$  as a measure of cross-modal interaction strength. Specifically, given a model  $f$ , we first take a gradient of  $f$  with respect to an input word (e.g.,  $x_1 = \text{dog}$ ), before taking a second-order gradient with respect to all input image pixels  $x_2$ , which should result in only the dog in the image being highlighted (see Figure 2 for examples on real datasets).

We implement a general module  $\text{CM}(f_\theta, y, x_1, \mathbf{x}_2)$  for cross-modal visualizations, taking in a trained model  $f_\theta$ , an output/feature  $y$ , the first modality's atom of interest  $x_1$ , and the entire second modality of interest  $\mathbf{x}_2$ .  $\text{CM}$  returns importance weights across atoms  $x_2$  of modality  $\mathbf{x}_2$ , and can build on top of any first-order unimodal attribution method, such as gradient visualization [32], LIME [86], or Shapley values [73].

### C.3 Multimodal representations

Given these highlighted unimodal and cross-modal interactions at the input level, the next stage aims to understand how these interactions are represented at the feature representation level. Specifically, given a trained multimodal model  $f$ , define the matrix  $M_z \in \mathbb{R}^{N \times d}$  as the penultimate layer of  $f$  representing (uninterpretable) deep feature representations implicitly containing information from both unimodal and cross-modal interactions. For the  $i$ th datapoint,  $z = M_z(i)$  collects a set of individual feature representations  $z_1, z_2, \dots, z_d \in \mathbb{R}$ . We aim to interpret these feature representations through both local and global analysis (see Figure 3 for an example):

**Local representation analysis ( $\mathbf{R}_\ell$ )** informs the user on parts of the original datapoint that activate feature  $z_j$ . To do so, we run unimodal and cross-modal visualization methods with respect to feature  $z_j$  (i.e.,  $\text{UNI}(f_\theta, z_j, \mathbf{x})$ ,  $\text{CM}(f_\theta, z_j, x_1, \mathbf{x}_2)$ ) in order to explain the input unimodal and cross-modal

interactions represented in feature  $z_j$ . Local analysis is useful in explaining model predictions on the original datapoint by studying the input regions activating feature  $z_j$ .

**Global representation analysis (R<sub>g</sub>)** provides the user with the top  $k$  datapoints  $\mathcal{D}_k(z_j) = \{(\mathbf{x}_1, \mathbf{x}_2, y)_{i=(1)}^k\}$  that also maximally activate feature  $z_j$ . By further unimodal and cross-modal visualizations on datapoints in  $\mathcal{D}_k(z_j)$ , global analysis is especially useful in helping humans assign interpretable language concepts to each feature by looking at similarly activated input regions across datapoints (e.g., the concept of color in Figure 3). Global analysis can also help to find related datapoints the model also struggles with for error analysis.

#### C.4 Multimodal prediction

Finally, the prediction step takes the set of feature representations  $z_1, z_2, \dots, z_d$  and composes them to form higher-level abstract concepts suitable for a task. We approximate the prediction process with a linear combination of penultimate layer features by integrating a sparse linear prediction model with neural network features [105]. Given the penultimate layer  $M_z \in \mathbb{R}^{N \times d}$ , we fit a linear model  $\mathbb{E}(Y|X = x) = M_z^\top \beta$  (bias  $\beta_0$  omitted for simplicity) and solve for sparsity using:

$$\hat{\beta} = \arg \min_{\beta} \frac{1}{2N} \|M_z^\top \beta - y\|_2^2 + \lambda_1 \|\beta\|_1 + \lambda_2 \|\beta\|_2^2. \quad (2)$$

The resulting understanding starts from the set of learned weights with the highest non-zero coefficients  $\beta_{\text{top}} = \{\beta_{(1)}, \beta_{(2)}, \dots\}$  and corresponding ranked features  $z_{\text{top}} = \{z_{(1)}, z_{(2)}, \dots\}$ .  $\beta_{\text{top}}$  tells the user how features  $z_{\text{top}}$  are composed to make a prediction, and  $z_{\text{top}}$  can then be visualized with respect to unimodal and cross-modal interactions using the representation stage.

Table 4: We scaffold the problem of interpreting multimodal models into the following stages for which algorithm design and analysis can occur. For each step, MULTIVIZ includes existing and newly proposed approaches for visualizing models across modalities and tasks.

Level	Methods		
Unimodal importance	LIME, Gradient, SHAP		
Cross-modal interactions	Cross-modal {LIME, Gradient, SHAP}, EMAP, DIME		
Multimodal representation	Local & global analysis		
Multimodal prediction	Sparse linear model		

Datasets			Models		
VQA 2.0	CLEVR	CMU-MOSEI	LXMERT	ViLT	CLIP
MIMIC	Flickr-30k	MM-IMDb	CNN-LSTM-SA	MuLT	LRTF

Analysis methods			Visualization tools		
LIME	FoG	SoG	LIME	Gradient	Sparse linear model
EMAP	DIME	Sparse linear model	visualizer	visualizer	visualizer

Figure 7: An illustration of the modules available in our code framework. Each **dataset** class provides data loading and label-answer mapping for a particular multimodal dataset; each **model** class is a wrapper for a particular model on a dataset and supports functionalities like making prediction and taking gradients; each **analysis** script performs a certain analysis method (such as LIME) on arbitrary input data point and model wrapper; and the **visualization** scripts are tools to visualize analysis results.

## D MULTIVIZ Visualization Tool

We summarize these proposed approaches for understanding each step of the multimodal process in Table 4, and show the overall pipeline in Algorithm 1 and Figure 1. To enable human studies, MULTIVIZ provides an interactive API where users can choose multimodal datasets and models and be presented with a set of visualizations at each stage.

In this section, we will include both introductions to our code framework that enables easy application of analysis visualization methods to datasets and models, and also present the MULTIVIZ website that showcases some examples of visualizations generated for each stage on different datasets and models.

### D.1 MULTIVIZ code framework

One additional major contribution of our works is that we designed a code framework in Python for easy analysis, interpretation and visualization of models on multimodal datasets with only a few lines of code. The framework is modularized and extendable to new datasets, models and visualization methods. Figure 7 is an illustration of the main modules of the code framework:

- Within the **datasets** module, we include scripts for retrieving information directly from the dataset, including getting specific data points from a split, getting the ground truth labels, label-id-to-answer and answer-to-label-id mappings, etc. Some dataset scripts also supports generating visualizations for data points (for example, the script for VQA supports generating pictures that contain both the image and the question).
- Within the **models** module, we write a wrapper for every supported model that inherits a common parent class called **analysismodel**, which defines a set of functionalities commonly used in various analysis methods. The functions in **analysismodel** include **forward** (just making a prediction on a specific data point), **forwardbatch** (forward but on multiple points in a batch), **getgrad** (compute gradient, if applicable), **getprelinear** (getting representation features), and many others. This design allows the same analysis

---

**Algorithm 2** Example of generating visualizations for VQA using our code framework.

---

```
from datasets.vqa import VQADataset # import the dataset
from models.vqa_lxmert import VQALXMERT # import the model
# import analysis methods
from analysis.unimodallime import rununimodallime
from analysis.dime import dime
from analysis.SparseLinearEncoding import get_sparse_linear_model
# import visualization tools
from visualizations.visualizelime import visualizelime
from visualizations.visualizesparselinearmodel import analyzepointandvisualizeall,
analyzefeaturesandvisualizeall, sparsityaccgraph

# get data, model, and predictions
datas = VQADataset('val')
analysismodel = VQALXMERT('cuda:0')
instance = datas.getdata(554)
predlabel = analysismodel.getpredlabel(analysismodel.forward(instance))
correctlabel = analysismodel.getcorrectlabel(instance)

# run and visualize unimodal importance on predicted label
explanation1 = rununimodallime(instance, 'image', 'image', analysismodel, [predlabel])
visualizelime(explanation1, 'image', predlabel, 'imagelime.png')
explanation2 = rununimodallime(instance, 'text', 'text', analysismodel, [predlabel])
visualizelime(explanation2, 'text', predlabel, 'imagelime.png')

# run and visualize cross-modal interactions on predicted label
instanceset = [datas.getdata(i*50+4) for i in range(100)]
explanations = dime(instanceset, 11, analysismodel, [predlabel])
visualizelime(explanations[0], 'image', 0, 'imagedimeunimodal.png')
visualizelime(explanations[0], 'image', 1, 'imagedimemultimodal.png')
visualizelime(explanations[1], 'text', 0, 'textdimeunimodal.png')
visualizelime(explanations[1], 'text', 1, 'textdimeunimodal.png')

# train sparse linear model and visualize
params, res = get_sparse_linear_model(analysismodel, 'trainfeats.pkl', 'valfeats.pkl', 'valfeats.pkl')
sparsityaccgraph(res, 'sparseplot.png')

# run local and global analysis on features
sampledata = datas.getseqdata(0, 20000)
# local analysis
analyzepointandvisualizeall(params, instance, analysismodel, predlabel, 'tmp/local', 'local')
# global analysis
analyzefeaturesandvisualizeall(params, instance, sampledata, analysismodel, predlabel, 'tmp/global', 'global')
```

---

script to work on vastly different models, as long as the models are wrapped by a class that shares these functionalities.

- Within the `analysis` module, we have scripts that can take in arbitrary data point and a model class (that inherits `analysismodel`) and perform various analysis methods such as LIME, DIME, EMAP, Sparse Linear Model, etc. These scripts generate the outputs in numerical format without visualizations, and users can choose to visualize them in arbitrary ways.
- Within the `visualizations` module, we have scripts that provide tools to visualize the analysis results from the analysis module.

In Algorithm 2, we showcase an example of running LIME, DIME, Sparse Linear Model and representation feature analysis (local and global), thus covering all stages of MULTIVIZ. As you can see, the code is actually very short (without the comments) for running this many analysis and visualizations. Our code framework is also easily extendible to support new datasets, models and analysis/visualization methods, by writing and adding scripts to the datasets/models/analysis/visualizations modules respectively.

## D.2 The MULTIVIZ website

We also created a visualization website accompanying MULTIVIZ which organizes visualizations of all stages on a particular datapoint of specific dataset-model pairs. The URL link of the webpage is available at <https://github.com/pliang279/MultiViz>.

Figure 8 is one example webpage for a data point in VQA. On the left there is a control panel that allows users to switch between different datasets and instances (i.e., data points), and then below the two boxes shows all information about the data point (image and question in the case of VQA) and also the ground truth ("GT") label and the predicted ("Pred") label. On the right side, we have a graph showing a simplified version of the Sparse Linear Model: we only show the top 5 features with the



Figure 8: An example of **MULTIVIZ** webpage for VQA (Overview page). Best viewed zoomed in and in color.

highest weights for each label (the weights are shown as numbers on the lines). Note that we will show both correct and predicted labels in the graph (so if the model got the answer wrong, there will be two labels shown under "classes" as shown in Figure 10, and clicking on each label will navigate to a webpage that shows visualizations with respect to that specific label). In the middle tab titled **Main View**, we show the visualizations from **U** and **C** stages. In the case of VQA we present unimodal LIME as **U** stage visualization (first column under **Main View**) and DIME as **C** stage visualization (second and third column under **Main View**). We call this webpage the **Overview** webpage. For each of the top five representation features shown within the graph, the user can access  $R_\ell$  and  $R_g$  visualizations of each feature by clicking on the circle in the graph representing that feature and the user will see a **feature** webpage like Figure 9. Under **Main View**, we include local analysis visualizations (unimodal lime with respect to the feature in the case of VQA) on the top and then global analysis visualizations on the bottom. To return to the **Overview** page, the user can just press the label circle under "classes" in the graph on the right again.

We also show additional example webpages: MM-IMDb (Figure 11 and Figure 12, with first order gradient for **U** stage, second order gradient for **C** stage), CMU-MOSEI (Figure 13 and Figure 14, with first order gradient for **U** stage, second order gradient for **C** stage) and MIMIC (Figure 15, with first order gradient for **U** stage). Note that we only ran **U** stage for MIMIC LF model because its cross-modal interactions are negligible (second order gradients are all zero) and there are too few representation features to do sparse linear models.

We have also used modified versions of these webpages to conduct all our experiments with human annotators. See Appendix F for details.

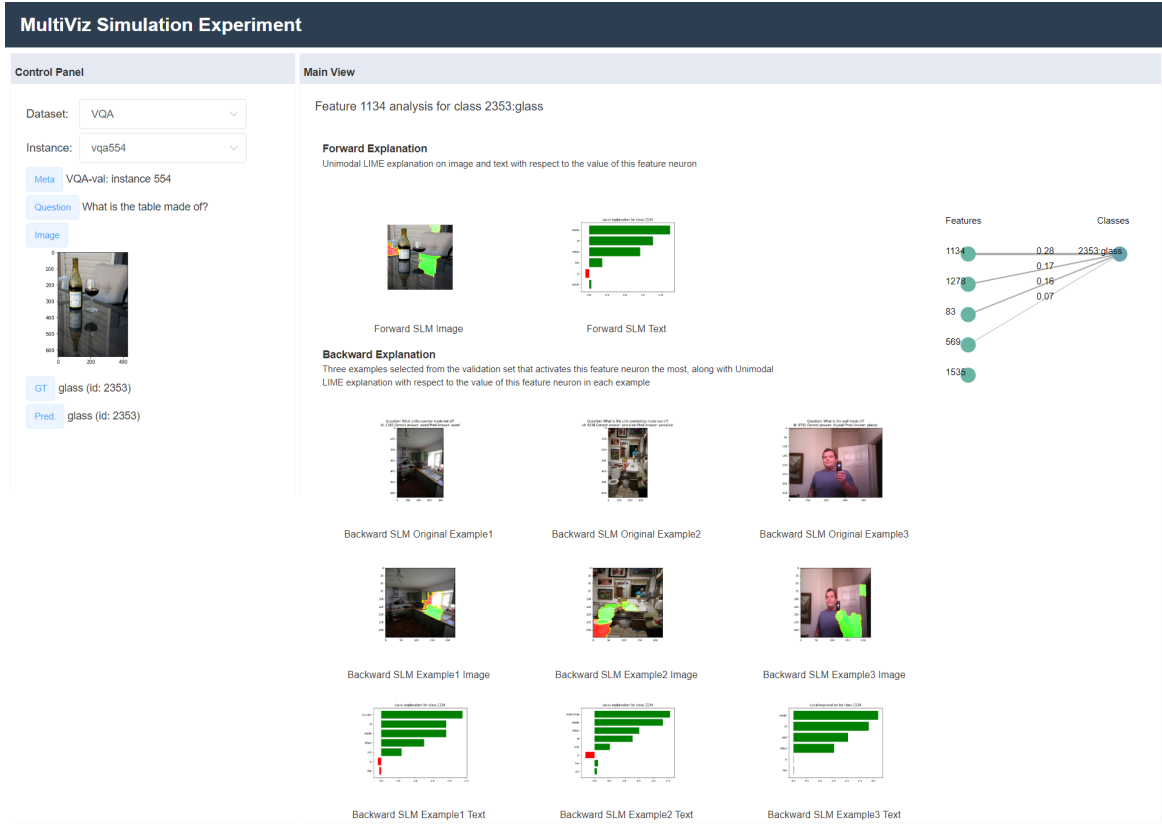


Figure 9: An example of MULTIVIZ webpage for VQA (Features page). Best viewed zoomed in and in color.



Figure 10: An example of MULTIVIZ webpage for VQA (Overview page). Best viewed zoomed in and in color.

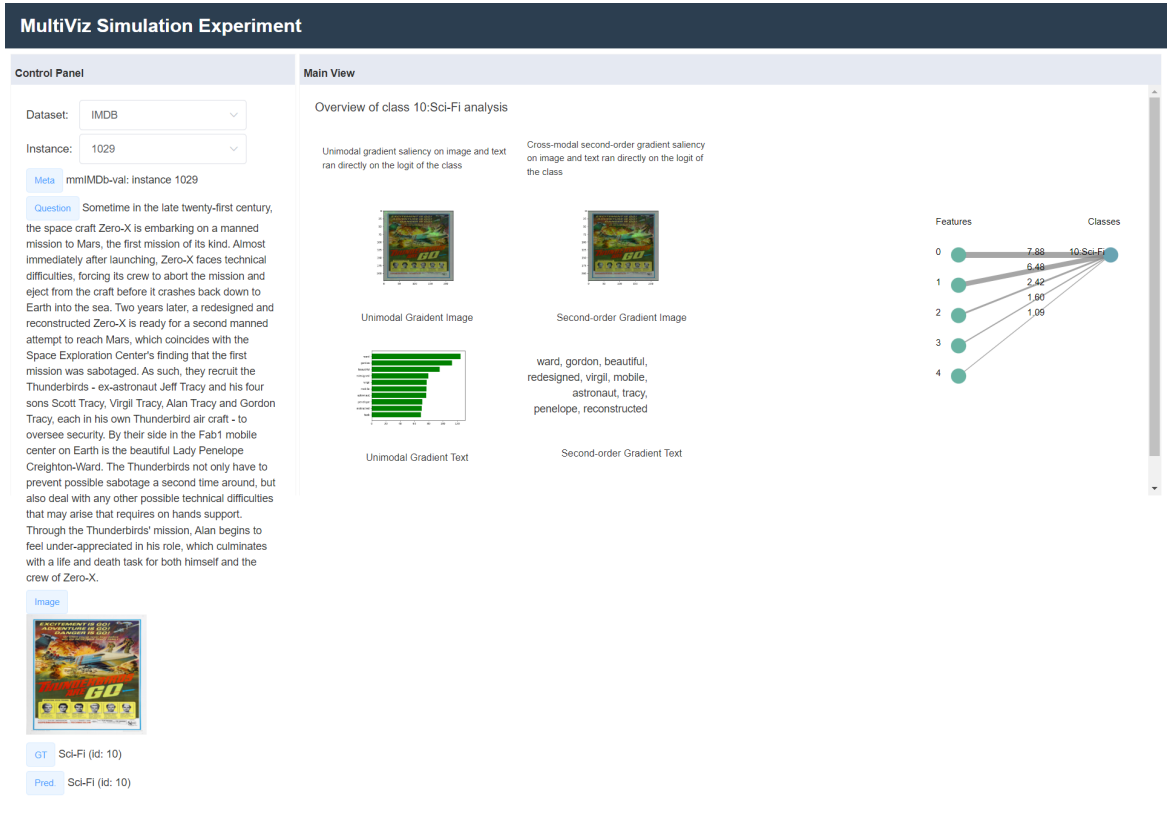
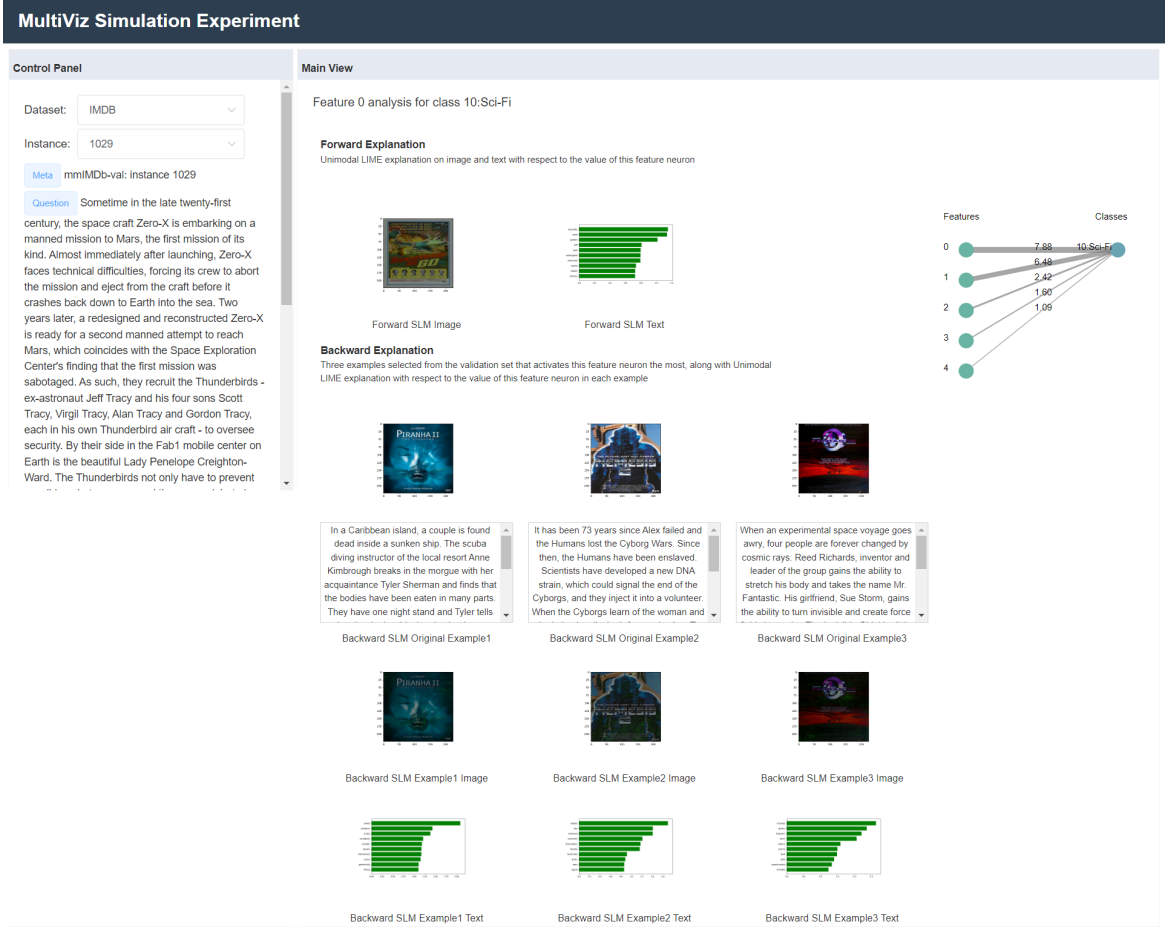


Figure 11: An example of MULTIVIZ webpage for VQA (Overview page). Best viewed zoomed in and in color.



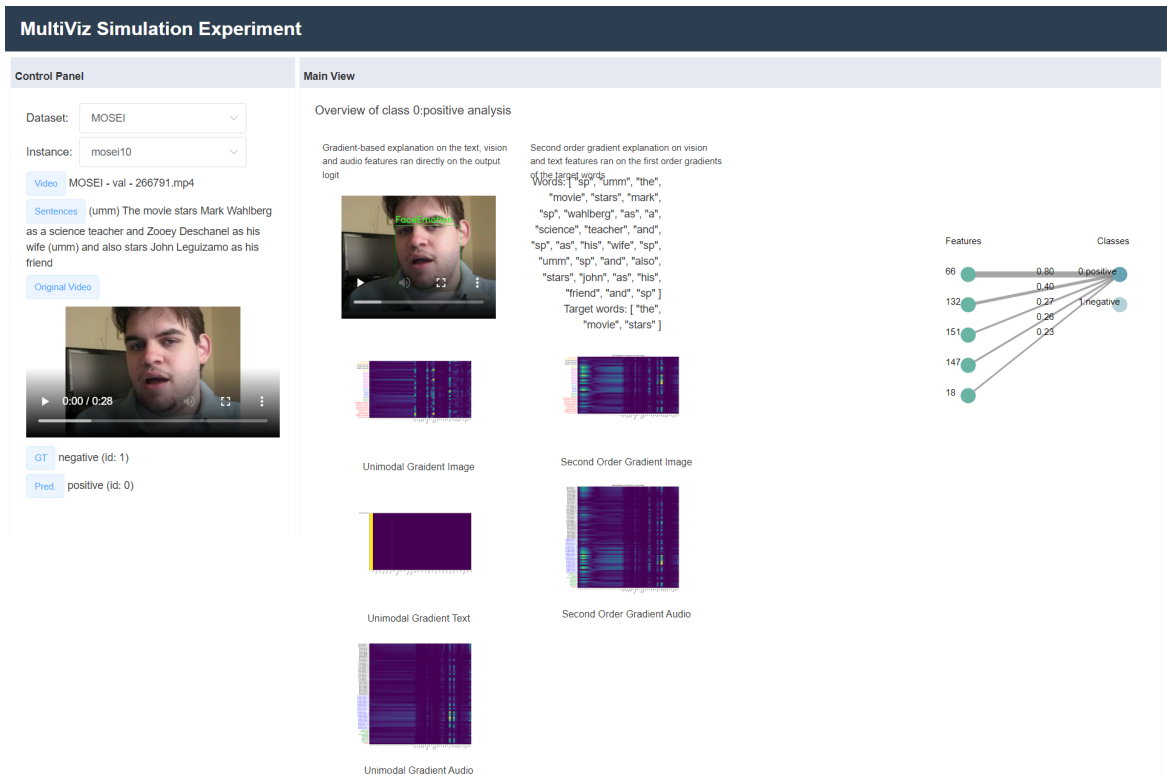


Figure 13: An example of MULTIVIZ webpage for CMU-MOSEI (Overview page). Best viewed zoomed in and in color.

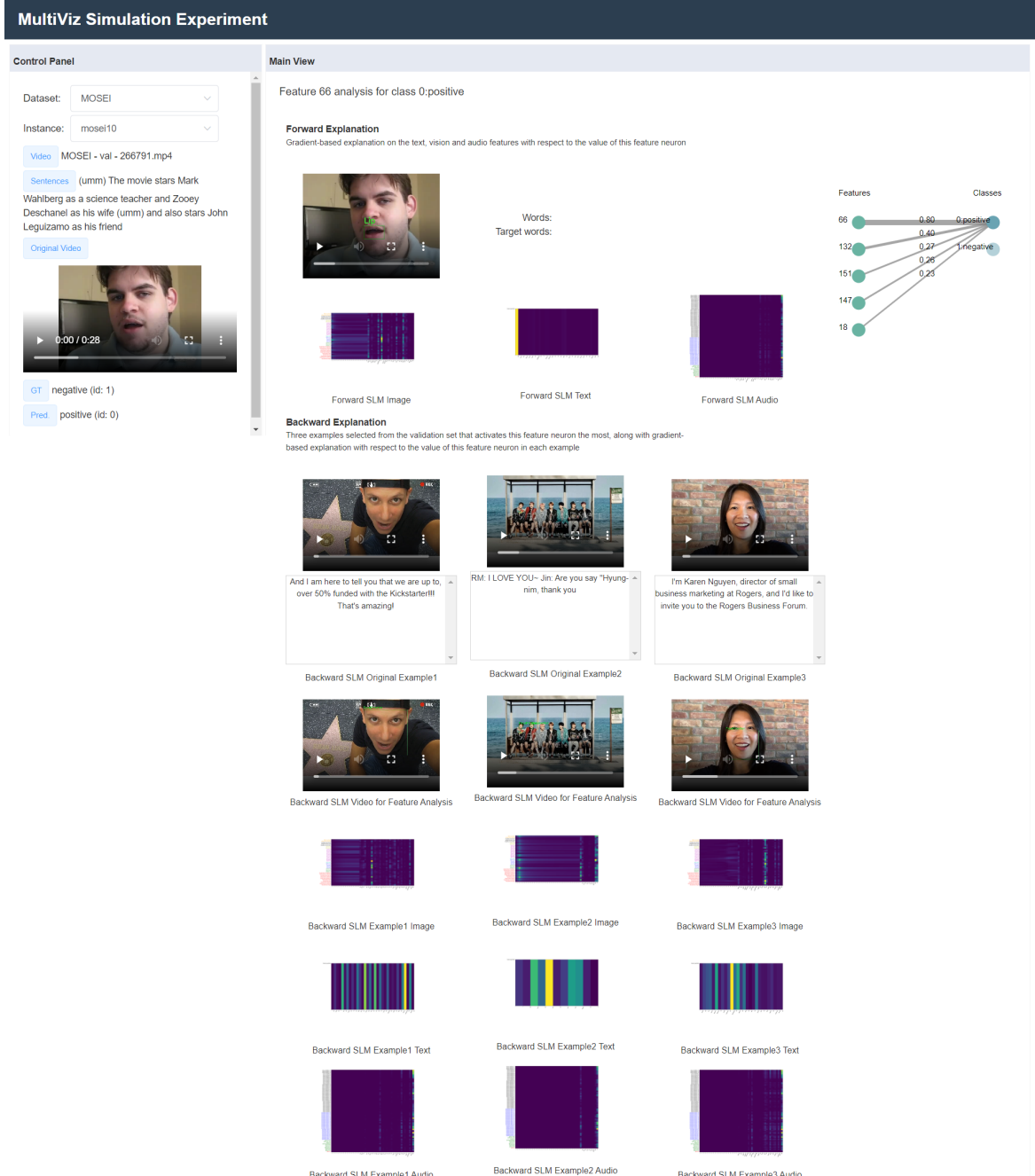


Figure 14: An example of MULTIVIZ webpage for CMU-MOSEI (Features page). Best viewed zoomed in and in color.

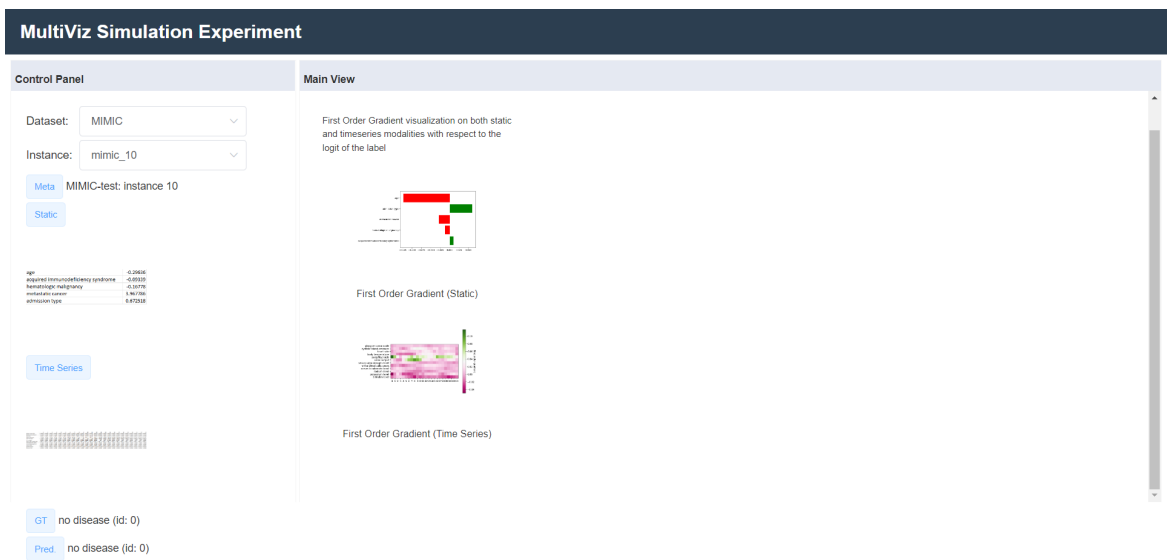


Figure 15: An example of MULTIVIZ webpage for MIMIC (Overview page). Best viewed zoomed in and in color.

## E Datasets and Models

All of our datasets build upon a diverse and standardized set of multimodal benchmarks in Multi-Bench [63]. We briefly describe the datasets and preprocessing here:

### E.1 Datasets provided in MULTIVIZ

#### E.1.1 Multimodal fusion

In multimodal fusion, the main challenge is to join information from two or more modalities to perform a prediction. Classic examples include audio-visual speech recognition, where visual lip motion is fused with speech signals to predict spoken words [24]. Information coming from different modalities have varying predictive power by themselves and also when complemented by each other (i.e., higher-order interactions). In order to capture higher-order interactions, there is also a need to identify the relations between granular units from two or more different modalities (i.e., alignment). When dealing with temporal data, it also requires capturing possible long-range dependencies across time (i.e., temporal alignment). MULTIVIZ contains the following datasets for multimodal fusion spanning:

**(1) CMU-MOSEI** is the largest dataset of sentence-level sentiment analysis and emotion recognition in real-world online videos [60, 115]. CMU-MOSEI contains more than 65 hours of annotated video from more than 1,000 speakers and 250 topics. Each video is annotated for sentiment as well as the presence of 9 discrete emotions (angry, excited, fear, sad, surprised, frustrated, happy, disappointed, and neutral) as well as continuous emotions (valence, arousal, and dominance). The diversity of prediction tasks makes CMU-MOSEI a valuable dataset to test multimodal models across a range of real-world affective computing tasks. The dataset has been continuously used in workshops and competitions revolving around human multimodal language.

**Access restrictions:** The authors are part of the team who collected the CMU-MOSEI dataset [115] so we have the license and right to redistribute this dataset. CMU-MOSEI was originally downloaded from <https://github.com/A2Zadeh/CMU-MultimodalSDK>.

**Licenses:** Permission is hereby granted, free of charge, to any person obtaining a copy of this software and associated documentation files (the “Software”), to deal in the Software without restriction, including without limitation the rights to use, copy, modify, merge, publish, distribute, sublicense, and/or sell copies of the Software, and to permit persons to whom the Software is furnished to do so, subject to the conditions in <https://raw.githubusercontent.com/A2Zadeh/CMU-MultimodalSDK/master/LICENSE.txt>

**Dataset preprocessing:** We follow current work [61, 115] and apply standard preliminary feature extraction for the CMU-MOSEI dataset.

**Train, validation, and test splits:** Each dataset contains several videos, and each video is further split into short segments (roughly 10 – 20 seconds) that are annotated. We split the data at the level of videos so that segments from the same video will not appear across train, valid, and test splits. This enables us to train user-independent models instead of having a model potentially memorizing the average affective state of a user. There are a total of 16, 265, 1, 869, and 4, 643 segments in train, valid, and test datasets respectively for a total of 22, 777 data points.

**(2) MM-IMDB** is the largest publicly available multimodal dataset for genre prediction on movies [7]. MM-IMDB starts from the movies of the MovieLens 20M dataset and expands this dataset by collecting genre, poster, and plot information for each movie. The final dataset contains ratings for 25, 959 movies. MM-IMDB is a realistic real-world multimodal dataset and is a popular benchmark for multimodal learning [7, 48, 79].

**Access restrictions:** While we do not have the license to this dataset, it is a public dataset free to download by the research community from <http://lisi1.unal.edu.co/mmimdb/> and <https://github.com/johnarevalo/gmu-mmimdb/>.

**Licenses:** MIT, see <https://github.com/johnarevalo/gmu-mmimdb/blob/master/LICENSE>

**Dataset preprocessing:** We used the same method as [7] to extract features from texts and images.

**Train, validation, and test splits:** The MM-IMDb dataset is split by genre into train, valid, and test datasets containing 15552, 2608, and 7799. The split was performed so that training, valid and test sets comprise 60%, 10%, 30% samples of each genre respectively.

**(3) MIMIC-III** (Medical Information Mart for Intensive Care III) [43] is a large, freely-available database comprising de-identified health-related data associated with over 40,000 patients who stayed in critical care units of the Beth Israel Deaconess Medical Center between 2001 and 2012. Following [83], we organized numerous patient data into two major modalities (using the 17 features in feature set A in [83]): time series modality, which is a set of medical measurements of the patient taken every 1 hour in a period of 24 hours where each measurement is a vector of size 12 (12 different measured numerical values); static modality, which is a set of medical information about the patient, represented in a vector of size 5. We use these modalities for 3 tasks: mortality prediction (6-class prediction on whether the patient dies in 1 day, 2 day, 3 day, 1 week, 1 year, or longer than 1 year), and 2 ICD-9 code predictions (binary classification on whether the patient fits any ICD-9 code in group 1 (140 – 239) and binary classification on whether the patient fits any ICD-9 code in group 7 460 – 519). MIMIC poses unique challenges in integrating time-varying and static modalities, reinforcing the need of aligning multimodal information at correct granularity.

**Privacy:** Before data was incorporated into the MIMIC-III database, it was first de-identified in accordance with Health Insurance Portability and Accountability Act (HIPAA) standards using structured data cleansing and date shifting. The de-identification process removed all eighteen identifying data elements listed in HIPAA, such as patient name, date of birth (for patients over 89 of age), telephone number, address, and dates. Protected health information was also removed from text fields, such as diagnostic reports and physician notes. We refer the reader to [83] for full de-identification details.

**Access restrictions:** We do not have the license and right to redistribute this dataset. Accessing MIMIC requires the completion of a training course and approval for access on PhysioNet (<https://physionet.org/about/database/>). However, we provide our own data preprocessing scripts for MIMIC, which transform the raw data into the standardized format for multimodal data and perform standardized splitting into the train, validation, and test splits. For a new user getting started with MIMIC data, all they would need to do is to complete the training course and obtain approval of access for scientific research from PhysioNet before they can use our public code to load all extracted features from the raw dataset in a version that can directly be used for machine learning studies.

**Licenses:** MIT, see <https://github.com/mit-lcp/mimic-code/blob/main/LICENSE>

**Dataset preprocessing:** We followed the instructions on <https://mimic.physionet.org/gettingstarted/access/> to download the dataset in the form of raw tables, then generated preprocessed data following the steps described in [https://github.com/USC-Melady/Benchmarking\\_DL\\_MIMICIII](https://github.com/USC-Melady/Benchmarking_DL_MIMICIII) (which takes 1 – 2 weeks running time) to get the data used for experiments. Specifically, we will use data in the file 24hrs/series/imputed-normed-ep\_1\_24-stdized.npz. When accessing this data from our code repo, set the imputed\_path of the npz file above in the get\_data.py and the script will generate the PyTorch data loader for the tasks (where we will normalize the data).

**Train, validation, and test splits:** We split the data into train/valid/test sets randomly (using a fixed random seed) in a 80 : 10 : 10 ratio (so 28,970 train, 3,621 valid, and 3,621 test data points) for a total of 36,212 data points.

### E.1.2 Multimodal retrieval

Another area of great interest lies in cross-modal retrieval [64, 116], where the goal is to retrieve semantically similar data from a new modality using a modality as a query (e.g., given a phrase, retrieve the closest image describing that phrase). The core challenge is to perform alignment of representations across both modalities. MULTIVIZ contains the following datasets for multimodal retrieval and grounding:

**(1) FLICKR-30K** [80] contains 32,000 images collected from Flickr, together with 5 reference sentences provided by human annotators enabling the tasks of text-to-image reference resolution, localizing textual entity mentions in an image, and bidirectional image-caption retrieval.

**Access restrictions:** While we do not have the license to this dataset, it is a public dataset free to download by the research community from <https://paperswithcode.com/dataset/flickr30k> and <https://shannon.cs.illinois.edu/DenotationGraph/>.

**Licenses:** Custom license (research-only, non-commercial), see <https://shannon.cs.illinois.edu/DenotationGraph/#:~:text=Downloads>

**Train, validation, and test splits:** The training items are generated from the captions of 25,000 images, and the test items are generated from a disjoint set of 3,000 images.

### E.1.3 Multimodal question answering

Within the domain of language and vision, there has been growing interest in language-based question answering (i.e., “query” modality) of entities in the visual, video, or embodied domain (i.e., “queried” modality). Datasets such as Visual Question Answering [3], Social IQ [113], and Embodied Question Answering [19] have been proposed to benchmark the performance of multimodal models in these settings. A core challenge lies in aligning words asked in the question with entities in the queried modalities, which typically take the form of visual entities in images or videos (i.e., alignment). MULTIVIZ contains the following datasets for multimodal question answering spanning several research areas:

**(1) CLEVR** [44] is a diagnostic dataset for studying the ability of VQA systems to perform visual reasoning. It contains 100,000 rendered images and about 853,000 unique automatically generated questions that test visual reasoning abilities such as counting, comparing, logical reasoning, and storing information in memory.

**Access restrictions:** While we do not have the license to this dataset, it is a public dataset free to download by the research community from <https://cs.stanford.edu/people/jcjohns/clevr/> and <https://github.com/facebookresearch/clevr-dataset-gen>.

**Licenses:** BSD license (research-only, non-commercial), see <https://github.com/facebookresearch/clevr-dataset-gen/blob/main/LICENSE>

**Train, validation, and test splits:** The complete dataset contains more than 608K train, 140K val and 140K test (question, image) pairs.

**(2) VQA 2.0** [33] is a balanced version of the popular VQA [3] dataset by collecting complementary images such that every question is associated with not just a single image, but rather a pair of similar images that result in two different answers to the question. This reduces the occurrence of spurious correlations in the dataset and enables training of more robust models.

**Access restrictions:** While we do not have the license to this dataset, it is a public dataset free to download by the research community from <https://visualqa.org/> and <https://paperswithcode.com/dataset/visual-question-answering-v2-0>.

**Licenses:** Commons Attribution 4.0 International License, see <https://visualqa.org/terms.html>.

**Train, validation, and test splits:** The complete balanced dataset contains more than 443K train, 214K val and 453K test (question, image) pairs.

## E.2 Documentation

We provide documentation for MULTIVIZ in the form of datasheets for datasets [29]:

### 1. Motivation

- (a) *For what purpose was the dataset created? Was there a specific task in mind? Was there a specific gap that needed to be filled? Please provide a description.*

The promise of multimodal models for real-world applications has inspired research in visualizing and understanding their internal mechanics with the end goal of empowering stakeholders to visualize model behavior, perform model debugging, and promote trust in machine learning models. However, modern multimodal models are typically black-box neural networks, which makes it challenging to understand their internal mechanics. How can we visualize the internal modeling of multimodal interactions in these models? MULTIVIZ aims to fill this gap as a method for analyzing the behavior of multimodal models by scaffolding the problem of interpretability into 4 stages: (1)

*unimodal importance*: how each modality contributes towards downstream modeling and prediction, (2) *cross-modal interactions*: how different modalities relate with each other, (3) *multimodal representations*: how unimodal and cross-modal interactions are represented in decision-level features, and (4) *multimodal prediction*: how decision-level features are composed to make a prediction.

MULTIVIZ is designed to operate on diverse modalities, models, tasks, and research areas. Through experiments on 8 trained models across 6 real-world tasks, we show that the complementary stages in MULTIVIZ together enable users to (1) *simulate* model predictions, (2) assign *interpretable concepts* to features, (3) perform *error analysis* on model misclassifications, and (4) use insights from error analysis to *debug* models. MULTIVIZ is publicly available, will be regularly updated with new interpretation tools and metrics, and welcomes inputs from the community.

(b) *Who created the dataset (e.g., which team, research group) and on behalf of which entity (e.g., company, institution, organization)?*

MULTIVIZ is created primarily by the MultiComp Lab in the Language Technologies Institute and Machine Learning Department of the School of Computer Science at Carnegie Mellon University, in collaboration with several other researchers at Georgia Tech and HKUST. The creation of MULTIVIZ is for purely research purposes only.

(c) *Who funded the creation of the dataset? If there is an associated grant, please provide the name of the grantor and the grant name and number.*

This material is based upon work partially supported by the National Science Foundation (Awards #1722822 and #1750439) and National Institutes of Health (Awards #R01MH125740, #R01MH096951, and #U01MH116925). PPL is partially supported by a Facebook PhD Fellowship and a Carnegie Mellon University’s Center for Machine Learning and Health Fellowship. RS is partially supported by NSF IIS1763562 and ONR Grant N000141812861. Any opinions, findings, conclusions, or recommendations expressed in this material are those of the author(s) and do not necessarily reflect the views of the National Science Foundation, National Institutes of Health, Facebook, Carnegie Mellon University’s Center for Machine Learning and Health, or Office of Naval Research, and no official endorsement should be inferred.

(d) *Any other comments?*

No.

## 2. Composition

(a) *What do the instances that comprise the dataset represent (e.g., documents, photos, people, countries)? Are there multiple types of instances (e.g., movies, users, and ratings; people and interactions between them; nodes and edges)? Please provide a description.*

We describe each dataset in detail in Appendix E.1. MULTIVIZ provides a comprehensive suite of multimodal datasets and models for visualization studies. It covers a diverse range of tasks (fusion, retrieval, and question answering) across several research areas (affective computing, healthcare, and multimedia), dataset sizes (small, medium, and large), and input modalities (in the form of  $\ell$ : language,  $i$ : image,  $v$ : video,  $a$ : audio,  $t$ : time-series,  $ta$ : tabular).

(b) *How many instances are there in total (of each type, if appropriate)?*

We describe each dataset’s statistics in detail in Appendix E.1 and Table 1. We chose datasets to span small, medium, and large sizes. The smallest dataset contains 22,777 instances (and training a model takes roughly an hour on a single GPU) while the largest one contains 1,100,000 instances (and fine-tuning a model takes roughly 2 weeks on a single GPU). This enables accessibility for researchers with limited computational resources, while also allowing for large-scale studies of multimodal datasets and models. For each dataset, we also include visualization studies for several state-of-the-art models spanning MULT [98], LRTF [66], LF [10], ViLT [49], CLIP [84],

CNN-LSTM-SA [44], MDETR [45], and LXMERT [97]. These cover models both pretrained and trained from scratch.

(c) *Does the dataset contain all possible instances or is it a sample (not necessarily random) of instances from a larger set? If the dataset is a sample, then what is the larger set? Is the sample representative of the larger set (e.g., geographic coverage)? If so, please describe how this representativeness was validated/verified. If it is not representative of the larger set, please describe why not (e.g., to cover a more diverse range of instances, because instances were withheld or unavailable).*

Each of the datasets are collected in different ways that we detail in Appendix E.1. To summarize, each dataset consists of samples from a larger set since it is impossible to include all videos/stock data/medical data/robotics data in the world. Each dataset is collected with the aim to be representative of the entire population.

(d) *What data does each instance consist of? “Raw” data (e.g., unprocessed text or images) or features? In either case, please provide a description.*

We describe in detail the raw data and processed features for each dataset in Appendix E.1. To summarize, MULTIVIZ contains both raw modality data and processed data with predefined feature extractors following current work.

(e) *Is there a label or target associated with each instance? If so, please provide a description.*

We describe in detail the labels for each dataset in Appendix E.1. To summarize, MULTIVIZ enables fine-grained analysis across 6 datasets spanning 3 research areas, 6 input modalities, and 8 models. We also plan to continuous expansion of MULTIVIZ with new multimodal datasets and models, and more visualization experiments with real-world stakeholders and users of multimodal models.

(f) *Is any information missing from individual instances? If so, please provide a description, explaining why this information is missing (e.g., because it was unavailable). This does not include intentionally removed information, but might include, e.g., redacted text.*

No, to the best of our knowledge, all datasets are provided in full.

(g) *Are relationships between individual instances made explicit (e.g., users’ movie ratings, social network links)? If so, please describe how these relationships are made explicit.*

We describe in detail the relationships between modalities for each dataset in Appendix E.1.

(h) *Are there recommended data splits (e.g., training, development/validation, testing)? If so, please provide a description of these splits, explaining the rationale behind them.*

Yes, MULTIVIZ provides a data loading pipeline that directly loads train, validation, and test splits according to current work, as well as trained models and their visualization results. We provide these details for each dataset in Appendix E.1.

(i) *Are there any errors, sources of noise, or redundancies in the dataset? If so, please provide a description.*

We do not know of any errors in each of the datasets included in MULTIVIZ. However, we will always be on the lookout for potential issues and update them via <https://github.com/pliang279/MultiViz>.

(j) *Is the dataset self-contained, or does it link to or otherwise rely on external resources (e.g., websites, tweets, other datasets)? If it links to or relies on external resources, a) are there guarantees that they will exist, and remain constant, over time; b) are there official archival versions of the complete dataset (i.e., including the external resources as they existed at the time the dataset was created); c) are there any restrictions (e.g., licenses, fees) associated with any of the external resources that might apply to a future user? Please provide descriptions of all external resources and any restrictions associated with them, as well as links or other access points, as appropriate.*

Most of the datasets in MULTIVIZ have been collected, stored, processed, and are self-contained. There are some datasets that depend on external resources which we explain below:

- i. MIMIC: We depend on the original dataset to be hosted on <https://mimic.physionet.org/gettingstarted/access/>. Unfortunately, since we are not allowed to redistribute the raw data and users need to complete training to access the raw data, we are unable to provide a self-contained version of the MIMIC dataset. We are currently planning to add several new multimodal datasets in the healthcare domain that can be self-contained after appropriate de-identification.

All other datasets are fully public and are commonly used for research purposes.

(k) *Does the dataset contain data that might be considered confidential (e.g., data that is protected by legal privilege or by doctor-patient confidentiality, data that includes the content of individuals' non-public communications)? If so, please provide a description.*

From the authors of MIMIC [43]: “The project was approved by the Institutional Review Boards of Beth Israel Deaconess Medical Center (Boston, MA) and the Massachusetts Institute of Technology (Cambridge, MA). Requirement for individual patient consent was waived because the project did not impact clinical care and all protected health information was de-identified.”

To the best of our knowledge, all other datasets do not contain confidential data and are publicly available for research purposes.

(l) *Does the dataset contain data that, if viewed directly, might be offensive, insulting, threatening, or might otherwise cause anxiety? If so, please describe why.*

We reviewed the datasets and found no offensive content. While there are clearly expressions of highly negative sentiment or strong displays of anger and disgust in the affective computing videos, there are no offensive words used or personal attacks recorded in the video. All videos are related to movie or product reviews, TED talks, and TV shows.

(m) *Does the dataset relate to people? If not, you may skip the remaining questions in this section.*

Yes, the MIMIC and CMU-MOSEI datasets relate to people. There might also be occurrences of people in the VQA and Flickr-30k datasets. The other datasets in MULTIVIZ do not.

(n) *Does the dataset identify any subpopulations (e.g., by age, gender)? If so, please describe how these subpopulations are identified and provide a description of their respective distributions within the dataset.*

The following datasets relate to people:

- i. CMU-MOSEI: This dataset does not identify any subpopulations in their modeling decisions. However, the raw data comes in the form of videos publicly available and free to download from YouTube. Sub-population and demographic information can be inferred from these raw videos.

- ii. MIMIC: According to the authors [43]: “The median age of adult patients is 65.8 years and 55.9% patients are male.”

(o) *Is it possible to identify individuals (i.e., one or more natural persons), either directly or indirectly (i.e., in combination with other data) from the dataset? If so, please describe how.*

The following datasets relate to people:

- i. CMU-MOSEI: One can see the person in the raw video, but the dataset contains no personal information. We do not explicitly use information regarding gender, ethnicity, identity, or video identifier in online sources. All pre-extracted features

are non easily invertible and only rely on general visual or audio features such as the presence of a smile or magnitude of voice [111, 115].

- ii. MIMIC: The MIMIC dataset has been rigorously de-identified in accordance with Health Insurance Portability and Accountability Act (HIPAA) such that all possible personal information has been removed from the dataset. Removed personal information includes patient name, telephone number, address, and dates. Dates of birth for patients aged over 89 were shifted to obscure their true age. Please refer to Appendix E.1 for de-identification details. Again, we emphasize that any multimodal models trained to perform prediction should only be used for scientific study and should not in any way be used for real-world prediction.

(p) *Does the dataset contain data that might be considered sensitive in any way (e.g., data that reveals racial or ethnic origins, sexual orientations, religious beliefs, political opinions or union memberships, or locations; financial or health data; biometric or genetic data; forms of government identification, such as social security numbers; criminal history)? If so, please provide a description.*

MULTIVIZ contains datasets with healthcare data. However, all these datasets are publicly available for research purposes. Healthcare data (MIMIC) has been rigorously de-identified in accordance with the Health Insurance Portability and Accountability Act (HIPAA) such that all possible personal information (patient name, telephone number, address, and dates, date of birth) has been removed from the dataset. Please refer to Appendix E.1 for de-identification details.

(q) *Any other comments?*

No.

**3. Collection Process**

- (a) *How was the data associated with each instance acquired? Was the data directly observable (e.g., raw text, movie ratings), reported by subjects (e.g., survey responses), or indirectly inferred/derived from other data (e.g., part-of-speech tags, model-based guesses for age or language)? If data was reported by subjects or indirectly inferred/derived from other data, was the data validated/verified? If so, please describe how.*

We include the collection process for each dataset in Appendix E.1.

- (b) *What mechanisms or procedures were used to collect the data (e.g., hardware apparatus or sensor, manual human curation, software program, software API)? How were these mechanisms or procedures validated?*

We include these details in Appendix E.1.

- (c) *If the dataset is a sample from a larger set, what was the sampling strategy (e.g., deterministic, probabilistic with specific sampling probabilities)?*

We include sampling methods for each dataset in Appendix E.1.

- (d) *Who was involved in the data collection process (e.g., students, crowdworkers, contractors) and how were they compensated (e.g., how much were crowdworkers paid)?*

We include annotation details for each dataset in Appendix E.1.

- (e) *Over what timeframe was the data collected? Does this timeframe match the creation timeframe of the data associated with the instances (e.g., recent crawl of old news articles)? If not, please describe the timeframe in which the data associated with the instances was created.*

We include timeframes for each dataset in Appendix E.1.

- (f) *Were any ethical review processes conducted (e.g., by an institutional review board)? If so, please provide a description of these review processes, including the outcomes, as well as a link or other access point to any supporting documentation.*

From the authors of MIMIC [43]: “The project was approved by the Institutional Review Boards of Beth Israel Deaconess Medical Center (Boston, MA) and the Massachusetts Institute of Technology (Cambridge, MA). Requirement for individual patient consent was waived because the project did not impact clinical care and all protected health information was de-identified.”

(g) *Does the dataset relate to people? If not, you may skip the remainder of the questions in this section.*

Yes, the healthcare, affective computing, and Kinetics (multimedia) datasets relate to people. The other datasets in MULTIVIZ do not.

(h) *Did you collect the data from the individuals in question directly, or obtain it via third parties or other sources (e.g., websites)?*

CMU-MOSEI dataset is collected from YouTube videos that follow the creative commons license and follow fair use guidelines of YouTube. According to the authors for the MIMIC dataset [43]: “Data was downloaded from several sources, including archives from critical care information systems, hospital electronic health record databases, and Social Security Administration Death Master File.”

(i) *Were the individuals in question notified about the data collection? If so, please describe (or show with screenshots or other information) how the notice was provided, and provide a link or other access point to, or otherwise reproduce, the exact language of the notification itself.*

CMU-MOSEI dataset is collected from YouTube videos that follow the creative commons license and follow fair use guidelines of YouTube. This is the standard way for content creators to grant someone else permission to use and redistribute their work. According to the authors for the MIMIC dataset [43]: “The project was approved by the Institutional Review Boards of Beth Israel Deaconess Medical Center (Boston, MA) and the Massachusetts Institute of Technology (Cambridge, MA). Requirement for individual patient consent was waived because the project did not impact clinical care and all protected health information was de-identified.”

(j) *Did the individuals in question consent to the collection and use of their data? If so, please describe (or show with screenshots or other information) how consent was requested and provided, and provide a link or other access point to, or otherwise reproduce, the exact language to which the individuals consented.*

CMU-MOSEI dataset is collected from YouTube videos that follow the creative commons license and follow fair use guidelines of YouTube which allows content creators to grant someone else permission to use and redistribute their work. According to the authors for the MIMIC dataset [43]: “Requirement for individual patient consent was waived because the project did not impact clinical care and all protected health information was de-identified.”

(k) *If consent was obtained, were the consenting individuals provided with a mechanism to revoke their consent in the future or for certain uses? If so, please provide a description, as well as a link or other access point to the mechanism (if appropriate).*

N/A.

(l) *Has an analysis of the potential impact of the dataset and its use on data subjects (e.g., a data protection impact analysis) been conducted? If so, please provide a description of this analysis, including the outcomes, as well as a link or other access point to any supporting documentation.*

N/A.

(m) *Any other comments?*

N/A.

#### 4. Preprocessing/cleaning/labeling

(a) *Was any preprocessing/cleaning/labeling of the data done (e.g., discretization or bucketing, tokenization, part-of-speech tagging, SIFT feature extraction, removal of instances, processing of missing values)? If so, please provide a description. If not, you may skip the remainder of the questions in this section.*

Yes, we followed the convention in prior research for any preprocessing done to the datasets. We explain these steps in Appendix [E.1](#).

(b) *Was the “raw” data saved in addition to the preprocessed/cleaned/labeled data (e.g., to support unanticipated future uses)? If so, please provide a link or other access point to the “raw” data.*

Yes, we include the raw data in MULTIVIZ in addition to the preprocessed features. The raw data (usually in the form of raw text, videos, audio, time series) are useful for users to perform their own feature extraction and also for robustness tests on raw data itself (e.g., imperfections in the raw text through spelling errors and missing words). There are certain cases where we are not allowed to distribute the raw data: for MIMIC where users must undergo training to download the raw data. For these datasets, we provide automated download and preprocessing scripts once the raw data is downloaded through the correct procedure by each user (see details in Appendix [E.1](#)).

(c) *Is the software used to preprocess/clean/label the instances available? If so, please provide a link or other access point.*

Yes, we provided all links and references to preprocessing steps in Appendix [E.1](#).

(d) *Any other comments?*

No.

## 5. Uses

(a) *Has the dataset been used for any tasks already? If so, please provide a description.*

Yes, MULTIVIZ contains several datasets that have been used in the multimodal ML community. We provide links to the original repositories of each dataset and their original citations in Appendix [E.1](#).

(b) *Is there a repository that links to any or all papers or systems that use the dataset? If so, please provide a link or other access point.*

We provide links to the original repositories of each dataset and their original citations in Appendix [E.1](#). Many of these methods have been tested by their original authors on a small subset of datasets in MULTIVIZ. In addition to these references, the leading authors maintain a reading list on topics in multimodal ML at [\[59\]](#) which contains links to papers, datasets, code, academic courses, conferences, and workshops relevant to the multimodal ML community.

(c) *What (other) tasks could the dataset be used for?*

In addition to interpreting these multimodal models, datasets and methods in MULTIVIZ can also be used for:

- i. Interpreting relationships between modalities.
- ii. Investigating alignment and cross-modal interactions between modalities.
- iii. Quantitative interpretations that are complementary to the qualitative visualizations currently of focus in MULTIVIZ.
- iv. Engagement with real-world users of multimodal and stakeholders via human-in-the-loop studies.

(d) *Is there anything about the composition of the dataset or the way it was collected and preprocessed/cleaned/labeled that might impact future uses? For example, is there anything that a future user might need to know to avoid uses that could result in unfair treatment of individuals or groups (e.g., stereotyping, quality of service issues) or other*

*undesirable harms (e.g., financial harms, legal risks) If so, please provide a description. Is there anything a future user could do to mitigate these undesirable harms?*

We are careful to outline all possible risks associated with each dataset in Appendix E.1 and also in our broader impact statement (Appendix A). We acknowledge that there could be risks regarding the privacy and security of data, as well as the real-world deployment of these methods whenever human-centric data is involved (e.g., in healthcare, affective computing, and multimedia). We discussed data demographics in the previous section, and it should be taken into consideration when making claims regarding the generalization of models to new users. We also emphasize that these multimodal datasets and methods should only be used for research purposes and not for actual real-world deployment until research can sufficiently verify their safety. Finally, we are carefully working with domain experts towards better understanding biases in these multimodal datasets and models as well as their real-world safety.

(e) *Are there tasks for which the dataset should not be used? If so, please provide a description.*

Yes, we emphasize that all multimodal models trained to perform prediction on these datasets should not in any way be used to harm individuals and should only be used as a scientific study. They should not be deemed safe for real-world deployment. In particular, the models used to make predictions of affective states, human actions, and health indicators are particularly sensitive and should not be used to inform any real-world decisions. All results must only be used as a scientific study of machine learning methods. See more details in Appendix A.

(f) *Any other comments?*

No.

## 6. Distribution

(a) *Will the dataset be distributed to third parties outside of the entity (e.g., company, institution, organization) on behalf of which the dataset was created? If so, please provide a description.*

Yes, the benchmark will be distributed to the public research community for theoreticians and practitioners to experiment on multimodal data.

(b) *How will the dataset be distributed (e.g., tarball on website, API, GitHub)? Does the dataset have a digital object identifier (DOI)?*

We plan to distribute MULTIVIZ via our public GitHub: <https://github.com/pliang279/MultiViz>. We also include a landing website page that includes an introduction to the benchmark, links to the relevant papers on multimodal datasets and algorithms, and a public leaderboard to keep track of current progress on these multimodal tasks.

(c) *When will the dataset be distributed?*

The dataset is currently available for use.

(d) *Will the dataset be distributed under a copyright or other intellectual property (IP) license, and/or under applicable terms of use (ToU)? If so, please describe this license and/or ToU, and provide a link or other access point to, or otherwise reproduce, any relevant licensing terms or ToU, as well as any fees associated with these restrictions.*

We release the benchmark and code under an MIT license: see <https://github.com/pliang279/MultiBench/blob/main/LICENSE>, which allows for sharing and distribution of the code for research purposes. Each of the datasets in MULTIVIZ has their own licenses which we detail in Appendix E.1.

(e) *Have any third parties imposed IP-based or other restrictions on the data associated with the instances? If so, please describe these restrictions, and provide a link or other access point to, or otherwise reproduce, any relevant licensing terms, as well as any fees associated with these restrictions.*

Yes, MULTIVIZ brings together a collection of several existing datasets in the multi-modal research that were built by their individual authors who have original licenses for these datasets. We only included the datasets with licenses that allow for redistribution (MIT or Creative Commons license) and are freely downloadable for research purposes. We detailed all dataset licenses in Appendix E.1.

(f) *Do any export controls or other regulatory restrictions apply to the dataset or to individual instances? If so, please describe these restrictions, and provide a link or other access point to, or otherwise reproduce, any supporting documentation.*

We are not aware of any such restrictions.

(g) *Any other comments?*

No.

## 7. Maintenance

(a) *Who is supporting/hosting/maintaining the dataset?*

The dataset is supported and hosted by the team of authors at CMU. The team will also lead the maintenance and expansion of MULTIVIZ. The team will also work with domain expert stakeholders to determine how helpful MULTIVIZ visualizations are.

(b) *How can the owner/curator/manager of the dataset be contacted (e.g., email address)?*

We provide all contact addresses at <https://github.com/pliang279/MultiViz>.

(c) *Is there an erratum? If so, please provide a link or other access point.*

All erratum and updates to the dataset will be tracked via GitHub commit histories at <https://github.com/pliang279/MultiViz>.

(d) *Will the dataset be updated (e.g., to correct labeling errors, add new instances, delete instances)? If so, please describe how often, by whom, and how updates will be communicated to users (e.g., mailing list, GitHub)?*

Yes, we plan for long-term maintenance and expansion of the dataset. All erratum and updates to the dataset will be tracked via GitHub commit histories at <https://github.com/pliang279/MultiViz>. Please refer to Appendix E.4 for details.

(e) *If the dataset relates to people, are there applicable limits on the retention of the data associated with the instances (e.g., were individuals in question told that their data would be retained for a fixed period of time and then deleted)? If so, please describe these limits and explain how they will be enforced.*

The individuals in question were not notified about the data collection. For YouTube videos, they are released under a creative commons license which is the standard way for content creators to grant someone else permission to use and redistribute their work. According to the authors for the MIMIC dataset [43]: “The project was approved by the Institutional Review Boards of Beth Israel Deaconess Medical Center (Boston, MA) and the Massachusetts Institute of Technology (Cambridge, MA). Requirement for individual patient consent was waived because the project did not impact clinical care and all protected health information was de-identified.”

(f) *Will older versions of the dataset continue to be supported/hosted/maintained? If so, please describe how. If not, please describe how its obsolescence will be communicated to users.*

Yes, we will maintain a GitHub history for all updates and older versions of datasets and code in MULTIVIZ.

(g) *If others want to extend/augment/build on/contribute to the dataset, is there a mechanism for them to do so? If so, please provide a description. Will these contributions be validated/verified? If so, please describe how. If not, why not? Is there a process for communicating/distributing these contributions to other users? If so, please provide a description.*

Yes, we will create a system where users can create pull requests on GitHub to include their datasets and models. The authors will verify that the additions are in the scope of multimodal learning and do not break the current experimental code. We will work with these authors to ensure that their data and algorithms can be included in MULTIVIZ.

(h) *Any other comments?*

No.

### E.3 Benchmark distribution

We plan to distribute the MULTIVIZ benchmark via our public GitHub: <https://github.com/pliang279/MultiViz>. We also include a landing website page that includes an introduction to the benchmark and links to the relevant papers on multimodal interpretation.

The GitHub and webpage will also allow feedback from the research community in suggesting and adding new datasets and algorithms. Finally, we plan to include a list of planned future updates to MULTIVIZ on the webpage, along with their target release dates.

### E.4 Hosting and maintenance

We have a long-term plan to continue the expansion and maintenance of MULTIVIZ. Here we summarize the main directions we plan to expand towards and leave details and other areas of future work to Appendix G.

- Maintenance: MULTIVIZ will be continuously hosted via GitHub which provides stable access to code and a landing page website. We guarantee that MULTIVIZ will be available for a long time through our distribution channels. The authors themselves are also actively working on interpreting multimodal learning. As a result of these long-term collaborative research efforts, the authors will continue to maintain and expand on the datasets and code provided in MULTIVIZ.
- Expansion of datasets: We plan to include more datasets and models that we will aim to interpret and visualize. We will encourage students taking the multimodal machine learning course at CMU (<https://cmu-multicomp-lab.github.io/mmml-course/fall2020/>) to use the visualization toolkit to analyze their proposed multimodal models and datasets and consider adding functionality to MULTIVIZ.
- Expansion of methods: The authors currently collect a very up-to-date reading list of core multimodal papers <https://github.com/pliang279/awesome-multimodal-ml> and plan to continuously update MULTIVIZ with new multimodal interpretation methods proposed by the community.

### E.5 Author statement

The authors carefully reviewed the information present in this document. To the best of our knowledge, the datasets in MULTIVIZ can be used for research purposes, following the methodology and licenses described in Section (Appendix E.1).

### E.6 License

Each of the datasets included in MULTIVIZ includes their own licenses, which we detail in Appendix E.1. We release all preprocessing code across all datasets using the MIT license. All other codes for multimodal interpretation algorithms in MULTIVIZ, as well as evaluation scripts, are also released via an MIT license: see <https://github.com/pliang279/MultiViz/blob/main/LICENSE.md>, which allows for sharing and distribution of the code for research purposes.

### E.7 Metadata

We have included structured metadata for MULTIVIZ on our landing page: <https://github.com/pliang279/MultiViz>.

### E.8 Persistence of MULTIVIZ

MULTIVIZ is publicly hosted on <https://github.com/pliang279/MultiViz>. For larger datasets that cannot be uploaded to GitHub, we plan to upload the processed dataset to CMU Box. We are still exploring the best options for sharing large datasets. Users need to download

these processed datasets, place them into a correct folder, and run the **MULTIVIZ** data loader and interpretation pipeline.

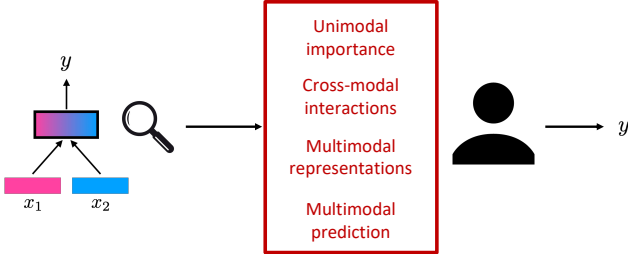


Figure 16: **Model simulation:** we use human studies to determine if users are able to simulate model predictions given only MULTIVIZ visualizations. If MULTIVIZ indeed generates human-understandable explanations, humans should be able to simulate model behavior accurately for both correct and incorrect model outputs.

## F Additional Experiments and Details

In this section, we provide additional details on the experiments and additional results on several other multimodal datasets.

**Computational resources:** Preparations for all experiments (i.e. generating the necessary visualizations for the points for each dataset) are done on a private server with 2 GPUs.

The preparation time for model simulation experiment using 2 GPUs is about 12 hours for VQA, 1 hour for MM-IMDb and 2 hours for CMU-MOSEI. For the representation interpretation experiment, we generated all visualizations for the VQA data points in the experiment in about 3 hours on 1 GPU. For the error analysis, in addition to the visualizations already present on the MultiViz website, we also have 1 GPU available live during the human annotation (so human annotators can request second order gradient analysis on specific words, each second order gradient computation only takes 2-3 seconds).

In all of the above analysis, we re-use the sparse linear model we had already trained for each dataset when building the main MultiViz webpage (the initial training can take some time - scaling the Sparse Linear Model to the large VQA took over 72 hours with 1 GPU).

Note that VQA visualization generation is much slower than those for MM-IMDb and CMU-MOSEI. This is because in VQA we used DIME for cross-modal interaction interpretation, but in MM-IMDb and CMU-MOSEI we use second-order gradient. The newly proposed second order gradient is much faster compared to DIME since it only requires running the model once instead of up to 10,000 times in DIME.

Overall, the proposed MULTIVIZ interpretation stages are efficient and only add negligible time on top of existing trained models, especially for our newly-proposed second-order gradient method.

**Participant risks and compensation:** Participation in these human studies were fully voluntary and without compensation. There are no participant risks involved. We obtained consent from all participants prior to each short study. All annotations are fully anonymous and we do not store any information regarding the participants at all.

### F.1 Model simulation

#### F.1.1 Setup

We design a large-scale use case of model simulation to determine if MULTIVIZ helps users of multimodal models gain a deeper understanding of model behavior, as shown in Figure 16. We design a human study to see what humans predict given MULTIVIZ explanations at each step (and across all steps). If MULTIVIZ indeed generates human-understandable explanations, humans should be able to make a prediction on the task given these explanations only. Specifically, we compare the full version of MULTIVIZ with a set of local ablations, each consisting of only 1 additional stage:

1. **U:** Users are only shown the unimodal importance (U) of each modality towards the prediction.
2. **U + C:** Users are shown both unimodal importance (U) and cross-modal interactions (C) highlighted towards the final prediction.

3. **U + C +  $\mathbf{R}_\ell$** : Users are shown unimodal importance (U) and cross-modal interactions (C) of the given datapoint highlighted towards the final prediction, as well as local analysis ( $\mathbf{R}_\ell$ ) of unimodal and cross-modal interactions of top ranked feature representations  $z_{\text{top}} = \{z_{(1)}, z_{(2)}, \dots\}$  with respect to that local datapoint.
4. **U + C +  $\mathbf{R}_\ell + \mathbf{R}_g$** : Users are additionally shown global analysis ( $\mathbf{R}_g$ ) through similar datapoints that also maximally activate those same top ranked feature representations.
5. **MULTIVIZ (U + C +  $\mathbf{R}_\ell + \mathbf{R}_g + \mathbf{P}$ )**: This constitutes the entire MULTIVIZ framework by including visualizations of the final prediction (P) stage: sorting all top ranked feature neurons  $z_{\text{top}} = \{z_{(1)}, z_{(2)}, \dots\}$  with respect to their coefficients  $\beta_{\text{top}} = \{\beta_{(1)}, \beta_{(2)}, \dots\}$  and showing these coefficients to the user.

We ask human annotators (who all have or are currently working towards a B.S. in a STEM field and have at least basic knowledge of machine learning models) to predict the output of a model analysis results and visualizations. In each of the following datasets (VQA 2.0, MM-IMDb, CMU-MOSEI), we divide 15 total human annotators into 5 groups of 3, each group getting one of the five settings above, and then we compute average accuracy and inter-rater agreement within each group. The full results are shown in Table 2.

### F.1.2 VQA 2.0

In this experiment, we will perform model simulation on VQA 2.0 dataset with pretrained LXMERT (<https://huggingface.co/unc-nlp/lxmert-vqa-uncased>). We randomly selected 22 points from the validation split of the VQA dataset under the following criterion: (1) it is not a yes/no question and (2) the answer to the question is not infrequent (i.e. it occurs at least 220 times over 220K+ validation points). For each of the point, we run MULTIVIZ analysis and visualization: for **U** stage we run LIME on each modality; for **C** stage we run DIME; for  **$\mathbf{R}_\ell$**  we run LIME with respect to the representation feature on this data point; and for  **$\mathbf{R}_g$**  we run LIME on each modality with respect to the representation feature on 3 examples that maximally activates the feature; and for **P** we show the top 5 representation features with the highest weights with respect to the predicted class in a Sparse Linear Model trained on the training set of VQA. The webpage for each datapoint is organized into **Overview** page (containing **U** and **C**) as well as five **Features** page ( **$\mathbf{R}_\ell$**  and  **$\mathbf{R}_g$**  for each of the top 5 representation features) as well as a "graph" on the right showing **P**. An example **Overview** page is shown in Figure 17 and an example **Features** page is shown in Figure 18. In settings (1)-(4), we will use versions of the webpage with certain stages removed (for example, Figure 19 is the webpage for setting (2), only showing **U** and **C**).

Within each of the five groups, on each of the 22 points, human annotators are asked to predict what the model (LXMERT) predicts given a website containing some or all of the stages of analysis visualizations (depending on the group's setting). In addition, they are given an answer sheet (see Figure 20) where they are given 4 answer choices for each data point to predict with, and they have to select one of the choices they think LXMERT most likely predicted as the answer to each data point. Before each annotator starts, they are taught how to interpret each analysis visualization, and then the instructor goes over 2 points together with the annotators as examples and the annotators need to finish the remaining 20 points on their own. Only the remaining 20 points counts towards the data collected in the experiment. We then compute average accuracy and inter-rater agreement score (Krippendorff's alpha) within each group. In addition, groups under settings (3), (4) and (5) are asked whether they found the **Overview** or **Features** page more helpful.

As shown in Table 2, in general, human annotators were able to better predict the model's predictions when they were given more information, as the groups that got more information almost always end up with both higher average accuracy and higher inter-rater agreement. Moreover, annotators in settings (3), (4), (5) reported that they found **Features** page most helpful compared to **Overview** page 31.7%, 61.7% and 80.0% of the time respectively, therefore showing that  $\mathbf{R}_g$  and **P** helps make representation analysis a lot more useful.

### F.1.3 MM-IMDb

In this experiment, we perform model simulation on MM-IMDb dataset with the LRTF model from MultiBench [63]. We randomly selected 21 points from the test split of MM-IMDb dataset. The original MM-IMDb dataset is designed for multi-label classification, but for simplicity, we only take the label with the highest prediction probability from LRTF as the predicted class, and effectively treat it as a single-label classification task during analysis, visualization and model simulation experiment.

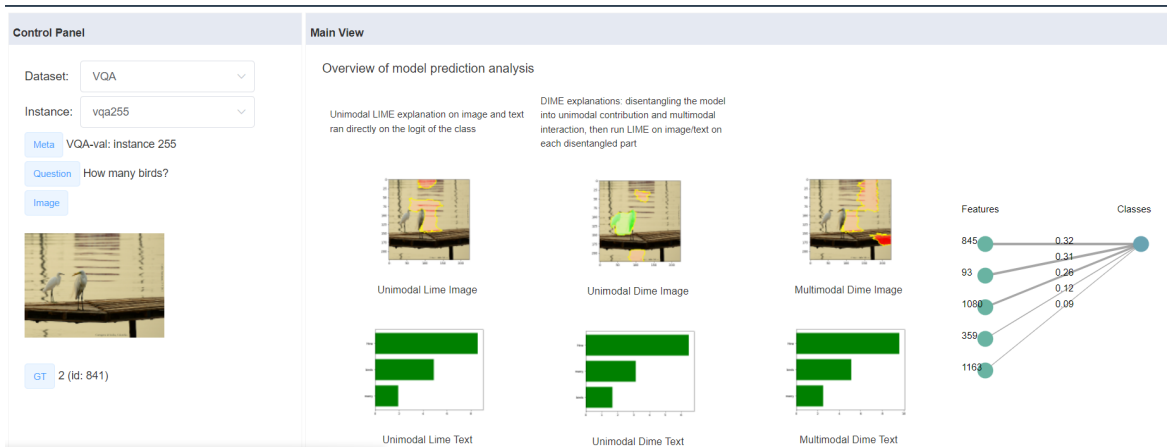


Figure 17: Simulation experiment for VQA: MultiViz website Overview page showing LIME and DIME explanations. Best viewed zoomed in and in color.

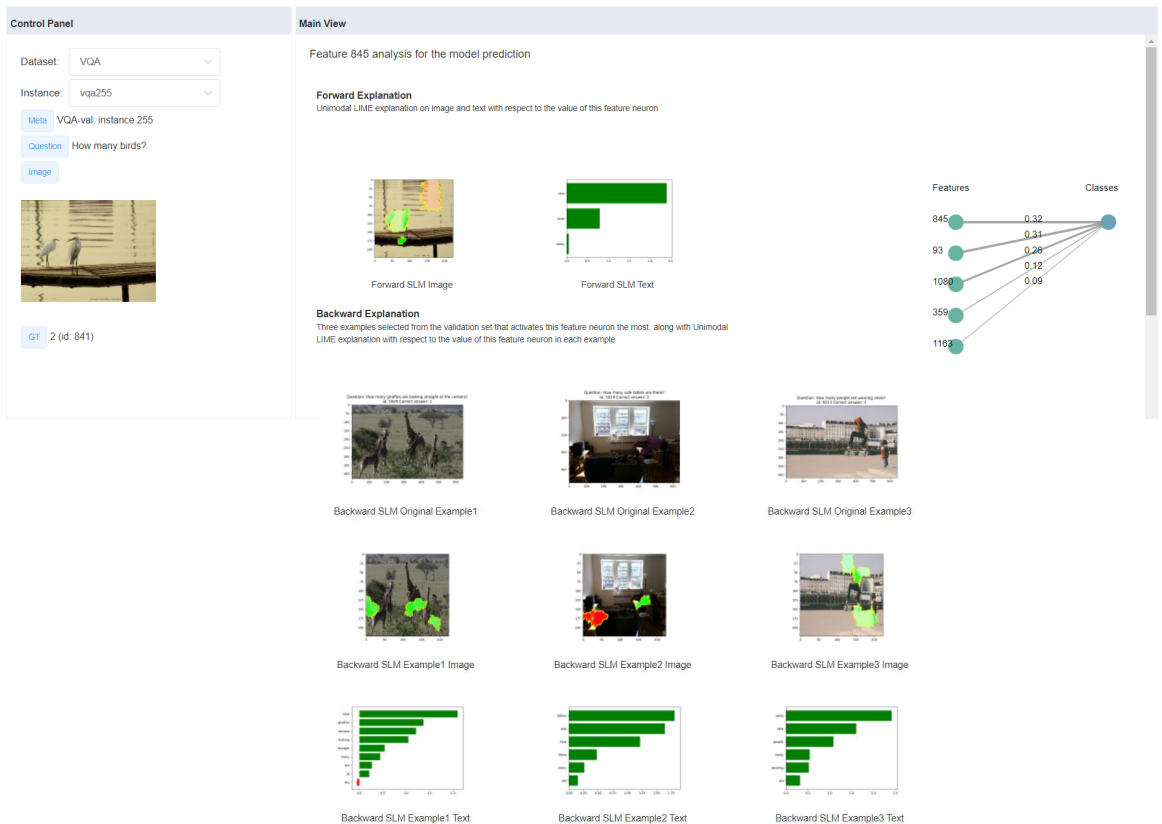


Figure 18: Simulation experiment for VQA: MultiViz website on a specific representation feature showing forwards and backwards analysis (a Features page). Best viewed zoomed in and in color.

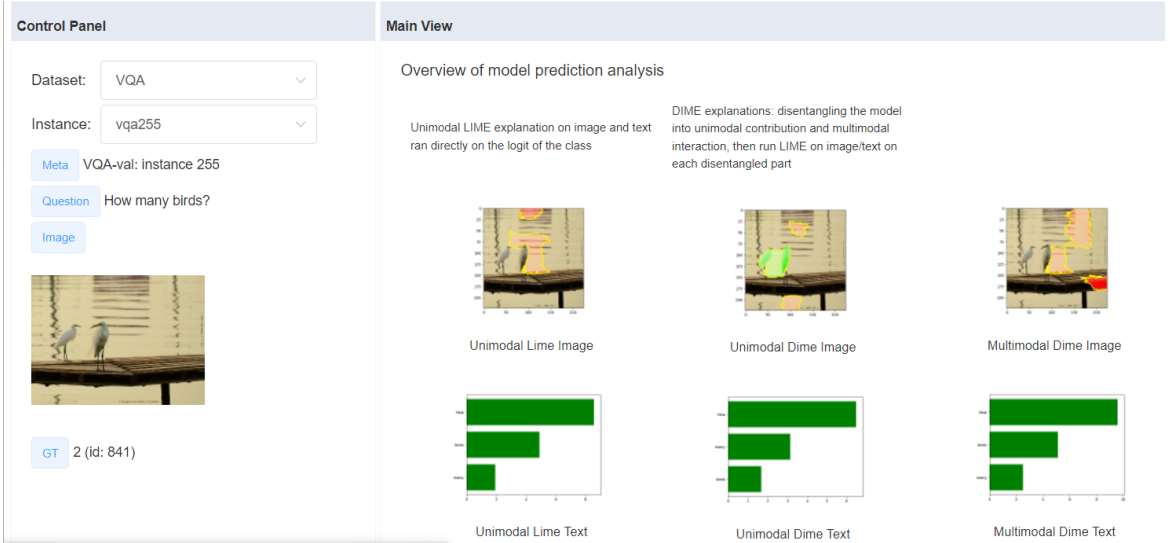


Figure 19: Simulation experiment for VQA: Setting 2 webpage with only LIME and DIME explanations. Best viewed zoomed in and in color.

	A	B	C	D	Answer
255		1	2	3	
1205	white	orange	blue	green	
2305	skis	snow	shoes	ground	
2605	male	female			
1905	0	1	2	3	
3205	man	woman	toddler	baby	
3255	0	1	2	3	
3405	white	orange	blue	green	
705	old	young			
2655	white	orange	blue	black	
855	left	right	up	down	
905	bus	car	SUV	ambulance	
955	0	2	4	6	
4155	0	1	2	3	
4255	0	1	2	3	
4755	white	orange	blue	green	
5555	red	yellow	blue	green	
5605	cat	dog	horse	cow	
6205	0	1	2	3	
6255	0	1	2	3	
4455	1	2	3	4	
7505	cat	dog	horse	cow	

Figure 20: Simulation experiment for VQA: Multiple choice answer sheet given to the annotators.

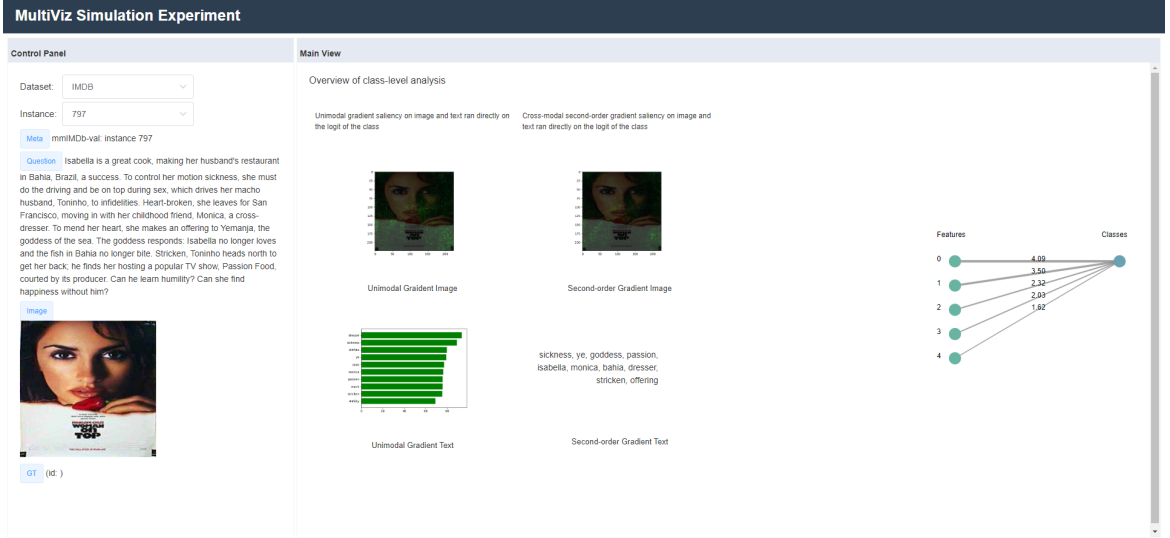


Figure 21: Simulation experiment for MM-IMDb: Sample Overview page. Best viewed zoomed in and in color.

For each of the points, we run **MULTIVIZ** analysis and visualization: for **U** stage we show first order gradient analysis on image and text; for **C** stage we perform second order gradient analysis on the top ten words with maximum first order gradient; for **R<sub>ℓ</sub>** we show first order gradient on image and text with respect to each representation feature; for **R<sub>g</sub>**, on each representation feature we present 3 data points that maximally activates the feature, and also show first order gradient visualization for each; for **P** stage we show the "graph" on the right that ranks the top 5 representation features from Sparse Linear Model analysis as well as their respective weights. The webpage organization is the same as the webpage for VQA with the Overview page (Figure 21) and Features pages (Figure 22).

Within each of the five groups, on each of the 21 points, human annotators are asked to predict what the model (LRTF) predicts given a website containing some or all of the stages of analysis visualizations (depending on the group’s setting). In addition, we give human annotators 10 possible movie classes that the model could predict for these 21 points ("Drama/Romance", "Crime", "Sci-Fi", "Comedy", "Thriller", "Western", "Action", "War", "Documentary", "Horror"). Note that in reality, some of these categories are not mutually exclusive, but we intentionally designed our experiment this way to see if human annotators were able to determine the model’s prediction by looking at what specific properties within the movie’s poster or description the model focused on during the prediction process. Before each human annotator starts, they are taught how to interpret each analysis visualization, and then the instructor goes over the first point together with the annotator as example and the annotator need to finish the remaining 20 points on their own. Only the remaining 20 points counts towards the data collected in the experiment. We then compute average accuracy and inter-rater agreement score (Krippendorff’s alpha) within each group.

As shown in Table 2, in general, human annotators were able to better predict the model’s predictions when they were given more information, as the groups that got more information almost always end up with both higher average accuracy as well as higher inter-rater agreement. We were especially surprised to find that including **C** stage actually helped, since MM-IMDb did not seem to be a task that relies much on cross-modal interaction.

#### F.1.4 CMU-MOSEI

In this experiment, we perform model simulation on CMU-MOSEI dataset with the MuLT model from MultiBench [63]. We randomly selected 20 points from the test split of CMU-MOSEI dataset. The original CMU-MOSEI dataset is designed for a 7-way sentiment classification (-3 to +3), but we follow the preprocessing in MultiBench and convert it into a binary classification problem (where -1, -2, -3 are "Negative" and 0,1,2,3 are "Positive"). For each of the points, we run **MULTIVIZ** analysis and visualization: for **U** stage we show first order gradient analysis on image, audio and

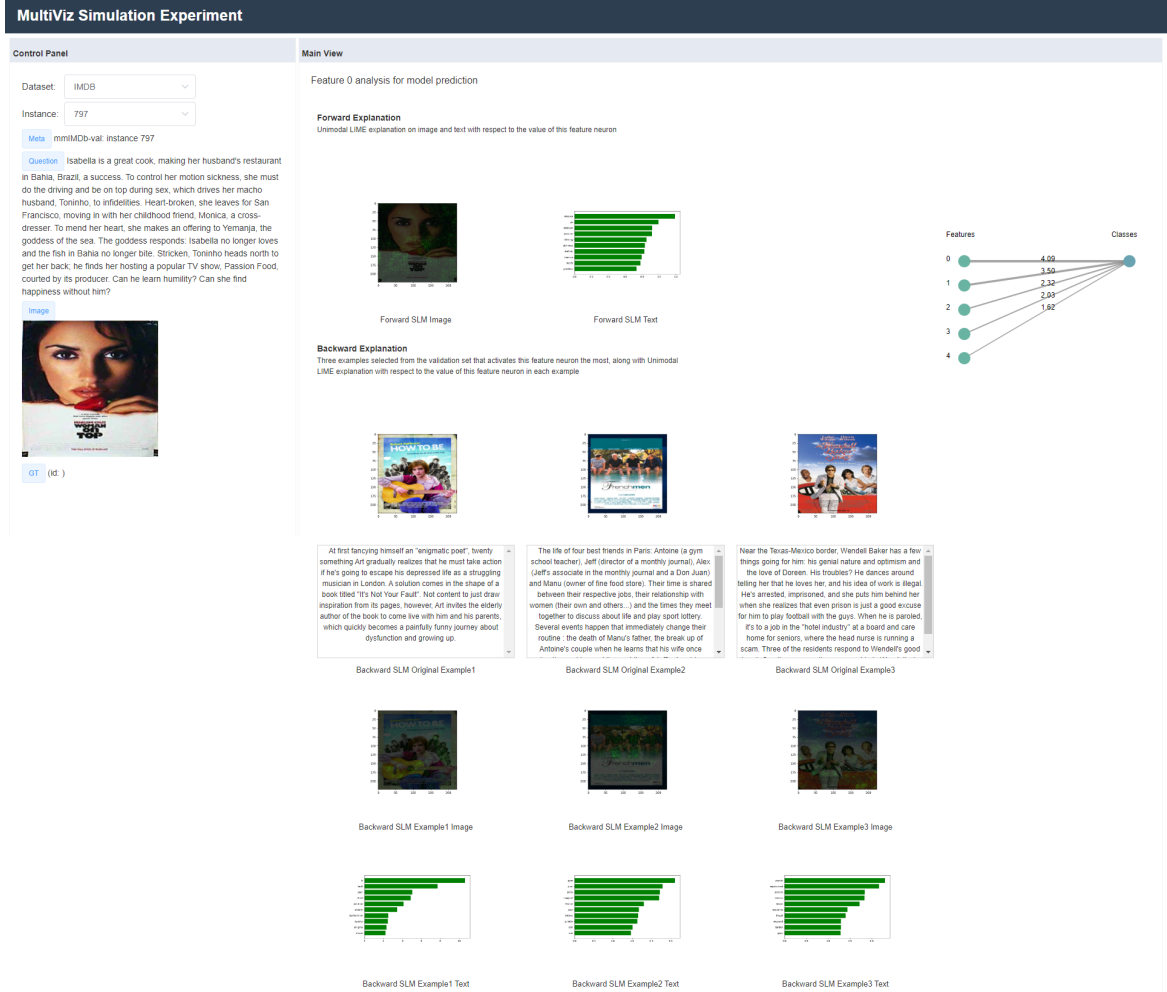


Figure 22: Simulation experiment for MM-IMDb: Sample Features page. Best viewed zoomed in and in color.

text (for image and audio, we compute gradient on each feature on each timestep, resulting in a 2d heatmap, while for text we just have a 1d heatmap), and we also show a processed video where we add bounding boxes around the visual features the model picked up (such as facial landmarks, facial expressions, lip movements, eye gaze, etc); for  $C$  stage we perform second order gradient analysis with selected words on image and audio; for  $R_\ell$  we show first order gradient on image, audio and text with respect to each representation feature; for  $R_g$ , on each representation feature we present 3 data points that maximally activates the feature, and also show first order gradient visualization for each; for  $P$  stage we show the "graph" on the right that ranks the top 5 representation features from Sparse Linear Model analysis as well as their respective weights. The webpage organization is the same as the webpage for VQA with the Overview page (Figure 23) and Features pages (Figure 24).

Within each of the five groups, on each of the 20 points, human annotators are asked to predict what the model (MultiT) predicts given a website containing some or all of the stages of analysis visualizations (depending on the group's setting). Before each human annotator starts, they are taught how to interpret each analysis visualization, and the annotator needs to finish the 20 points on their own. We then compute average accuracy and inter-rater agreement score (Krippendorff's alpha) within each group.

As shown in Table 2, in general, human annotators were able to better predict the model's predictions when they were given more information, as the groups that got more information almost always end

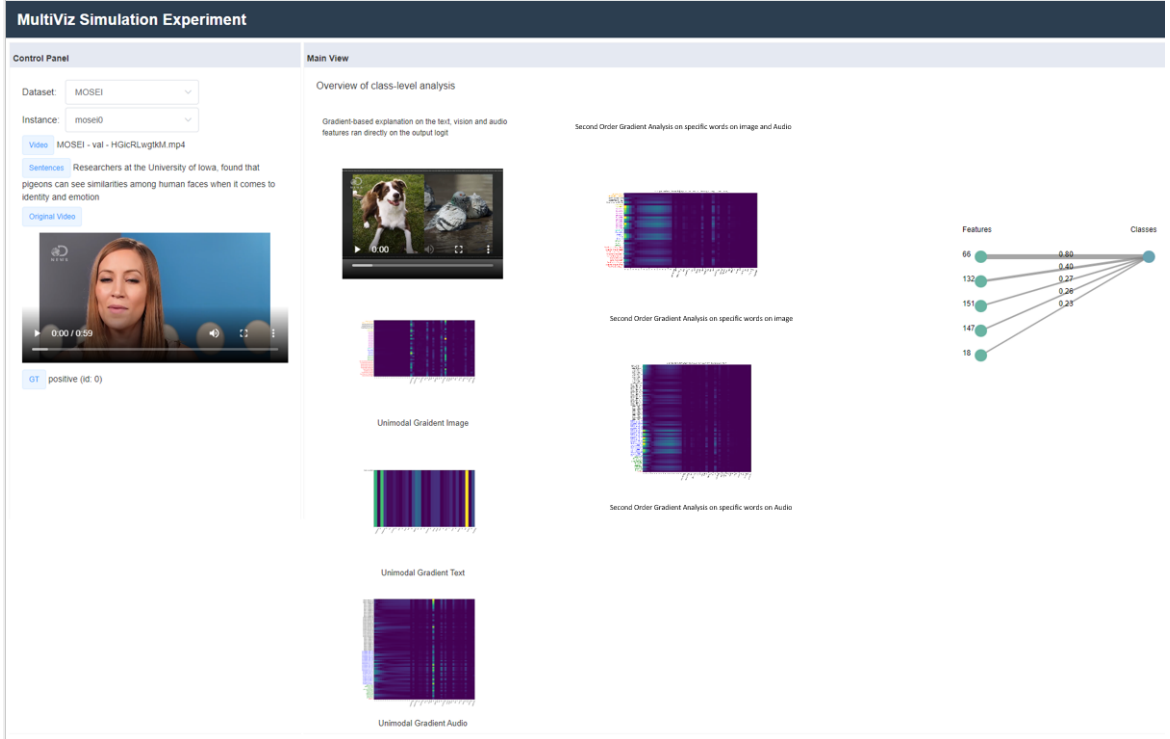


Figure 23: Simulation experiment for CMU-MOSEI: Sample Overview page. Best viewed zoomed in and in color.

up with both higher average accuracy and higher inter-rater agreement. Moreover, human annotators were able to get perfect accuracy and agreement in settings (4) and (5), showing that including global analysis  $\mathbf{R}_g$  provides enough information to simulate model predictions.

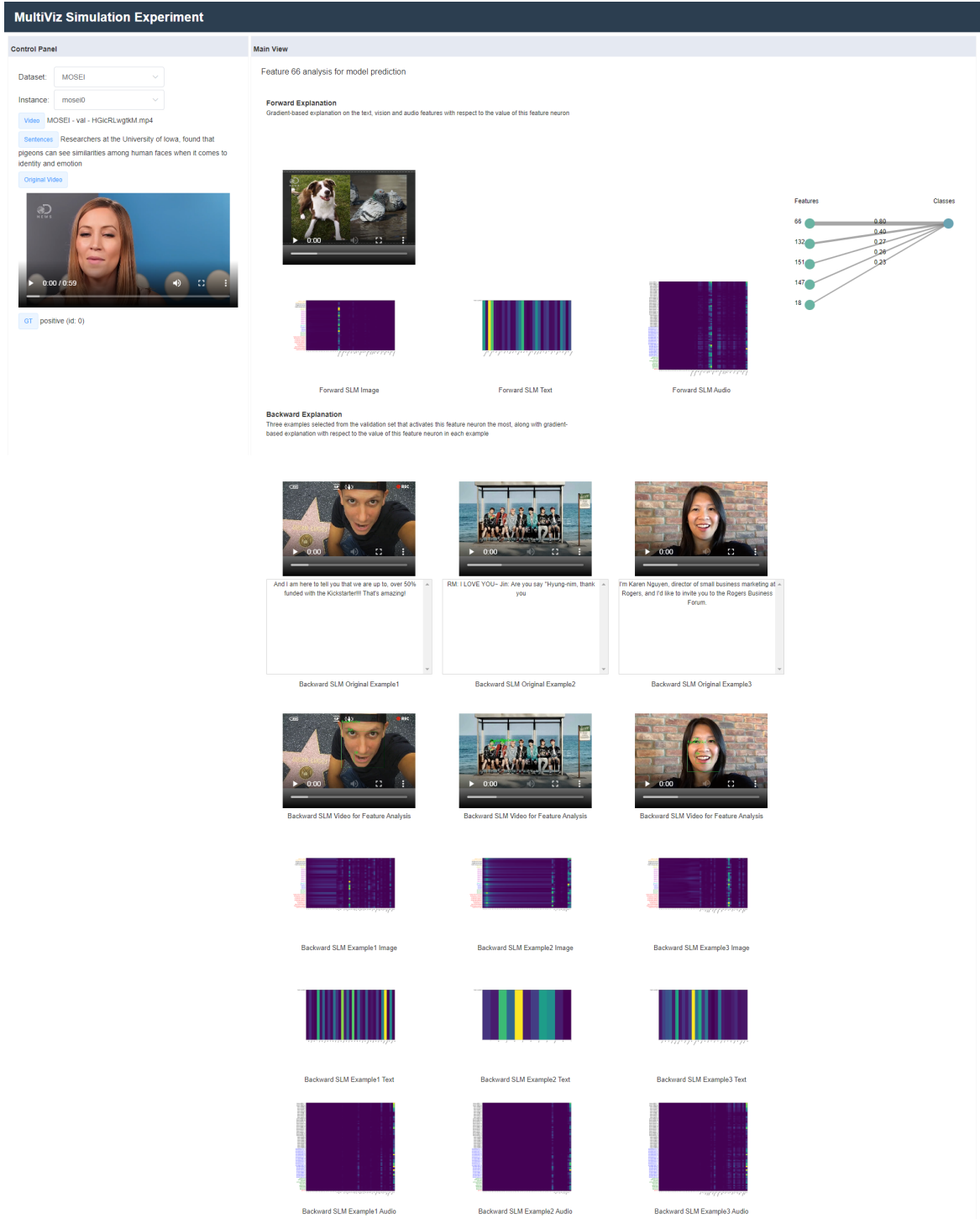


Table 5: Local faithfulness evaluations on visualizing cross-modal interactions.

Method	Dataset	Model	Model Accuracy	Top 1 alignment accuracy	Top 2 alignment accuracy
Second Order Gradient	CLEVR	MDETR [45] CNN+LSTM+SA [44]	99.5% 68.5%	55.8% 21.2%	80.7% 32.7%

## F.2 Cross-modal interactions

In order to verify local faithfulness of interpreting cross-modal interactions, we take a closer look at the qualitative and quantitative performance of our proposed second-order gradient method.

### F.2.1 CLEVR

One gold standard for evaluating visualizations of cross-modal interactions involves using CLEVR [44] (for image question answering), because in this dataset we are given ground truth bounding boxes of each object and there are often cross-modal alignments that are obvious and without any controversy. We picked two representative models: MDETR [45], which is near-perfect (with 99.5% accuracy); and CNN+LSTM+SA [44], which was the best model amongst the baselines included in the paper that introduced CLEVR dataset [44]. We randomly selected 52 ground-truth alignment pairs, all of which aligns between a phrase in the question (1-4 words) and the one single object in the image. Then, for each pair, we compute the first-order gradient of each word with respect to the sum of all entries in the prediction logit vector, sum up the absolute gradients of the words in the phrase, before taking the gradient of each pixel with respect to the sum. We end up with a second-order gradient (SOG) on each pixel. Then, we then compute the average absolute SOG per pixel within bounding boxes of each object (given by CLEVR). We compute 2 metrics: alignment picked up by top 1 bounding box (how often does the aligned object match with the bounding box with the highest average SOG) and alignment picked up by top 2 bounding box (how often does the aligned object match with one of the bounding boxes with top 2 highest average SOG).

We show the results in Table 5. We found that under near-perfect setting (MDETR) where it is safe to assume that the model actually picks up all ground-truth alignments, our method was able to pick up over 80% of the alignments using top-2 bounding boxes, thus indicating that our method is quite faithful to the model’s actual prediction process. Moreover, we found that CNN+LSTM+SA, which is a relatively simple late fusion model with relatively poor performance, was much less likely to pick up the correct alignments according to our method, which makes sense. Below, we show examples of when the model picks up or is unable to pick up the ground-truth alignments in Figure 25.

### F.2.2 FLICKR-30K

In addition, we perform a similar experiment for Flickr-30k image-text retrieval by modifying the above approach slightly. We select 20 image-text pairs from the annotated dataset, and for each of them we take between 8-15 phrases to find the second-order-gradient (SOG) on each pixel. We take the ground-truth boxes from Flickr30k Entities [80] and calculate the average SOG for a given object per pixel across all the available boxes for the object. Additionally, we match the phrase against ground-truth phrase annotations to find relevant boxes. Finally, we calculate what percentage of the objects were recovered by double gradient from the ground-truth annotations, if any. For ViLT [49] model, we observe that second-order gradient is able to do so with 44% matching accuracy, as compared to 34% using random matching (see some examples of detected interactions in Figure 26). For CLIP, the matching performance is worse (35%) as the gradients are very scattered across examples, making it hard to localize one particular object (see some examples of detected interactions in Figure 27). Both these findings indicate potential future directions towards quantifying intermediate cross-modal interactions learned by a model beyond looking at final task performance.

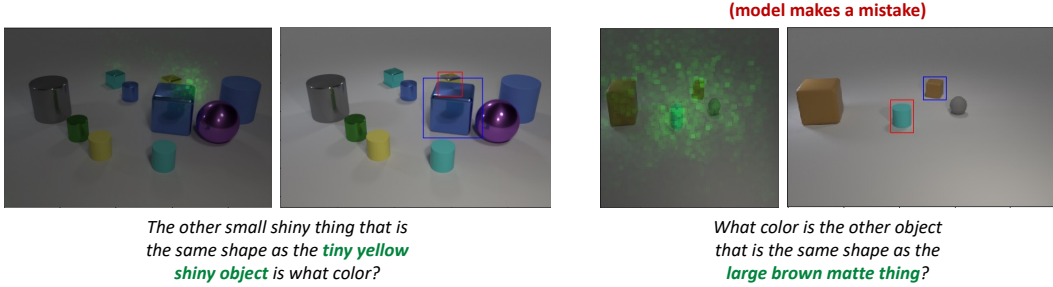


Figure 25: Examples of cross-modal interactions on CLEVR captured by our proposed second-order gradient method. Left: an example with the MDETR model, where it picks up the correct cross-modal interaction and predicts the correct answer. Right: an example with the CNN+LSTM+SA model, where it does not pick up the correct cross-modal interaction and results in an incorrect answer. (Within each of the two example, the image on the left side is heatmap on absolute second order gradient for each pixel, and on the right shows top 2 bounding boxes with highest average absolute second order gradient per pixel, top 1 box in red, top 2 box in blue).

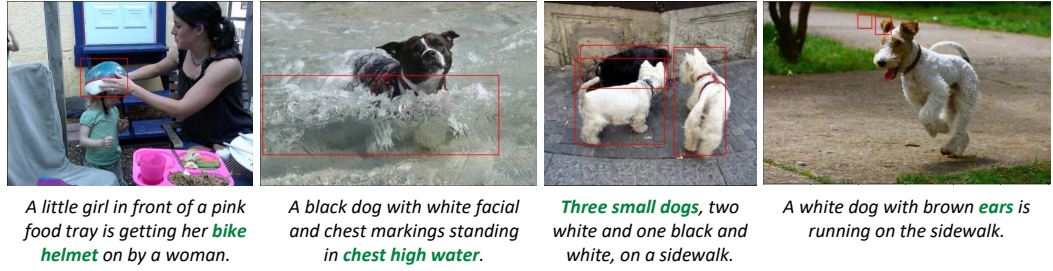


Figure 26: Examples of cross-modal interactions captured by ViLT on Flickr-30k dataset discovered by our proposed second-order gradient approach.



Figure 27: Examples of cross-modal interactions captured by CLIP on Flickr-30k dataset discovered by our proposed second-order gradient approach.



Figure 28: Example of  $R_\ell$  example with Unimodal LIME explanation given to annotators in the representation feature interpretation experiment.

### F.3 Representation interpretation

We now take a deeper look to check that MULTIVIZ generates accurate explanations of multimodal representations. Using local and global representation visualizations, can humans consistently assign interpretable concepts in natural language to previously uninterpretable features?

#### F.3.1 VQA 2.0

For VQA 2.0 dataset, we perform a representation interpretation experiment, where we give human annotators some visualizations on a particular representation feature and ask them to describe what concept they think that feature represents. We found 9 human annotators (with same qualifications as those in model simulation experiment), and divide them into 3 groups of 3. Each group is given a different setting (with different amounts of MULTIVIZ visualizations available):

1.  **$R_\ell$ :**  $R_\ell$  only, i.e. one random example and Unimodal LIME explanation on the example with respect to this example. See Figure 28 for example.
2.  **$R_\ell + R_g$  (no viz):** In addition to  $R_\ell$  with LIME, we also provide  $R_g$  (top 3 examples that maximizes the feature's value and top 3 examples that minimizes the feature's value), but no LIME visualizations for  $R_g$ . See Figure 29 for example.
3.  **$R_\ell + R_g$ :** Same as setting 2, but we also provide Unimodal LIME visualizations for all examples in  $R_g$ . See Figure 30 for example.

We gave the same 13 representation features to all 9 human annotators, where the first feature serves as an example and the other 12 are the ones we actually record for the experiment. The instructor first explains to each annotator what each visualization means, and then goes over the first feature together. Then, the annotator must write down a concept for the other 12 features on their own. We also ask each annotator to rate a confidence of 1-5 on how confident they are that this feature indeed represents this concept.

Once we have collected all 108 annotations (9 annotators each on 12 features), we manually cluster these into 29 distinct concepts that we show in Figure 31. For example, annotations like "things to wear", "t-shirts" and "clothes" all belong to "clothes" concept; all color-related annotations belong to "colors" concept; "material question", "made-of question" and "material of object" all belongs to "material" concept. We then compute inter-rater agreement score on each feature within each group of 3 annotators using Krippendorff's alpha with 29 possible categories. We report both inter-rater agreement and average confidence in Table 3.

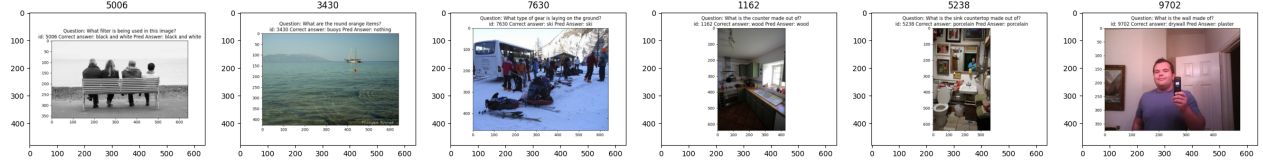


Figure 29: Example of  $R_g$  examples without Unimodal LIME explanation given to annotators under Setting 2 together with  $R_\ell$  visualizations in the representation feature interpretation experiment. Note that the left 3 examples are the ones that minimize the feature’s value, while the right 3 examples are the ones that maximize the feature’s value.

As shown in Table 3, as we give annotators more information, they were able to assign concepts more consistently (higher inter-rater agreement) and more confidently (higher average confidence score). Under setting 3 with full MULTIVIZ visualizations on feature representations, the 3 annotators completely agreed with each other on 8 out of 12 features, which is really impressive since there are so many possible concepts annotators could assign to each feature. Therefore, this shows that our visualizations, i.e.  $R_\ell$  and  $R_g$ , really helps humans to better understand what concept (if any) that each feature in representation represents, and that  $R_g$  examples and visualizations are especially helpful.

### F.3.2 CLEVR

A few examples of interpreted representations are shown in Figure 32, in addition to the examples in Figure 4 of the main paper.

### F.3.3 MM-IMDb

A few examples of interpreted representations are shown in Figure 33, in addition to the examples in Figure 4 of the main paper.

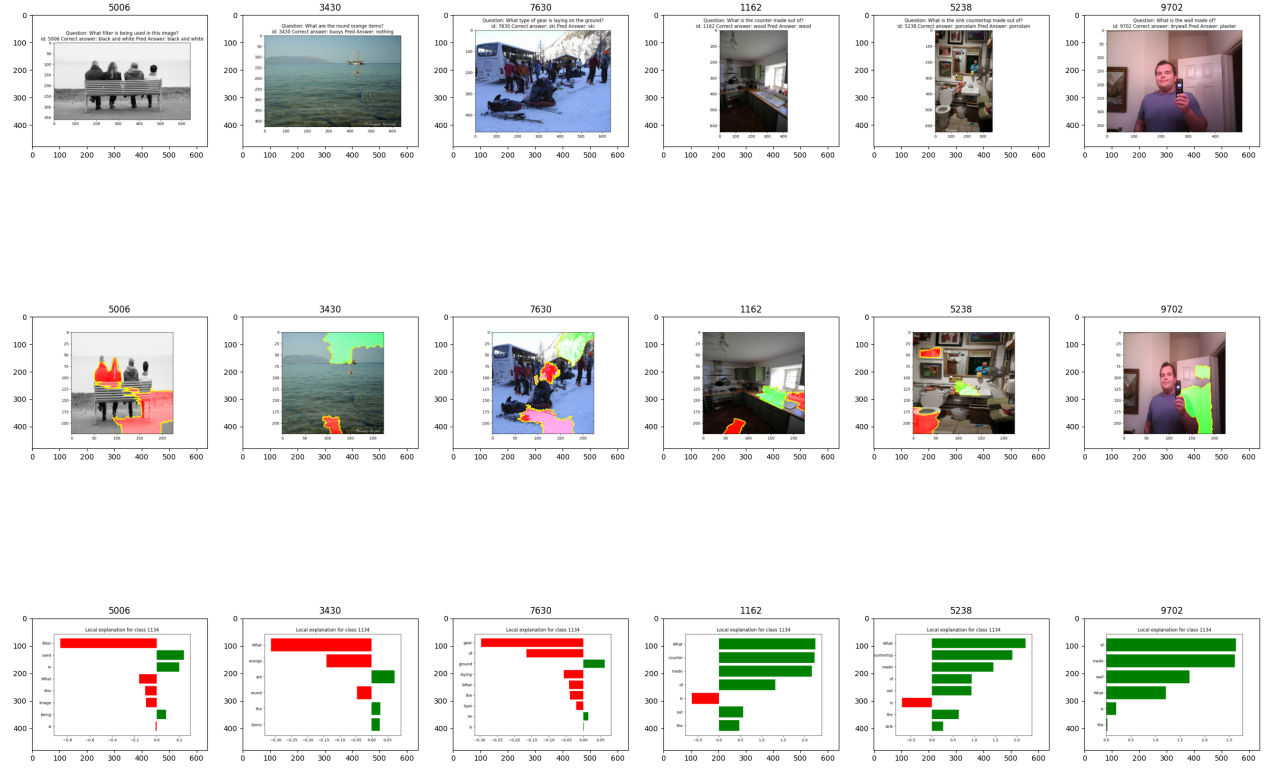


Figure 30: Example of  $R_g$  examples without Unimodal LIME explanation given to annotators under Setting 3 together with  $R_\ell$  visualizations in the representation feature interpretation experiment. Note that the left 3 columns are the ones that minimize the feature’s value, while the right 3 columns are the ones that maximize the feature’s value. Within each column, from top to bottom in order: the example data point, unimodal image LIME visualization, and unimodal text LIME visualization. Best viewed zoomed in and in color.

none	what	objects above/under relationship
plants	street	modifiers on an idea
numbers	vegetable juice	bathroom
colors	train	man and baby
plane	sky	motorcycle
pizza	plate	kitchen
rooms in house	identifying things	near-building objects
material	brush teeth	
clothes	something covering another	
airport	people with hands on plate	
food	poles	

Figure 31: The 29 concepts that we grouped all 108 annotations (12 features  $\times$  9 annotators) into in order to compute categorical inter-rater agreement.

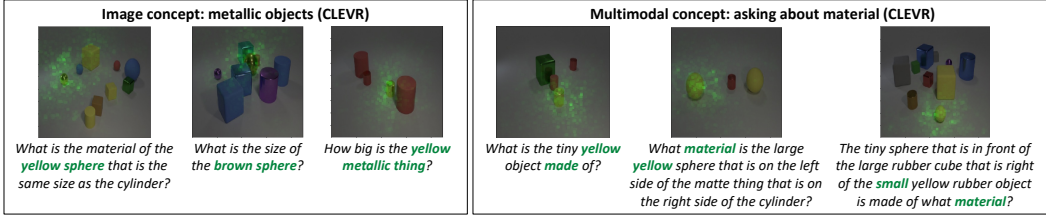


Figure 32: Examples of human-annotated **concepts** using MULTIVIZ on feature representations. We find that the features separately capture image-only, language-only, and multimodal concepts.

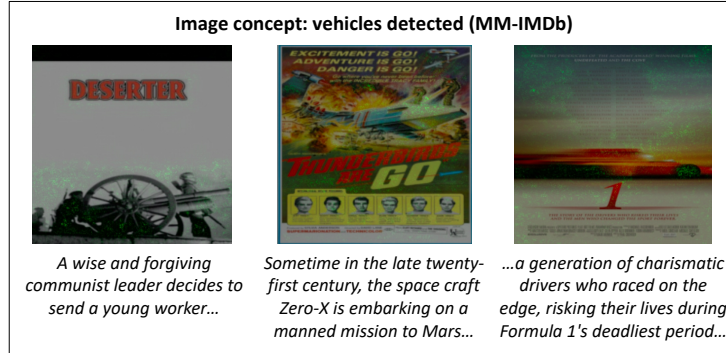


Figure 33: More examples of human-annotated concepts using MULTIVIZ on feature representations. We find that the features separately capture image-only, language-only, and multimodal concepts.

## F.4 Error analysis

In this section, we conduct an experiment to see if human annotators will be able to categorize the reasons why the model fails to predict the correct answer.

### F.4.1 Setup

We present three categories of errors:

1. **Unimodal perception error:** The model fails to recognize certain unimodal features or aspects. (For example, in Figure 5 top left example, the FRCNN object detector was unable to recognize the thin red streak as an object).
2. **Cross-modal interaction error:** The model fails to capture important cross-modal interactions such as aligning words in question with relevant parts or detected objects in image. (For example, in Figure 5 first one in middle column, the model is erroneously aligning "creamy" with the piece of carrot).
3. **Prediction errors:** The model is able to perceive correct unimodal features and their cross-modal interactions, but fails to reason through them to produce the correct prediction. (For example, in Figure 5 top right example, the model was able to both perfectly identify the chair with object detector and associate it with the word "chair" in the question (as shown by second-order-gradient analysis), but the model was still unable to reason with the given information correctly to predict the correct answer).

For each of the 2 datasets we used in this experiment (VQA and CLEVR), we found 4 human annotators and divide them into 2 groups of 2, one group for each setting: (1) under MULTIVIZ setting, for each data point, the human annotator is given access to full MULTIVIZ webpage as well as live Second-Order Gradient (i.e. the human annotator may request to compute second order gradient for a specific subset of words in the question, and he will be presented with the resulting second order gradient result); (2) under **No Viz** setting, the human annotator is given nothing but the original data point, the correct answer and the predicted answer. Each human annotator needs to classify each point into one of the three categories above, and they are also asked to rate their confidence in categorizing the error on a scale of 1-5.

### F.4.2 VQA 2.0

In this experiment, we perform error analysis on VQA 2.0 with LXMERT. We first randomly selected 24 data points which the model got wrong, and then we ask 4 human annotators to categorize each point into one of the 3 categories above (2 annotators under MULTIVIZ setting and 2 annotators under **No Viz** setting). The webpage that the human annotators under MULTIVIZ setting sees is the same as the ones described in Appendix D. In addition, since the LXMERT prediction pipeline is differentiable with respect to the detected objects by FRCNN object detector but not with respect to each pixel in the original image, the human annotators under MULTIVIZ setting will also be given all the bounding boxes of objects detected by FRCNN and also which ones have the highest second order gradient with respect to the specific words they picked. See Figure 34 for an example of all bounding boxes detected by FRCNN as well as second-order gradient analysis results for LXMERT.

During the experiment, the instructor first informs the annotators what each of the 3 categories of errors mean, and then explains each part of the visualizations they are given (if under MULTIVIZ setting). Then the instructor goes over the first data point together with the human annotators, and the human annotators must categorize the remaining 23 points on their own, and only those 23 points' annotations will count towards the final result.

The result for VQA error analysis experiment is shown in Table 3. As shown in the table, on average the human annotators are much more confident in categorizing each error, and also tend to agree with each other a lot more often when given MULTIVIZ compared to **No Viz**. This shows that MULTIVIZ can indeed help humans identify types of errors within a multimodal model. In addition, human annotators from the MULTIVIZ setting report that they can tell whether a model is able to perceive unimodal information correctly via **U** stage analysis as well as the bounding boxes produced by FRCNN, and they found second order gradient requested on specific words most helpful among all **C** stage visualizations (such as DIME) when determining if the model was able to find the correct cross-modal interactions. The data point presented in Figure 34 is one good example of this.

**Error breakdown:** Out of the 23 total errors, human annotators reported that on average 8.5 of them are category 1 (unimodal perception error), 8.5 of them are category 2 (cross modal interaction

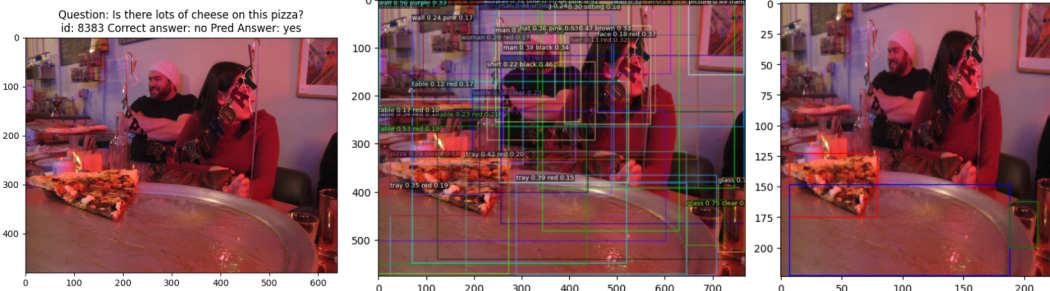


Figure 34: Examples of second-order gradient request by human annotators during error analysis. Left: input image. Middle: all bounding boxes detected by FRCNN image encoder. Right: top 3 bounding boxes with the highest second order gradient with respect to the word "pizza" (red is top 1, blue is top 2, green is top 3). In this data point, we can clearly see that the model was able to detect the pizza (as it was included in a bounding box by FRCNN) and was able to associate the pizza in the image with the word "pizza" in the question (as shown by second order gradient analysis). Therefore, through MULTIVIZ visualizations, both human annotators agreed that this point is a category 3 prediction error. Best viewed zoomed in and in color.

error), and 6 of them are category 3 (prediction error). This suggests that the majority of errors present in LXMERT is still caused by misunderstanding the basic unimodal concepts and cross-modal alignments rather than high-level reasoning of the perceived information, and that one possible future direction for improving the model pipeline is to use better unimodal encoders (than FRCNN) and find out some way to force the model to learn to align visual and text concepts correctly.

#### E.4.3 CLEVR

In this experiment, we perform error analysis on CLEVR with CNN+LSTM+SA model. We first randomly selected 11 data points which the model got wrong, and then we ask 4 human annotators to categorize each point into one of the 3 categories above (2 annotators under MULTIVIZ setting and 2 annotators under **No Viz** setting). The webpage that the human annotators under MULTIVIZ setting sees is the same as the ones described in Appendix D. In addition, the human annotators under MULTIVIZ setting can request the second-order gradient analysis result on specific words or phrases they pick, both the pixel-wise heatmap and top 2 bounding boxes with the highest average absolute gradient per pixel (same procedure as described in Appendix F.2). See the bottom half of Figure 25 for an example of second-order gradient analysis result of CNN+LSTM+SA.

During the experiment, the instructor first informs the annotators what each of the 3 categories of errors mean, and then explains each part of the visualizations they are given (if under MULTIVIZ setting). Then the instructor goes over the first data point together with the human annotators, and the human annotators must categorize the remaining 10 points on their own, and only those 10 points' annotations will count towards the final result.

The result for CLEVR error analysis experiment is shown in Table 3. As shown in the table, on average the human annotators are much more confident in categorizing each error, and also tend to agree with each other a lot more often when given MULTIVIZ compared to **No Viz**. This shows that MULTIVIZ can indeed help humans identify types of errors within a multimodal model.

**Error breakdown:** Out of the 10 total errors, human annotators on average reported 6 of them belonging to category 2 (cross modal interaction error). This suggests that the major weakness of CNN+LSTM+SA is that it is not great at aligning phrases in text with the object the phrase refers to. This is expected because CNN+LSTM+SA is a late fusion model, which is known to be not great at capturing low-level cross-modal interactions.

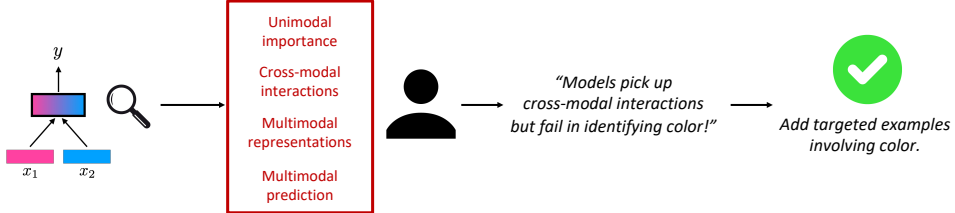


Figure 35: **Model debugging**: we ask humans to use MULTIVIZ visualizations and identify bugs that a multimodal model exhibits. Following this, we will attempt to fix the bug given a fixed budget of additional datapoints that the model is allowed access to. If MULTIVIZ indeed helps humans to identify the correct reason for model failure, the targeted data given to the model should improve performance more so than a same amount of randomly sampled data.

## E.5 Model debugging

### E.5.1 VQA 2.0

Following error analysis, we take a deeper investigation into one of the errors on a pretrained LXMERT [97] model fine-tuned on VQA 2.0 [33].

We compute the penultimate features (the input to the last linear layer in the classification head) of the V set, and train a linear model that best maps the absolute values of these penultimate features to a binary label where 0 means the original LXMERT model got this point right and 1 means the original LXMERT model got this point wrong. Then, we pick the top 5 dimensions in the penultimate feature with the highest positive weight in the linear model, and task human annotators to inspect these neurons carefully through MULTIVIZ local and global representation analysis. Human annotators found that 2 of the 5 neurons were consistently related to questions asking about color, which highlighted the model’s failure to identify color correctly (especially blue). The model has an accuracy of only 5.5% amongst all blue-related points (i.e., either have blue as correct answer or predicted answer), and these failures account for 8.8% of all model errors. We show examples of such datapoints and their MULTIVIZ visualizations in Figure 6. Observe that the model is often able to capture unimodal and cross-modal interactions perfectly, but fails to identify color at the prediction stage.

In this section, we describe our initial attempt at fixing this color-related bug by adding targeted data in an active learning scenario. If MULTIVIZ indeed provides accurate insights for model debugging, we should be able to improve model performance using less data as compared to a control experiment that adds randomly sampled data (see Figure 35).

We first split the validation set (about 220K points) into 3 parts: the first 110K were called the V set (stands for "val"), the next 50K were called the U set (stands for "unlabeled"), and the last 60K were called the T test (stands for "test"). We are simulating a situation where in addition to the 450K training set, we have a labeled 110K validation set (V set), another 50K unlabeled points (U set), and 60K held-out test set (T set). Our goal is to debug or improve the given model (LXMERT) by selecting N points from U set to label and finetune the model with these N points.

We compare the following settings:

1. **Random:** We randomly sample  $N$  points from the U set.
2. **Uncertainty:** A common active learning baseline which selects the top  $N$  datapoints from the U set that the model is uncertain about based on the entropy of its predicted label distribution [55, 56, 89].
3. **MULTIVIZ 2 color:** For each of these 2 erroneous features, we picked  $\frac{N}{2}$  points from the U set that has the highest absolute values on the feature, and together these points form the N points related to color that we select from the U set. Note that we do not use label information about these additional datapoints.
4. **MULTIVIZ no color:** Same as above, but we use 2 features that do not represent color.
5. **MULTIVIZ 1 color:** Same as above, but we use 1 feature that represents color and 1 that does not represent color.

Table 6: **Model debugging:** we task 3 human users to use MULTIVIZ visualizations and highlight the bugs that a model exhibits (see Figure 35), and find 2 penultimate-layer neurons which highlighted the model’s failure to identify color. The model has an accuracy of only 5.5% amongst all blue-related points (i.e., either have blue as correct answer or predicted answer), and these failures account for 8.8% of all model errors. By providing the model with 500 additional datapoints asking specifically about color (in an active learning setup), we improve the model, especially on the targeted points.

Research area Dataset Model	QA	
	VQA 2.0 [33]	
	LXMERT [97]	
Metric	Targeted accuracy $\Delta$	Overall accuracy $\Delta$
Random	$+1.4 \pm 0.3$	$+0.3 \pm 0.1$
Uncertainty [55, 56, 89]	$+0.0 \pm 0.0$	$+0.1 \pm 0.0$
MULTIVIZ no color	$+2.5 \pm 1.3$	$+0.1 \pm 0.0$
MULTIVIZ 1 color	$+27.5 \pm 1.9$	$+1.0 \pm 0.1$
MULTIVIZ 2 color	<b><math>+30.5 \pm 4.9</math></b>	<b><math>+1.2 \pm 0.2</math></b>

Under each of these active learning settings, we finetune the last layer of LXMERT with the N selected points from U set for one epoch (batch size 32, learning rate tuned to the best performance), and the result is evaluated on the T set. In addition, since through MULTIVIZ analysis we found out that LXMERT is particularly bad on data points that either have ground truth correct answer "blue" or the original LXMERT predicts as "blue", we define a subset of T set we call "bluelist" that contains all 1729 points in the T set that either have ground truth correct answer "blue" or the original LXMERT predicts as "blue". The original LXMERT only has a 6% accuracy on bluelist. We try each setting 10 times (with different random seeds) and report average and standard deviation on improvement in accuracies on both the entire T set and bluelist over the original LXMERT.

We show these results in Table 6 and find that MULTIVIZ significantly improves upon either random or uncertainty-based sampling as measured by performance on the overall VQA 2.0 test set. To obtain a deeper look at performance, we further evaluate performance on a targeted test set only containing questions asking about color (reflecting the main bug we found in the model). On this targeted test set, MULTIVIZ significantly improves performance by 30% as compared to only 1.4% for random sampling. Using more features related to color also improved performance: 27% with 1 feature and 30% with both features. Surprisingly, we find uncertainty sampling had no effect (0.0%) since the model predicted these incorrect answers on color-related questions with *high certainty*, so none of these color-related questions were additionally introduced to the model.

## F.6 Summary of takeaway messages

From these results, we emphasize the main take-away messages:

1. From the model simulation experiment, we found that on all 3 settings of datasets and models, human annotators were able to get higher accuracy and better agreement when given strictly more stages of visualization from MULTIVIZ. This suggests that each stage in MULTIVIZ is complementary to helping humans better understand the models' decision-making process.
2. Through a deeper inspection of cross-modal interaction visualization, we showed that second-order gradient is faithful to what the model internally aligns most of the time (over 80% using top 2 alignment accuracy on MDETR).
3. From the representation interpretation experiment, we found that having both local and global representation visualizations helps human annotators assign interpretable concepts in natural language to deep features with higher confidence and agreement.
4. From the error analysis experiment, we showed that MULTIVIZ can help users locate the stage of model that caused the error when the model makes a mistake, which provides insights for model error analysis and debugging.
5. Finally, we showcase a real-world model debugging case study: using each stage of MULTIVIZ to localize the error, we were able to locate a real bug in the HuggingFace Transformers LXMERT library.

## G Future Directions

We plan to ensure the continual availability, maintenance, and expansion of MULTIVIZ. Several immediate future directions include expansions in the datasets and models used for interpretation with MULTIVIZ, interpretation algorithms implemented in MULTIVIZ, and holistic evaluation of interpretation methods.

### G.1 New datasets and models

There are a suite of new datasets in MultiBench [63] that we plan to include in MULTIVIZ, including those in the multimodal reinforcement learning [68] (e.g., RTFM [117] and SILG benchmark [118]) and multimodal co-learning [114] research fields (e.g., transferring information from CMU-MOSI to SST, CMU-MOSEI to SST [114], GLOVE word embeddings for CIFAR10 image classification [92], and knowledge graphs to image classification on Visual Genome dataset [52, 72]).

We attempted to include several models in the neuro-symbolic category [4, 71], but found them incompatible with gradient-based interpretation methods as well as LIME-based methods. We plan to investigate ways to analyze these models as well, perhaps in architecture-specific ways. There have also been recent attempts at building multimodal models that are interpretable by design, such as through soft [77] and hard attention mechanisms [16], graphs [61, 115] or routing networks [99]. We plan to investigate the tradeoffs between black-box post-hoc interpretable models versus those interpretable by design, with respect to model simulation, error analysis, and debugging with stakeholders, as well as performance.

### G.2 New classes of interpretation tools

MULTIVIZ is designed to be modular and support interpretation tools at each stage. While we have explored some directions, we plan to include the following interpretation methods in future work:

#### G.2.1 Unimodal importance

We also plan to include methods for segmenting data into atoms: a basic unit of real-world data in that modality which cannot (or rather, the user chooses to not) be broken down into further units. For example, when working with text, a user may choose the level of words or characters as the most basic unit. We plan for MULTIVIZ to provide a standard set of segmentations for each modality’s raw data, such as words for sentences or object bounding boxes for images. At the same time, it also allows the user to flexibly segment their own modalities of choice. Given segmented atoms, representations are learned for each atom to capture unimodal meaning contextualized in the presence of other atoms in the same modality. While the included datasets provide relatively clear segmentation, this task becomes nontrivial in the face of new datasets we plan to include, such as videos and graphs.

#### G.2.2 Cross-modal interactions

There have been several attempts at building multimodal models that are interpretable by design, with a particular focus on cross-modal interactions. Many of these involve parameterizing cross-modal interactions through attention models [38, 67] or graph-based models [61, 115]. As a result, there have been several approaches to study these specific types of cross-modal interactions, such as M2Lens [104], an interactive visual analytics system to visualize multimodal models for sentiment analysis through both unimodal and cross-modal contributions, and VL-InterpreT [1], an interactive visualization tool for interpreting vision-language transformers. We plan to include these in MULTIVIZ to compare black-box post-hoc interpretation of cross-modal interactions versus models interpretable by design.

#### G.2.3 Multimodal prediction

For future work beyond linear prediction, we also plan to investigate 2 other parameterizations to interpret the multimodal prediction process:

**Tree:** Insights from integrating neural networks with decision trees [103] can enable us to generalize linear reasoning into one based on compositionality defined by a decision tree. Specifically, we will investigate replacing the final layer of a black-box multimodal model with a learned decision tree to generalize linear prediction to hierarchical tree-structured prediction.

**Hierarchical:** How can we extend these ideas towards visualizing general compositionality of multimodal evidences, either predefined by the user or learned by the model? We propose knowledge distillation as a general paradigm for understanding the reasoning process in multimodal models.

For example, we may attempt to distill the knowledge in a black-box ViLBERT [67] model into a neuro-symbolic model with predefined multimodal composition (e.g., Neural Module Networks [6] or Neuro-Symbolic VQA [108]). This results in a model that preserves the interpretable benefits of predefined reasoning while at the same time enjoying the benefits of large-scale pretraining. By comparing the decisions made by the ViLBERT model before and after distillation, we can also obtain a measure of the reasoning capabilities of these black-box models.

### G.3 Evaluating interpretability

Progress towards interpretability is challenging to evaluate [14, 20, 41, 90, 94]. Model interpretability (1) is highly subjective across different population subgroups [8, 53], (2) requires high-dimensional model outputs as opposed to low-dimensional prediction objectives [77], and (3) has desiderata that change across research fields, populations, and time [74]. We plan to continuously expand MULTIVIZ through community inputs for new metrics to evaluate interpretability methods. Some metrics we have in mind include those for measuring faithfulness, as proposed in recent work [14, 20, 41, 70, 90, 94, 106].

### G.4 Engagement with real-world stakeholders

Finally, we have plans for engagement with real-world stakeholders to evaluate the usefulness of these multimodal interpretation tools. We plan to engage these stakeholders in the healthcare domain to evaluate interpretability on the MIMIC dataset and those in the affective computing domain to evaluate interpretability on the CMU-MOSEI dataset. We also refer the reader to recent work examining the issues surrounding real-world deployment of interpretable machine learning [11, 17, 53].